Geophysical investigation of the West Antarctic continental margin between Wrigley Gulf and the Amundsen Sea Embayment

DISSERTATION

zur Erlangung des Grades Dr. rer. nat.

Fachbereich für Geowissenschaften der Universität Bremen

vorgelegt von

Thomas Horst Kalberg

Gutachter

Prof. Dr. Heinrich Miller

Prof. Dr. Cornelia Spiegel

Bremerhaven, den 30. Juli 2015

Kolloquium 20.11.2015

Universität Bremen AWI ALFRED-WEGENER-INSTITUT HELMHOLTZ-ZENTRUM FÜR POLAR- UND MEERESFORSCHUNG

Per asperga ad astra - Durch das Rauhe zu den Sternen

Erklärung

Hiermit erkläre ich,

Thomas Horst Kalberg
wohnhaft in der Hasenheide 10 in 29313 Hambühren, dass ich

- die vorliegende Arbeit ohne fremde Hilfe angefertigt habe,
- keine anderen als die von mir angegebenen Quellen und Hilfsmittel verwendet habe,
- die den benutzten Werken wörtlich oder inhaltlich entnommenen Stellen als solche kenntlich gemacht habe.

Bremerhaven, 30. Juli 2015

Zusammenfassung

Das Amundsen See Embayment und das Marie Byrd Land inklusive des vorgelagerten Wrigley Golf sind Teil des westantarktischen Kontinentalrandes. Beide Gebiete liegen zwischen dem Ross Meer und der Antarktischen Halbinsel. Die gesamte Region entstand während des Abbrechens und der darauf folgenden Trennung der Westantarktis von Neuseeland in der Kreidezeit. Das Gebiet spielt eine zentrale Rolle bei der tektonischen Rekonstruktion des westantarktischen Kontinentalrandes sowie des gesamten Südpazifiks.

Fundierte Kenntnisse der tektono-magmatischen Entwicklung dieser Region und der daraus resultierenden Architektur der Lithosphäre sind zudem unverzichtbare Parameter bei der Berechnung und Interpretation detaillierter Modelle der Dynamik des westantarktischen Eisschildes. Es gilt als erwiesen, dass jener Teil des westantarktischen Eisschildes, welcher in die Amundsen See mündet, der mit Abstand am schnellsten abschmelzende Eisschild der gesamten Antarktis ist.

Das Amundsen See Embayment überdeckt eine Fläche von ca. 320000 km^2 und ist von gedehnter kontinentaler Kruste unterlagert. Geophysikalische Untersuchungen angrenzender Regionen wie des Pine Island Rifts, des westlich der Amundsen See gelegenen Marie Byrd Landes oder des Ross Meeres zeigen Krustenmächtigkeiten von 21-24 km bzw. 25-28 km. Die Krustenmächtigkeit des Amundsen See Embayment ist mit 24-28 km entlang eines 2D Profiles nur sehr ungenau bekannt. Das kontinentale Hinterland der Amundsen See befindet sich mehr oder weniger auf Meeresniveau. Einflüsse des westantarktischen Riftsystems sowohl auf die Entwicklung dieses Hinterlandes als auch des Amundsen See Embayment selbst werden zwar vermutet, konnten aber noch nicht verbindlich geklärt werden.

Weiterhin sind sowohl die Krustenstruktur als auch die Entstehung des Wrigley Golfs und des hinterlandigen Marie Byrd Landes ebenfalls nur sehr punktuell bekannt. Eine singuläre Receiver Funktion, welche südwestlich des Marie Byrd Land Domes gemessen wurde, liefert eine Krustenmächtigkeit von 21-24 km. Im Gegensatz zum Hinterland des Amundsen See Embayment liegt das Hinterland des Wrigley Golf auf einer Höhe von maximal 3 km über Meeresniveau. Diese Erhöhung steht in Zusammenhang mit dem Marie Byrd Land Dome. Als Ursache hierfür wird ein rezenter Mantel Plume vermutet, welcher grosse Teile des Marie Byrd Landes unterlagert.

Kontrovers diskutiert wird in diesem Zusammenhang, ob dieser Plume bereits zum Zeitpunkt des Abspaltens Neuseelands von diesem Teil der Antarktis in der Kreidezeit existierte. Damit direkt verbunden ist die These, ob sich die Region zum Zeitpunkt des Aufbruches bereits auf erhötem Niveau befunden hat oder nicht. Ein Indiz dafür, dass dies nicht der Fall ist, liefert die Tatsache, dass sich der konjugierende Kontinentalrand auf Meeresniveau befindet.

In den Jahren 2006 und 2010 wurden auf zwei Schiffsexpeditionen des Forschungsschiffes Polarstern in die Amundsen See und den Wrigley Golf geophysikalische Daten erhoben um die Lithosphären- und Sedimentstruktur sowie die tektonomagmatische Entwicklung beider Regionen zu erforschen.

In meiner Arbeit präsentiere ich basierend auf diesem Datensatz unter anderem P-Wellen Geschwindigkeitsmodelle entlang zweier Profile, welche in der Amundsen See gemessen wurden. Darauf basierend präsentiere ich ein ca. 540 km langes 2D Dichtemodell entlang eines Profiles, welches von der Tiefsee auf den mittleren Schelf der Amundsen See verläuft. Des weiteren zeige ich Ergebnisse einer Tiefenabschätzung durch Spektralanalyse von Gravimetrie und Magnetikdaten.

Das 2D Dichtemodel wird durch ein 3D Dichte- und ein 3D Magnetikmodel der Amundsen See erweitert. Beide Modelle werden durch Reflexionsseismik unterstützt. Abgerundet werden die Ergebnisse durch die Berechnung der lithosphärischen Rigidität (Biegefestigkeit) der Amundsen See.

Meine Krustenmodelle der Amundsen See bestätigen und erweitern frühere Arbeiten, nach denen die Kruste von gedehnter kontinentaler Natur ist. Die Kruste ist unter dem Kontinentalrand 10-14 km dick und bis zu 29 km unter dem Schelf. Eine Schicht erhöhter Dichte und variabler Mächtigkeit bis max. 10 km unterlagert die gesamte untere Kruste der Amundsen See. Diese Schicht impliziert überregionale magmatische Aktivitäten, welche ich mit einem beobachteten kontinentalen Magmaflusses in Richtung der Marie Byrd Unterseevulkane korreliere.

Ein Vergleich der Resultate der 3D Schweremodellierung mit der 3D Magnetikmodellierung zeigt zudem im östlichen Amundsen See Embayment eine höhere Korrelation zwischen Intrusionen erhöhter Dichte und magnetischen Störkörpern als im westlichen Embayment. Ich interpretiere diese Beobachtung als Indiz für eine vermehrte Intrusion mafischen Gesteins im östlichen Embayment, welche ich wiederum mit einem prominenten mafischen Intrusionskörper, dem Dorrel Rock Intrusions Komplex, unter dem östlichen Marie Byrd Land korreliere.

In Kombination mit tektonischen Lineamenten, welche aus Potentialfeldanalysen abgeleitet wurden, sowie Ergebnissen einer Berechnung der Biegefestigkeit der Lithosphäre, postuliere ich ein dominierendes tektono-magmatisches Ereignis im Oligozän, welches durch mehrstufige tektonische Prozesse überlagert wurde. Diese tektonischen Prozesse wiederum interpretiere ich als Resultat einer Ausweitung des West Antarktischen Riftsystemes in die Amundsen See.

Des weiteren präsentiere ich vier verschiedene Schweremodelle entlang eines ca. 280 km langen Profiles von der Tiefsee auf den kontinentalen Schelf des Wrigley Golf. Basierend darauf diskutiere ich die Existenz und den Einfluss eines möglichen Mantelplumes auf die Lithosphäre des Marie Byrd Landes. Unter Zuhilfenahme von Reflexionsseismik entlang des Schweremodels diskutiere ich den Zeitpunkt der Anhebung des Marie Byrd Landes sowie die klimatischen Veränderungen seid dem Aufbruch.

Mein finales Model zeigt Pratt kompensierte gedehnte kontinentale Kruste, welche einen anomalen Mantel überdeckt. Die Kruste ist 10-12 km dick am Kontinentalhang und 27 km unter dem kontinentalen Schelf. Die Mantelanomalie korreliere ich mit einer bekannten Niedergeschwindigkeitszone unter der Region, welche durch mein Model bestätigt wird.

Die hochkompakten Sedimente des inneren Schelfes des Wrigley Golf neigen sich mit ca. 4°. Dies ist durchschnittlich 2° steiler als an anderen antarktischen Schelfen. Eine wechselende Reflektivität der Sedimentgesteine auf dem Kontinentalhang impliziert einen Wechsel des Klimas zwischen kälteren und wärmeren Phasen während der Sedimentation. In Kombination mit einem oberen Mantel niedriger Dichte und der Abwesenheit sogenannter Flutbasalte interpretiere ich diese Ergebnisse als Beleg dafür, dass das zentrale Marie Byrd Land durch einen anomalen Mantel nach der Trennung von Neuseeland angehoben wurde.

Summary

The Amundsen Sea Embayment and the Marie Byrd Land including Wrigley Gulf off Hobbs Coast are part of the West Antarctic continental margin. The area is bounded in the East by the Antarctic Peninsula and by the Ross Sea in the West. The whole region was created during Cretaceous breakup and the corresponding separation between greater New Zealand and West Antarctica and plays a major role in plate tectonic reconstructions of the entire South Pacific and the West Antarctic continental margin.

Knowledge of the tectono-magmatic development and the resulting architecture of the lithosphere of the continental margin of West Antarctica are also indispensable for detailed modelling of the dynamics of the West Antarctic Ice Sheed. It is evident that the part of the West Antarctic Ice Sheed which flows into the Amundsen Sea, melts with the highest rates observed in entire Antarctica.

However, the Amundsen Sea Embayment covers an area of about 320000 km^2 and is underlain by stretched continental curst. Geophysical investigations of adjacent areas such as the Pine Island Rift, the Marie Byrd Land or the Ross Sea reveal crustal thicknesses of about 21-24 or 25-28 km. Crustal thickness of the Amundsen Sea Embayment itself is with 24-28 km only imprecisely known along a single profile. An influence of the West Antarctic Rift System on the development of the Amundsen Sea Embayment and its hinterland, which is more or less around mean sea-level, has been discussed but remains speculative.

Additionally, the crustal structure and the development of Wrigely Gulf and the Marie Byrd Land are also less known. A single receiver function, determined southwest of the Marie Byrd Land dome, reveals a crustal thickness of 21-24 km. Contrary to the hinterland of the Amundsen Sea Embayment, Marie Byrd Land is elevated by around 3 km above mean sea-level. This elevation is the so-called Marie Byrd Land dome. Reason for this elevation is a recent mantle plume which is suspected to underlie great parts of central Marie Byrd Land.

Controversially discussed in this context is the question whether this plume existed already at breakup of greater New Zealand from this part of Antarctica in the Cretaceous. Closely related to this discussion is the issue of whether the region was elevated in breakup times or not. An indication for a non-elevated breakup is that the conjugated New Zealand continental margin is near sea-level.

In the years 2006 and 2010 during two expeditions with the research vessel Polarstern in the Amundsen Sea and Wrigley Gulf off Hobbs Coast, geophysical data were collected to investigate the lithospheric and sedimentary structure including the tectono-magmatic development of both regions.

In my dissertation, I present P-wave velocity models along two profiles in the Amundsen Sea. Based on this, I present two 540 km long 2D density-depth models along a continental-rise to shelf profile in the Amundsen Sea. Furthermore, I show results of a depth estimation based on a spectrum analysis of gravity and magnetic data.

I build on my 2D density-depth model to generate a 3D density-depth and a 3D susceptibility-depths model of the Amundsen Sea. Both models are supported by seismic reflection measurements. The results are complemented by a calculation of the lithospheric rigidity of the Amundsen Sea.

My crustal models confirm and extend earlier studies of the Amundsen Sea which show stretched crust of continental nature. The crust of the continental rise is 10-14 km thick at the continental rise and up to 29 km under the shelf. A high-density layer of variable thickness up to max. 10 km underlies the whole crust of the Amundsen Sea. This layer implies a supra-regional mamgmatic process which I correlate with a postulated continental insulation flow towards the Marie Byrd submarine volcanoes.

A comparison of the 3D density-depth modelling results with a 3D magnetic model shows a stronger correlation between high-density intrusions and magnetic source bodies in the eastern than in the western embayment. I interpret this as an indication of more intrusions of mafic rocks in the eastern embayment which I correlate with the presence of a prominent mafic intrusive body, the Dorrel Rock intrusive complex, under the eastern Marie Byrd Land.

In combination with tectonic lineaments interpreted from potential field data and an estimation of the lithospheric rigidity, I postulate a dominating tectono-magmatic event which occured simultaneously with several minor tectonic processs during Oligocene. I interpret these processes as results of the propagation or relocation of the West Antarctic Rift System into the Amdunsen Sea.

Furthermore, I present four distinct gravity models along a 280 km long continental rise to shelf profile in the Wrigley Gulf. Based on this models, I discuss the existence and influence of a possible mantle plume to the lithosphere of the Marie Byrd Land. Including a coincident 2D seismic reflection profile along the gravity model, I discuss the uplift of Marie Byrd Land and the variations of climate conditions during and since break up.

My final model shows Pratt-type compensated stretched continental crust above an anomalously warm/low-density upper mantle. Further, the model shows 10-12 km thick crust at the continental rise and 27 km under the continental shelf. The mantle anomaly confirms the presence of a low-velocity area known from earlier works.

Wrigley Gulf sediments dip with around 4° towards the shelf edge which is around 2° steeper than observed at other Antarctic shelf regions. Changing reflectivity of the continental rise sediments implies changes of the climate conditions during sedimentation. In combination with a low-density upper mantle and the absence of flood basalts, I interpret the previous results as indication for an uplift of Marie Byrd Land after break up from New Zealand.

Acknowledgments

Ich danke Herrn Prof. Dr. Heinrich Miller und Frau Prof. Dr. Cornelia (Conny) Spiegel, dass sie eingewilligt haben diese Dissertationsschrift zu begutachten und damit den einhergehenden Zeit- und Arbeitsaufwand auf sich nehmen.

Herrn Dr. Karsten Gohl danke ich für die Betreuung meiner Promotion. Er war stets für Fragen erreichbar und hat mich erfolgreich re-motivieren und auf den rechten Pfad der Tugend zurückführen können. Frau Dr. Gabriele Uenzelmann-Neben und Herrn Dr. Graeme Eagles danke ich für kritische Anmerkungen und wissenschaftliche Beistandschaft während der Anfertigung meiner Dissertationsschrift.

Die Arbeit am AWI und die Teilnahme an Tagungen und Expeditionen sowohl in die Arktis, die Antarktis und die Fidji Inseln haben mir sehr viel Freude bereitet und wird immer einen sehr spannenden Anteil in meinem Leben einnehmen.

Es ist schon etwas ganz besonderes.

Contents

List of Figures

1 Introduction and Motivation

Geoscientists all around the world deal with one fundamental question: Which factors control the climate system of our planet? In 2014, the *Intergovernmental Panel on Climate Change* (IPCC) published the 5th Assessment Report representing the latest view of scientific knowledge relevant to climate changes (http://www.ipcc.ch/). The essence of this report is: The anthropogenic induced climate change can no longer seriously be denied.

However, beside the investigation of identified human induced influences on the environment such as the accumulation of climate forcing gases like CO_2, a legitimate interest in the distribution of landmasses including its responsible tectonic processes and the circulation of oceanic currents exists as their behavior is indirectly and directly related to climate (e.g. Hay, 1996). For example, the horizontal displacement of landmasses has a direct connection to climate through changing the latitudial distribution of continental blocks. Moreover, the closing and opening of gateways between oceanic basins influence the flowpathes of global oceanic circulation patterns and hence the transport of thermal energy from the equator to the polar regions.

Of greater interest in this context is the reconstruction of tectonically and geodynamically induced changes of the architecture of the polar regions including their basins and gateways. This in turn is indispensable to understand the Cenozoic and Mesozoic climate evolution of the Earth from greenhouse to a bipolar icehouse. However, the contribution of oceanic currents to the mean poleward heat transport is small (e.g. Trenberth and Caron, 2001; Czaja and Marshall, 2006; Fasullo and Trenberth, 2008) but its influence to the global heat balance is important as they may trigger global climate transitions for example from greenhouse to icehouse.

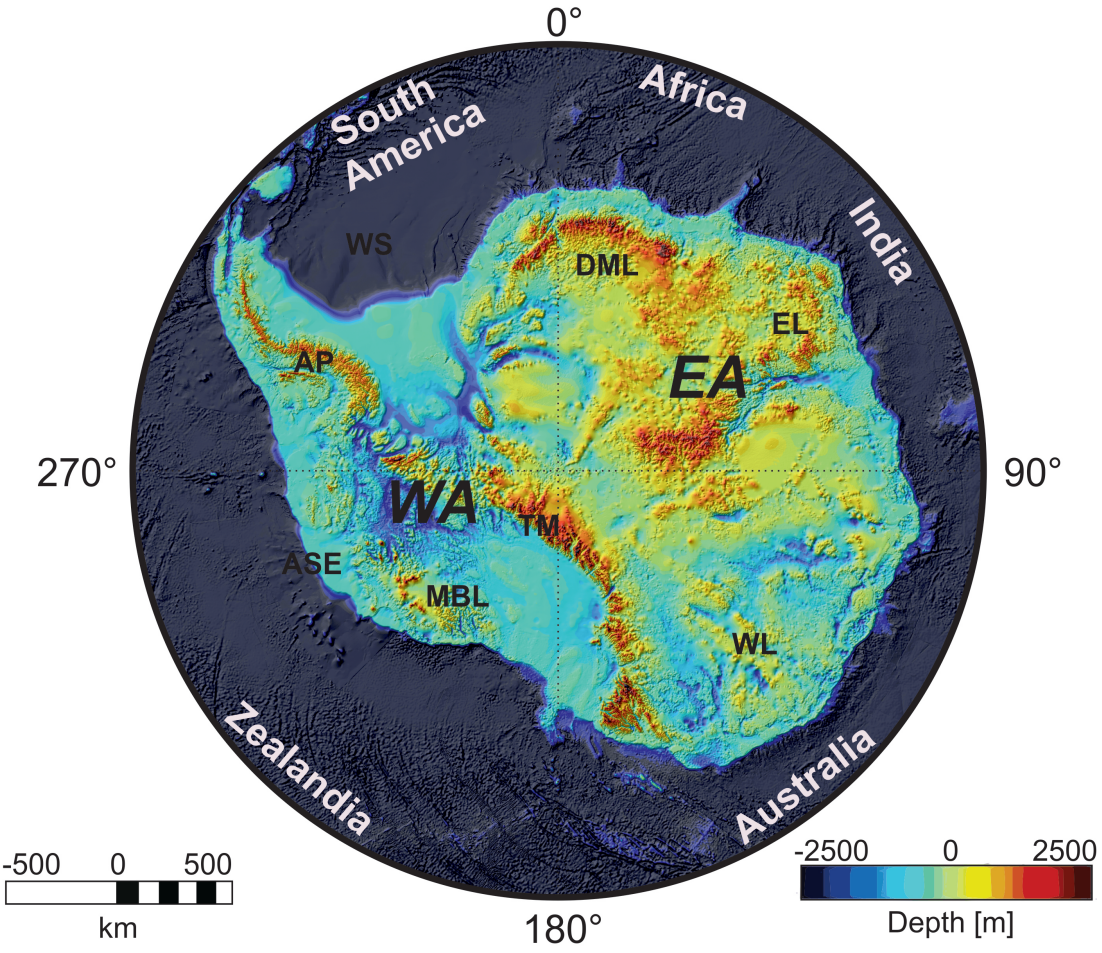

Figure 1: Topographic map of Antarctica showing the continental setting derived from BEDMAP2 (Fretwell et al., 2013). WA: West Antarctica, EA: East Antarctica, ASE: Amundsen Sea Embayment, TM: Transantarctic Mountains, MBL: Marie Byrd Land, WS: Weddel Sea, WL: Wilkens Land, EL: Ellsworth Land, DML: Dronning Maud Land, AP: Antarctic Peninsula.

The continent Antarctica (Fig. 1) was the center point from which all other continental plates like South America or Africa moved northwards after continental break-up of the ancient Southern Hemisphere supercontinent Gondwana in Early Jurassic (e.g. Storey, 1991). Hence, Antarctica plays a fundamental role in global plate tectonic reconstructions from break-up of the supercontinent Gondwana to Present. The opening of the Drake Passage and the corresponding deepening of the Tasmanian Gateway in the Cenozoic led to the onset of the modern Antarctic Circumpolar Current (ACC) (e.g. Stickley, 2004; Barker et al., 2007 a, b; Livermore et al., 2007). This in turn has been interpreted to be the cause for glaciation of Antarctica as the ACC works as natural boundary or isolator between warm equatorial water and coastal Antarctica.

But the ACC is not the only suggested reason for the build-up of the Antarctic Ice Sheed. The paleo onshore topography of West Antarctica seems to be also a prominent factore leading to the onset and the preservation of ice sheeds as most of onshore West Antarctica was above sea-level in Oligocene and hence seperates large ice sheeds from warm oceanic water (Wilson et al., 2013).

To accurately reconstruct West Antarcticas paleotopography, a detailed picture of the present day architecture is indispensable. Latest tectonic reconstructions of several regions of West Antarctica, for example of the Amundsen Sea Embayment, suffer from the lack of knowledge of the lithosphere in this region (e.g. Eagles et al., 2004a; Wobbe et al., 2012). Moreover, recent climate simulations and paleo ice shield models often take only the present day topography of West Antarctica into account.

Current knowledge of the lithospheric structure and the tectonic development in West Antarctica is based mostly on geophysical studies in the Ross Sea (Cooper et al., 1991; Trey et al., 1999; Luyendyk et al., 2001, Luyendyk et al., 2003), Marie Byrd Land (LeMasurier and Landis, 1996; Winberry and Anandakrishnan, 2004; LeMasurier, 2008) and the Pine Island Glacier region (Jordan et al., 2010) (Fig 2).

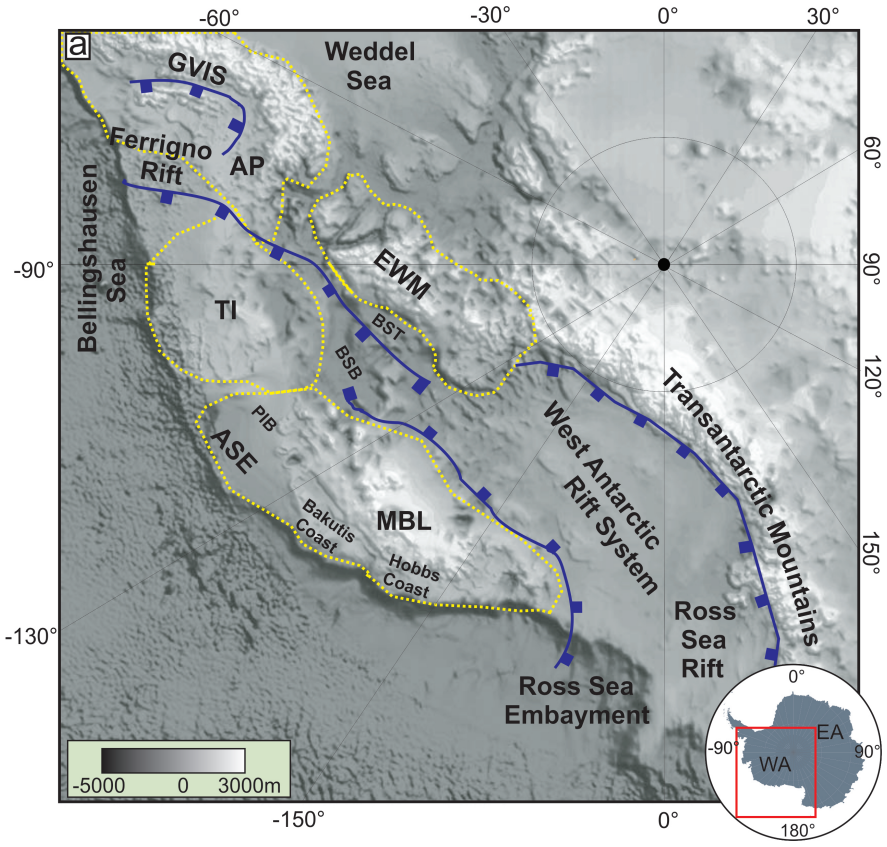

Figure 2: Topographic map of West Antarctica showing the regional setting derived from BEDMAP2 (Fretwell et al., 2013). Tectonic blocks (Dalziel and Elliot, 1982) are marked by yellow-dotted areas: WA: West Antarctica, EA: East Antarctica, EWM: Ellsworth-Whitmore Mountains, TI: Thurston Island, AP: Antarctic Peninsula, MBL: Marie Byrd Land, ASE: Amundsen Sea Embayment and PIB: Pine Island Bay. Rift structures such as the West Antarctic Rift System, Ferrigno Rift (FR) and George IV Sound (GIVS) are indicated with blue lines.

The Amundsen Sea Embayment:

In this context, the Amundsen Sea Embayment of West Antarctica (Fig. 2) is a key region as it provides critical boundary conditions for tectonic reconstructions of the pacific margin of West Antarctica. Furthermore, a sufficient reconstruction of the region is indispensable for a better understanding of the present as well as the past dynamic behavior of the West Antarctic Ice Sheet (WAIS), which is currently undergoing rapid ice loss in the Amundsen Sea sector (e.g. Rignot et al., 2008; Pritchard et al., 2009). This melting, thinning and retreating of the ice is one of the largest present-day changes documented in the Antarctic ice sheet (e.g. Rignot et al., 2011).

The dynamic behavior of the WAIS was subject of several studies in the past (e.g. Pollard and DeConto, 2009, Rignot et al., 2011). In this context it is interesting that beside serious scientific studies, the change of the WAIS arouses, in contrast to other scientific analysed areas, the interest of the public community. For example, the The New Yorker in May 2014 featured an article entitled: The West Antarctic Ice Sheet Melt: Defending the Drama. The Guardian in 2014 emphasised that: Western Antarctic ice sheet collapse has already begun, scientists warn - loss of ice sheet is inevitable.

However, in the last decade an intensely debated hypotheses asks whether the Amundsen Sea Embayment has been conditioned in its ice drainage role by the West Antarctic Rift System (WARS) (Fig. 2), one of the largest rift systems in the world and the dominating tectonic feature in West Antarctica (e.g. Gohl et al., 2013). The WARS itself encompasses the Ross Sea, the area under the Ross Ice Shelf and a part of West Antarctica (Fig. 2) but its influence to the Amundsen Sea Embayment is unclear.

Marie Byrd Land:

Eastward of the Amundsen Sea Embayment the Marie Byrd Land dome rises up (Fig. 2). This dome is an elevated portion of the WARS and covers an area of 1200 km x 500 km and was affected by volcanism in Oligocene times (Rocchi et al, 2006). This volcanism, as part of a Pacific Diffuse Alkaline Magmatic Province, has been related to the presence of an anomalous underlying mantle (Finn et al., 2005). The spatial distribution and temporal development of this mantle anomaly and its influence on the geomorphological development of the West Antarctic continental margin and the entire South Pacific have been subject of vigorous debate (e.g. LeMasurier and Landis, 1996; LeMasurier, 2008; Sutherland et al., 2010). The Marie Byrd Land itself is with an area of 1610000 km^2 by far the largest single unclaimed territory on Earth.

Two opposite theories embrace the geomorphology of Marie Byrd Land and conjugate greater New Zealand during continental break-up in Cretaceous times (Eagles et al., 2004; Wobbe et al., 2012). One hypothesis suggests that the conjugate margins were near sea-level during break-up, and then Marie Byrd Land uplifted thereafter (LeMasurier and Landis, 1996; Rocchi et al., 2006). The other hypothesis postulates that Marie Byrd Land was already elevated during continental break-up as a result of the presence of a mantle anomaly. (Luyendyk et al., 2001; Sutherland et al., 2010).

1.1 Research Questions

Several studies of the tectono-magmatic history of the Amundsen Sea Embayment and Wrigley Gulf off Hobbs Coast (Fig 2) (e.g. LeMasurier and Landis, 1996; Luyendyk et al., 2001; Larter et al., 2004; Rocchi et al., 2006, Sutherland et al., 2010 and Wobbe et al., 2012) have been presented in the last two decades. All these studies unfortunately provide an incomplete view due to an insufficient knowledge of the lithospheric and sedimentary architecture of the region between the Ross Sea and the Antarctic Peninsula (Fig. 1). In the next two chapters, I briefly summarize the most important results to set the major research questions of my dissertation into a broader context.

1.1.1 Tectonic development of the West Antarctic Continental margin and the Amundsen Sea Embayment

The tectonic blocks of West Antarctica (Dalziel and Elliot, 1982) are separated from the tectonically different and stable East Antarctic craton by the Transantarctic Mountains and the West Antarctic Rift System, which is one of the largest continental rift systems in the world (Fig. 1). The structural composition of the West Antarctic Rift System is comparable to other major continental rift zones such as the East African Rift or the Basin and Range Province (Behrendt et al., 1991; Tessensohn and Wörner, 1991; LeMasurier and Landis, 1996; LeMasurier, 2008).

The Amundsen Sea Embayment was formed as a consequence of the break-up of the former Gondwana supercontinent blocks of West Antarctica and greater New Zealand (e.g. Eagles et al., 2004a; Wobbe et al., 2012). The evolution of the Pacific margin of West Antarctica since the Late Cretaceous break-up included several distinct tectonic phases. South-westward propagation of rifting and break-up started with the separation of Chatham Rise from the eastern Marie

Byrd Land margin as early as 90 Ma and continued to around 83 Ma with the break-up of Campbell Plateau from central Marie Byrd Land (e.g. Mayes et al. 1990; Bradshaw et al., 1991; Larter et al., 2001; Eagles et al., 2004a, Wobbe et al., 2012).

From about 80-79 Ma, the Bellingshausen Plate began acting as an independent tectonic plate, and continued to do so until about 61 Ma (e.g. Larter et al., 2002; Eagles et al., 2004a,b). Its incorporation into the Antarctic Plate at this time occurred as part of a major plate reorganisation in the South Pacific (Cande et al., 2000). Kipf et al. (2014) postulated that at about 65-56 Ma the Marie Byrd Seamounts were formed from magmatic material that was transported from beneath the West Antarctic continental crust by a continental insulation flow.

The eastern shelf of the ASE has been suggested as the site of a Paleozoic-Mesozoic crustal boundary between the Thurston Island crustal block in the east and the MBL block in the west, whose apparent paleomagnetic polar wander paths differ significantly (Dalziel and Elliot, 1982; Storey, 1991; Grunow et al., 1991). Müller et al. (2007) considered that the WARS east of the Ross Sea started acting in dextral strike-slip or extensional motion east of the ASE between chrons 21 and 8 (48-26 Ma.). They postulated that this motion was connected to a Pacific-Phoenix-East Antarctica triple junction at the southwestern Bellingshausen Sea margin via the Bentley Subglacial Trench (Fretwell et al., 2013) and the Byrd Subglacial Basin.

Moho depth estimates under the Byrd Subglacial Basin and the Pine Island Rift reveals thin crust of only 19 km thickness (Jordan et al., 2010). The same authores estimated the elastic thickness of the lithosphere is around 5 km in the same area (Jordan et al., 2010). These results infer continental rifting in this part of West Antarctica which they interpreted as a distributed Cretaceous rifting

followed by Cenozoic narrow-mode rifting (Jordan et al., 2010). Latest analysis of geophysical data from the Amundsen Sea Embayment shelf shows that sedimentary sub-basins and tectonic lineaments cross the shelf, of which some can be related to an eastern branch of the West Antarctic Rift System (Gohl et al., 2013a,b). Wobbe et al., (2012) suggest the crust of the Embayment is highly stretched crust of continental affinity.

Recent Apatite-He age trends derived from rock samples of the eastern Pine Island Bay infer rift-related block faulting (Lindow et al., 2011). It seems likely that the topographic depression of the present glacially formed Pine Island Trough on the eastern Embayment shelf may be a product of pre-glacial tectonic activity which can be correlated to tectonic processes related to the West Antarctic Rift System. West of Pine Island Bay, thermochronological analysis show different signatures of the Mt. Murphy block compared to its neighbouring areas. This can be interpreted as an indication for a major fault system in this part of Marie Byrd Land, which was active during or after the Oligocene (Lindow et al., 2011).

Although the lithoshere of the Amundsen Sea Embayment was identified as highly stretched continental crust, but what is the thickness of the crust in Amundsen Sea Embayment? Was there magmatic underplating related to a proposed continental insulation flow or synbreak-up magmatism? What were the timing and character of the rifting processes leading to the present day architecture of the embayment? Are there indications for WARS activity in the embayment?

1.1.2 Lithospheric structure and sedimentary architecture in Wrigley Gulf and uplift of Marie Byrd Land

Marie Byrd Land is part of the West Antarctic continental margin and bounded by the West Antarctic Rift System in the south and an elevated, dome-like structure in the north which has been attributed to plume-related tectonic uplift (LeMasurier and Landis, 1996; LeMasurier, 2008) (Fig. 2). This so-called Marie Byrd Land dome and its volcanic products seem to be similar in petrologic character, geologic history and size to the Kenyan and Ethiopian domes (LeMasurier, 2008).

In contrast to the mantle plume hypothesis, other studies of the Marie Byrd Land propose that the elevated surface is the result of a warm Pacific mantle rising beneath it following the end of subduction at the Marie Byrd Land continental margin. Further, its volcanoes are suggested to be part of a much larger SW Pacific Diffuse Alkaline Magmatic Province (Finn et al., 2005). Other studies propose two hot mantle anomalies of which the larger one is centred on the Ross Sea sector, resulting in up to 1 km of dynamic topography (Spasojevic et al., 2010). Sutherland et al. (2010) illustrated this topography in the seafloor off West Antarctica, which is elevated by 0.5 to 1.2 km above the level of its conjugate area south of New Zealand and predictions using the lithospheric age-subsidence relationship (e.g. Stein and Stein, 1992).

It is widely accepted, that beneath the continents mantle upwelling can lead to tectonic uplift and widespread magmatism (Cox, 1989) such as observed in the Afar region of the East African Rift System (e.g. Marty et al., 1993; Marty et al., 1996) or the western cordillera in the United States (Parsons et al., 1994). LeMasurier and Landis (1996) or Sieminski et al. (2003) suggested that a mantle plume led to uplift of central Marie Byrd Land, beginning as early as 30 to 28

Ma and coinciding with the inception of alkaline volcanism in the region (Hole and LeMasurier, 1994).

However, two different hypotheses can explain the geomorphology of Marie Byrd Land and greater New Zealand during their Cretaceous continental break-up. One hypothesis suggests that the conjugate margins were at or near sea-level during break-up, and than MBL uplifted thereafter (LeMasurier and Landis, 1996; Rocchi et al., 2006). A contrary hypothesis postulates that the region was already elevated during continental break-up because of the presence of a mantle anomaly which causes uplift (Luyendyk et al., 2001; Sutherland et al., 2010).

Both the timing and the source of the Marie Byrd Land uplift are debated. First order questions in this context are: What is the crustal architecture of Wrigley Gulf off Hobbs Coast? Can the sedimentary architecture solve the question of timing of uplift of the central Marie Byrd Land? Was Marie Byrd Land already elevated during break-up in Cretaceous?

2 Dataset, Methods and Processing

In the following chapter, I present the scientific methods which I used for data acquisition, data processing and modelling. At first, I give a brief introduction into each used geophysical method. Afterwards, I show data examples and discuss the credibilities and the difficulties of each method. The final results and interpretation of the data are then shown in three scientific contributions presented in chapters 4, 5 and 6.

The geophysical data I evaluate in this study were acquired during the research cruise legs of *RV Polarstern* ANT-XXIII/4 in 2006 to the Bellingshausen and Amundsen seas (Gohl et al., 2007) and during ANT-XXVI/3 in 2010 into the Amundsen Sea Embayment including the Pine Island Bay (Gohl et al., 2010) (Fig. 2). Additionally, sediment echosounding and multibeam bathymetry data were recorded during both cruises continuously. At several locations in the Amundsen Sea Embayment, the geothermal heat flux was measured during ANT-XXII/4 but will not be evaluated in this study. The cruise in 2006 was a cooperation between the Alfred Wegener Insitute (AWI), the TU Dresden, the British Antarctic Survey (BAS) and the Vernadsky Institute for Geochemistry (Moskow). The partners of the AWI for the 2010 cruise were the University of Bremen, BAS and the Institute of Geological and Nuclear Sciences (GNS Science) (New Zealand).

My dissertation focusses on the development of a regional crustal model of the Amundsen Sea Embayment and Wrigley Gulf off Hobbs Coast (Fig. 2). Based on these models, I draft a possible tectono-magmatic history of the Amundsen Sea Embayment from the Cretaceous to Present. The used seismic profiles were set up from the continental rise through the shelf edge and over the middle shelf of the western Amundsen Sea Embayment which is of Cretaceous age and hyper extended (e.g. Wobbe et al., 2012). A third seismic refraction profile was used to de-

termine sediment densities in the eastern embayment (Gohl et al., 2012). Further, I process and interpret gravity data which comprise the satellite-derived Free-Air anomaly from McAdoo and Laxon (1997) and ship-borne gravity data which were collected continuously during both expeditions. The Free-Air anomaly was used to calculate the Bouguer anomaly. Additionally, I use a magnetic anomaly grid of the Amundsen Sea Embayment which was compiled by Gohl et al. (2013a) from magnetic data collected during the two RV Polarstern expeditions in 2006 and 2010.

Based on this dataset, I calculate two distinct 2D continental rise-to-shelf gravity models and a 3D gravity model of the Amundsen Sea Embayment between 120°W to 104°W and 70°E to 74°E. Additionally, I calculate a 3D forward magnetic model of the Amundsen Sea Embayment between -120°E to -104°E and -70°S to -74°S. I interpret the lithospheric architecture, several intrusive bodies and the responsible tectono-magmatic processes which forms the present morphology of the embayment.

Finally, I interpret a 2D continental rise-to-shelf seismic reflection transect that was collected in Wrigley Gulf off Hobbs Coast during the expedition in 2010. Based on this dataset, I calculate a 2D forward gravity model and I discuss the crustal architecture, the tectonic uplift of central Marie Byrd Land including the consequences for the tectono-magmatic development of this part of the West Antarctic continental margin.

2.1 Seismic experiments

On both expeditions, an extensive dataset was acquired consisting of high-resolution seismic reflection and wide-angle seismic refraction measurements. The aim of the seismic reflection experiment was to map the sedimentary cover and the top-of-basement morphology along the continental margin and the shelf region of the Amundsen Sea Embayment and the Wrigley Gulf off Hobbs Coast. Additionally, seismic refraction experiments were conducted to portray the lithospheric architecture and the velocity-depth distribution of the sedimentary layer and the underlying crust.

Figure 3: Airgun array used during expedition ANT-XXIII/4 in 2006.

The seismic source used during the expedition in 2006 consisted of 8 G-Guns (68.17 liters in total) and a Bolt air gun (32 liters) mounted astern on a metal frame (Fig. 3) (Gohl et al., 2007). The shot interval for the seismic refraction experiments was 60 s corresponding to an average shot-spacing of 150 m. For all seismic-reflection measurements, a shot interval of 10 s was used. Seismic measurements carried out during the expedition in 2010 were conducted by using 3 GI-guns, fired every 10 s (Gohl et al., 2010). Along all seismic profiles, the water depth was measured continuously by using a Hydrosweep DS-III system from ATLAS Hydrographic which works with a sampling rate of 1 s.

2.1.1 Seismic refraction experiment

Figure 4 illustrates an Ocean Bottom Hydrophone (OBH) which was used during the expedition in 2006. Technical details of the OBH are listed in the cruise report of the expedidion in 2006 (Gohl et al., 2007).

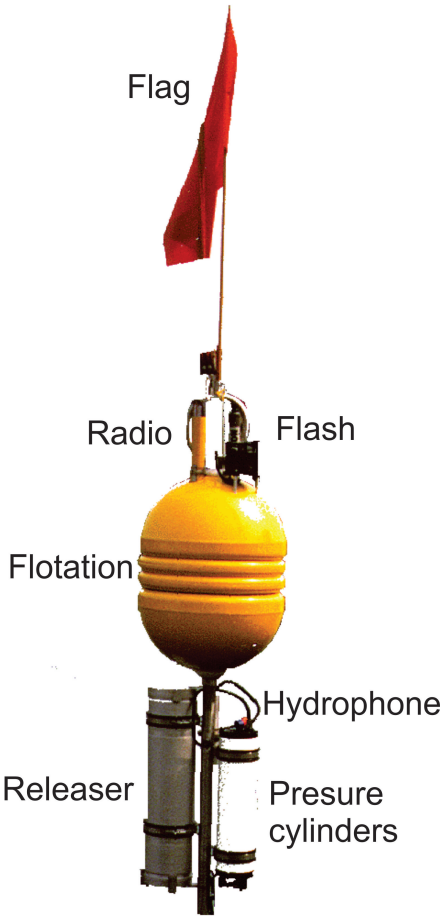

Figure 4: OBH used during ANT-XXIII/4 with components labelled

Figure 5 illustrates an Ocean Bottom Seismometer (OBS) which was used during the expedition in 2010. Technical details of the OBS are listed in the cruise report of the expedition in 2010 (Gohl et al., 2010).

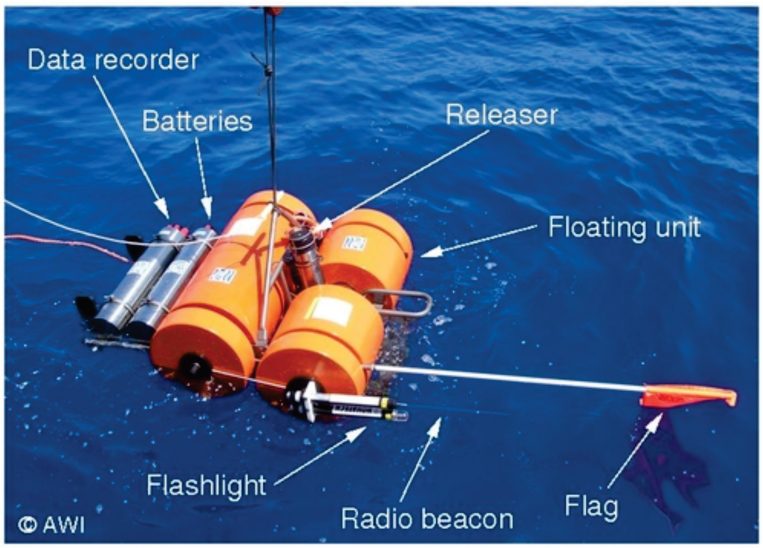

Figure 5: OBS used during ANT-XXVI/3 with components labelled (modified after http://www.awi.de/typo3temp/pics/bbfac7f294.jpg)

In the following, I explain the standard procedure of a marine seismic refraction experiment from deployment of the OBS/OBH to data extraction.

- The OBH/OBS are deployed at equal intervals along a defined profile line. The OBH/OBS sinks down to the sea-bottom due to anchors which are mounted under the OBH/OBS as additional weight

- Air-guns deployed behind the ship emitted seismic pulses along the defined profiles. Hydrophones mounted on the OBH/OBS recorded seismic signals and the data are recorded on a hard disk inside of a pressure cylinder.

- After the ship crosses the last OBH/OBS and reaches the end of the profile, the ship returns to the first OBH/OBS location.

- To recover each OBH/OBS, an accoustic signal is transmitted into the water to open the releaser unit, which holds the additional weight to the OBH/OBS.

- After disconnection from the anchor, the OBH/OBS floats up to the water-surface and can be collected.
- After data extraction from the hard disk, the data are transfered to a PC and saved.

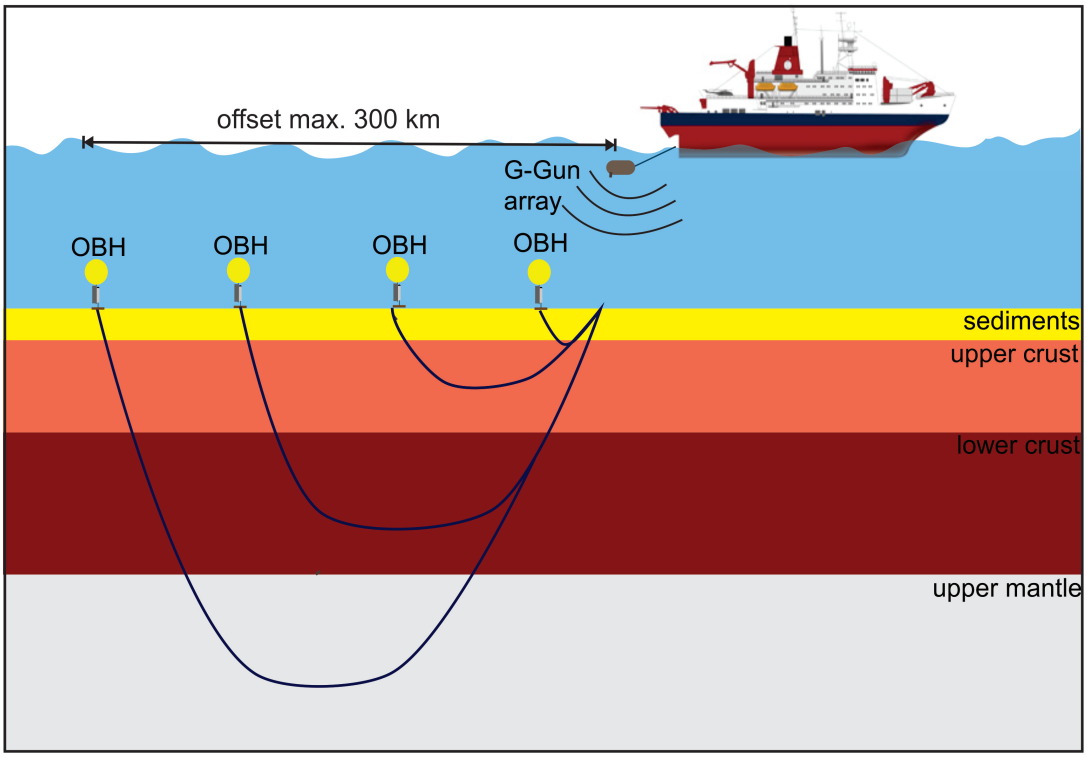

Figure 6: Principle of a seismic refraction experiment

The data were derived from signals recorded continuously by a hydrophone (OBH) or a three-component seismometer (OBS) and saved to an internal hard disk. After data extraction, I cut the data into 60 s long traces corresponding to the shot intervall. Afterwards, I relocalize the position of each OBS/OBH at the sea-bottom by using direct waves. I pick the direct wave followed by a shift of the shortest travel-time signal to zero-offset (Fig. 7). After relocalization, the OBH/OBS data are ready to further processing, travel-time picking with the software ZP2 and modelling.

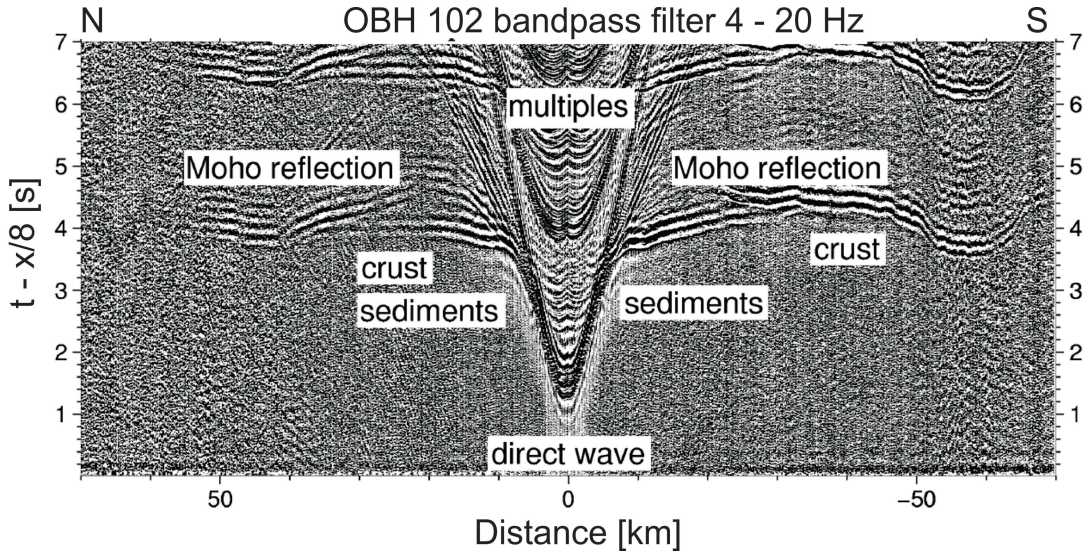

Figure 7: Seismic section of OBH 102. Identified phases are assigned. The data are bandpass-filtered.

2.1.2 Seismic refraction data and P-wave modelling

In general, seismic refraction measurements are conducted for observing subsurface layers and crustal structures by recording the travel times of acoustic waves propagating through the Earths interior. Because of its long offset configuration (up to 200 km), seismic refraction measurements allow the recording of wide-angle reflections and refracted waves of deep structures in the subsurface.

From a geophysical point of view, a subsurface layer boundary is an interface of an accoustic impedance contrast. The accoustic impedance of a media is defined by the product of its density and seismic velocity. In this context, seismic refraction observations reveal velocity and density information about the lithosphere and sediments. The velocity is then the slope of an observed phase in time versus offset. To derive the crustal thickness and the seismic velocity from measured data, I use a two dimensional (2D) ray-tracing algorithm, which can be used both for inversion and forward modelling of refracted and reflected seismic

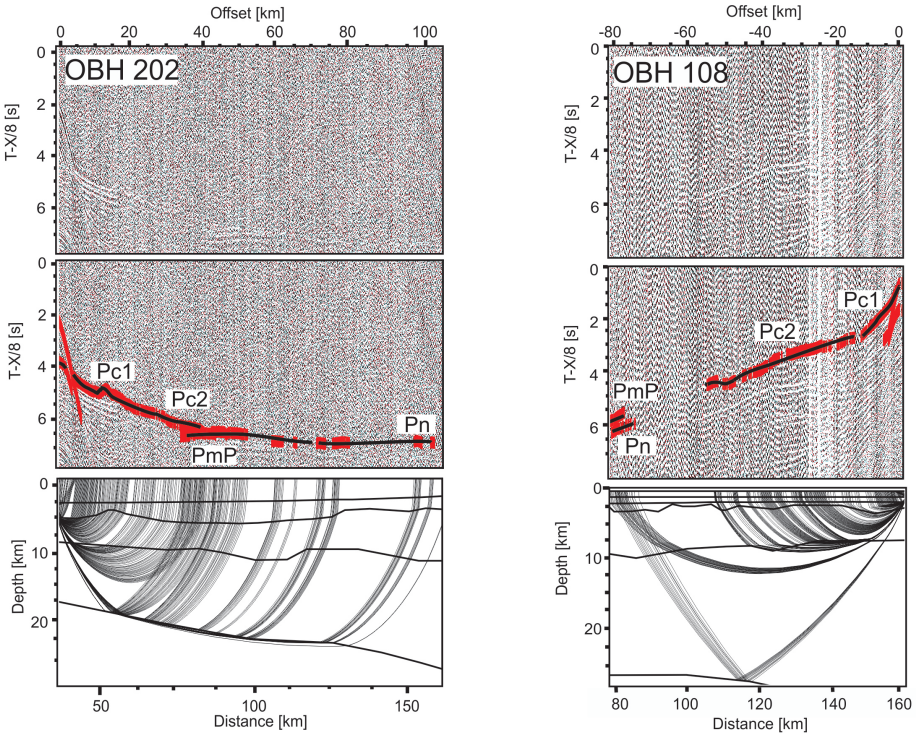

Figure 8: Top panel: part of seismic section from OBH 202 and 108 (lines AWI-20060100 and AWI-20060200, both plotted with a reduction velocity of 8 km/s and a bandpass filter of 4-20 Hz. Middle panel: Same section with modelled phases (black lines) and picked signals (red bars with bar length representing the pick uncertainty). Bottom panel: Ray tracing results with ray coverage in the velocity-depth model

phases (Zelt and Smith, 1992). Figure 9 shows a flow chart from data acquisition to modelling and interpretation after a seismic refraction experiment.

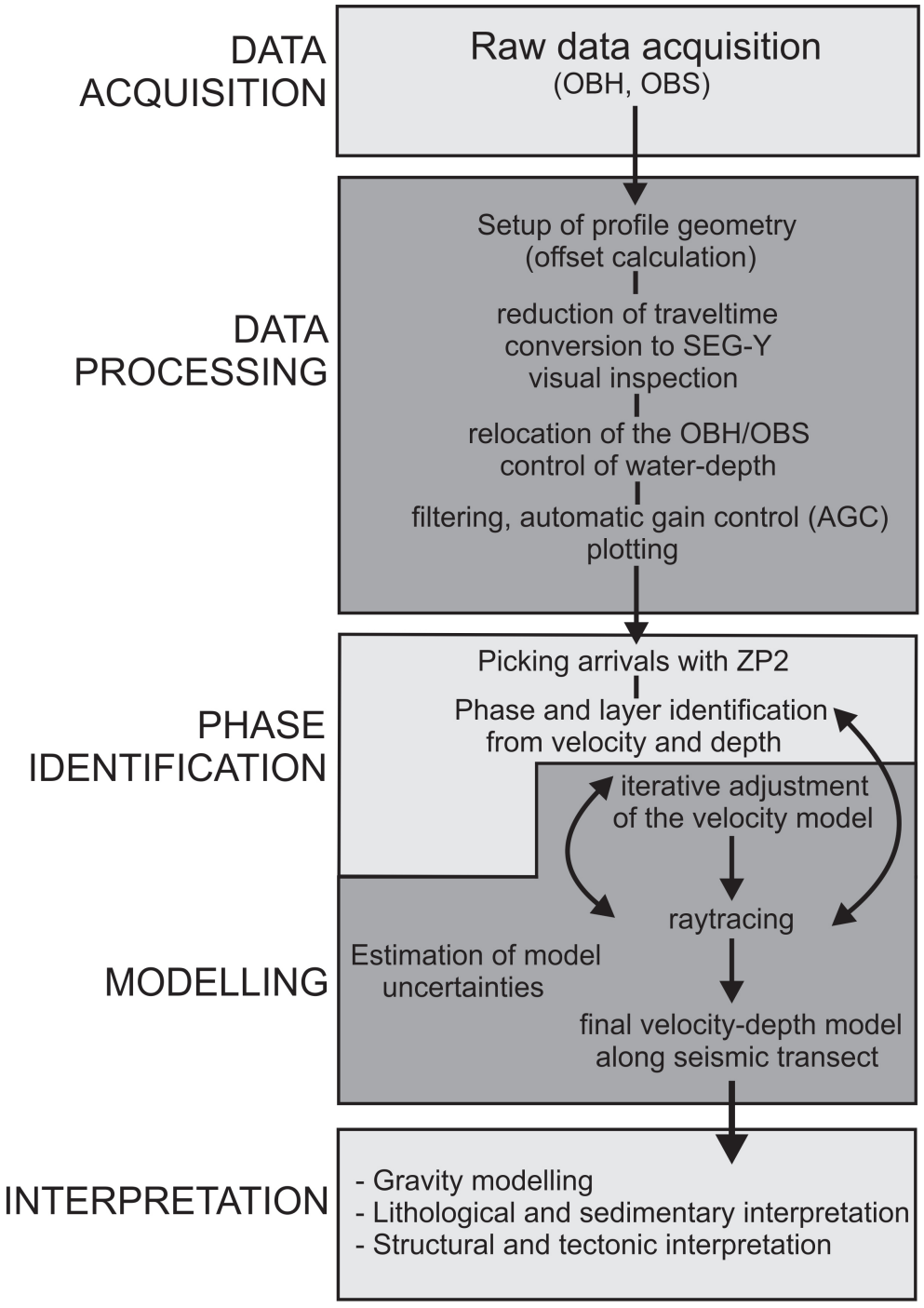

Figure 9: Flowchart of a seismic refraction experiment from data collection to interpretation.

2.1.3 Seismic reflection experiment

Seismic reflection measurements are a standard technique for geophysical observations of subsurface structures in sediments, at the top-of-basement and in the upper crust. Compared to seismic refraction measurements, the offset configuration of a seismic reflection observation is shorter. Hence, the observation depth is shallower but due to the number of active channels of higher resolution.

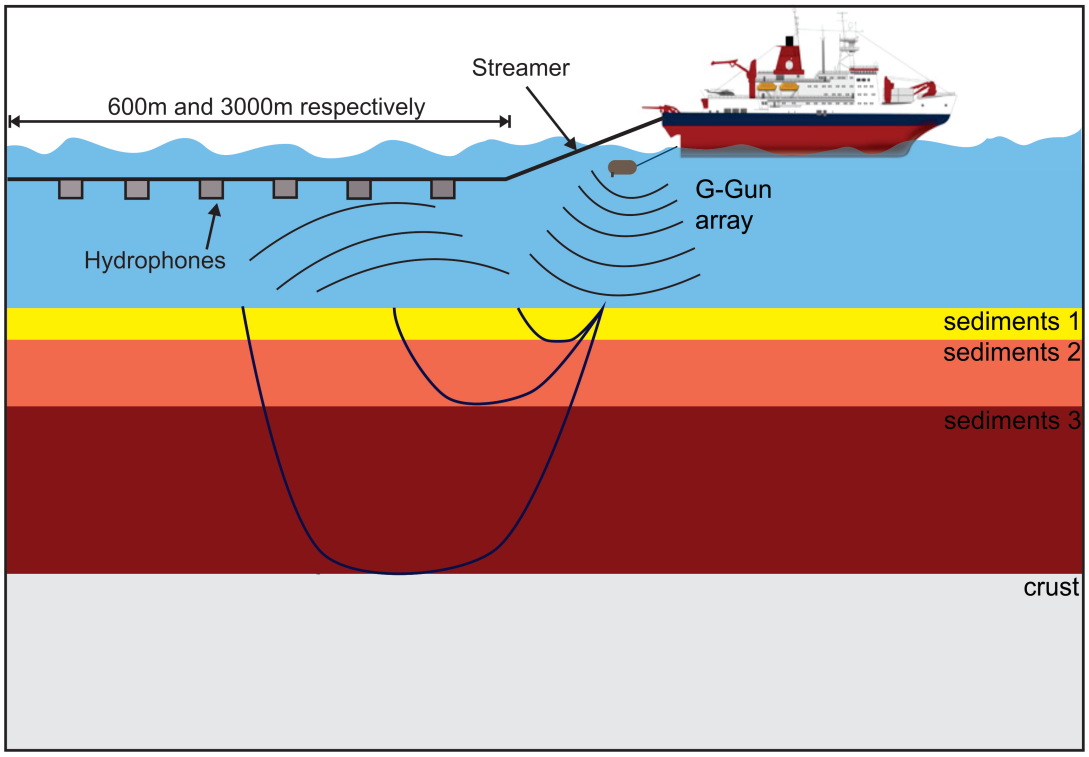

Figure 10: Principle of a seismic reflection experiment

During a seismic reflection survey, a long cable named a streamer is towed behind the vessel (Fig. 10). The data were recorded continuously on a harddisk and demultiplexed onboard afterwards. Parallel to data recording, a visual real time control is set up to check if all registration channels are active. At the end of a seismic survey, all data must be transfered to a PC and merged with the ships navigation information. This step is necessary to be able to set up the right geometry of the seismic survey. The streamer used during the expedition in 2006 was an analogue streamer with a length of 600 m and 96 active channels. The streamer used in 2010 was a 3 km long digital streamer with 240 channels online.

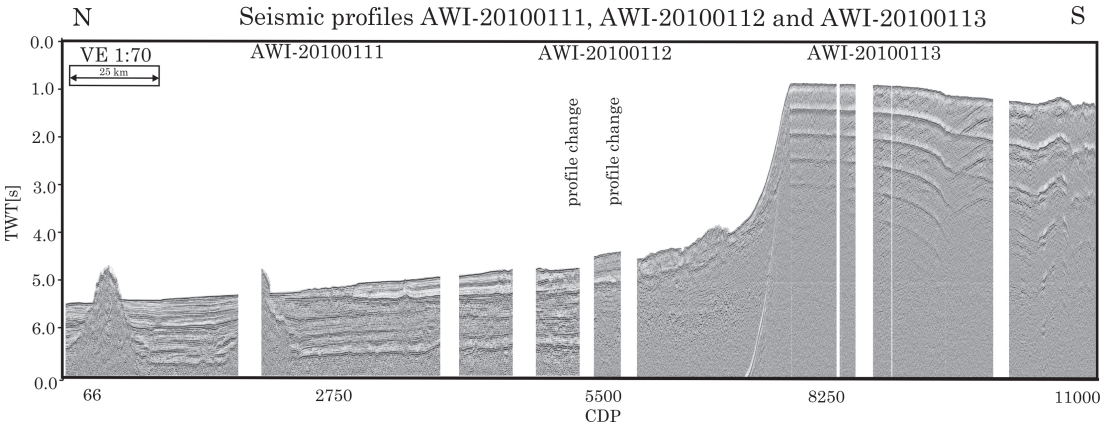

Figure 11: Example of seismic reflection data. The profile is a compilation of a seismic transect from the continental rise to the inner shelf of Wrigley Gulf off Hobbs Coast. Gaps in the data are airgun shutdowns due to sea-mammals. CDP distance: 25m.

Figure 11 shows the three seismic reflection profiles AWI-20100111-113 collected in Wrigley Gulf off Hobbs Coast in 2010. The profiles were combined to make a continental rise to shelf transect. A detailed description of the processing steps is documented in chapter 7 and in the flow-chart shown in figure 12.

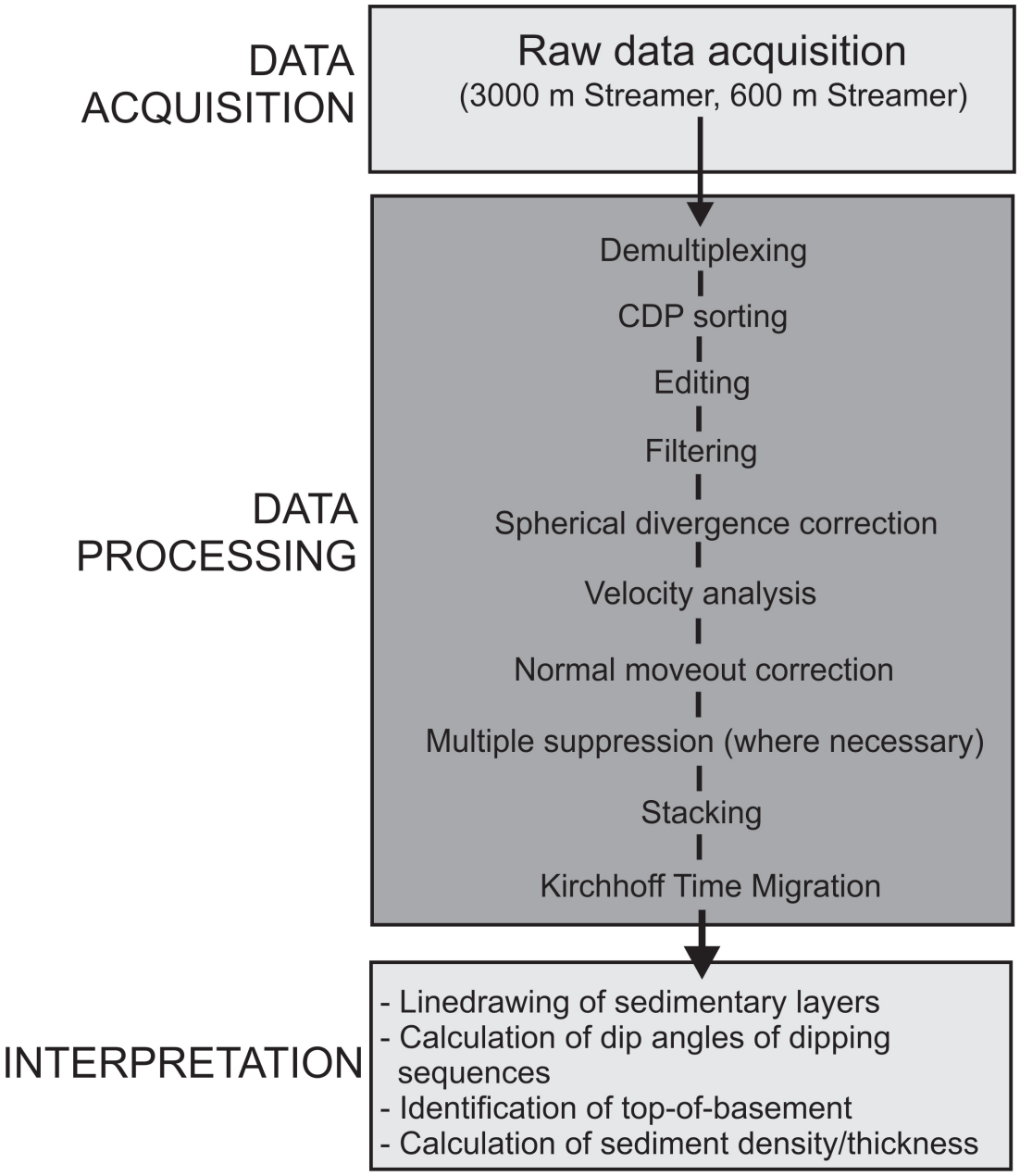

Figure 12: Flowchart of a seismic reflection experiment from data collection to interpretation.

2.2 Potential field data

Gravity and magnetic data are used to map the effects of density variations and magnetic susceptibility contrasts in the subsurface. Hence, potential field data are usefull to highlight rift structures, magmatic provinces and other products of tectono-magmatic processes. In combination with seismic measurements, which can be used as constraints for potential field modelling, the data can be interpreted in a regional geological context.

2.2.1 Gravity data

The recorded signal of the gravity effect of a mass anomaly in the subsurface is superposed by a suite of effects based on the registration method and the earth itself. Hence, a suite of corrections must be applied to the measured signal before it can be used further such as in spectral analysis, modelling and interpretation. In the next chapter, I briefly present these necessary correction steps.

Latitude correction:
The first correction which must be applied to the data is the latitude correction. The Earth is a rotational ellipsoid and therefore of non-spherical shape due to different angular velocities from the poles to the equator. The centripedal force causing different distances from the surface to the centre of the earth and hence, the gravity force to a body on the surface varies with the latitude on the surface of the Earth. To correct this effect from the data, I calculate the latitude effect by using the International Gravity Formula (IGF):

$$g = 978049(1 + 0.0052884 sin^2\Phi - 0.0000059 sin^2 2\Phi) \tag{2.1}$$

In this formula, Φ is the latitude. After that, I subtract the result from the ship-borne measurements.

Eötvös correction:

The next effect which influences the measurements is the Eötvös effect. This effect is the result of a moving platfrom (e.g. ship or aircraft) on a rotating earth and the relative movement of this platform to it. This effect is determined by the cruise speed v_s in knots [1 knot is around 1.85 km/h], the latitude Φ and the heading H by the formular:

$$g_E = 7.503 v_s cos\Phi sinH + 0.004 v^2 \tag{2.2}$$

Free-Air anomaly (FAA) and Bouguer anomaly (BA):

The next effect which must be taken into account is the effect of the topographic elevation of the surface of the earth. This correction is necessary because it compensates the topographic effect of the surface and projects the data onto mean sea-level. This so-called *Free-Air Correction* results in the FAA and is generally used in marine geophysics, where the gravity meter is near mean sea-level and all topographic highs (bathymetry) are below sea-level.

For regions above mean sea-level the BA is nothing else but the application of a Bouguer correction (BC) to the FAA, thus the effect of an additional mass which was substracted from the FAA:

$$\Delta g_B = \Delta g_{FAA} \tag{2.3}$$

with Δg_B = BA, Δg_{FAA} = Free-Air Anomaly and BC = Bouguer correction, where:

$$BC = 0.0419(\rho \times h) \tag{2.4}$$

In this formular ρ is the average density of the additional plate and h the thickness. In marine regimes, gravity is in general measured at mean sea-level. In the strict sense the BA and the FAA are equivalent, because the measurement hight of the gravity is already at mean sea-level.

In the case that h = 0 (mean sea-level), the equation is:

$$\Delta g_{BA} = \Delta g_{FAA} \tag{2.5}$$

However, the water density is significantly less than the underlying crust. Hence, it is possible to calculate the BA very easily. If water density and depth are known, the oceanic basin can be considered as a missing mass. To apply a BC, this mass deficit can be approximated by an infinite plate with the thickness of the water column (water depth). The plates density is therefore the difference density between the water density and the mean crustal density.

$$\Delta BC_O = 0.0419 - (\rho \times h) = 0.0419 - ((\rho_w - \rho_h) \times h_w) \tag{2.6}$$

Here BC_O is the Bouguer correction for marine regimes, ρ_w the water density, ρ_c the crustal density and h_w the observed water depth. If we set $\rho_w = 1030\ kg/m^3$ and $\rho_c = 2670\ kg/m^3$, the BC for marine regimes can be simplified to:

$$\Delta BC_O = 0.0419 - (-1640 kg/m^3) \times h_w = -(0.0687(mGal)/m) \times h_w \tag{2.7}$$

As mentioned above, BC must be substracted from the FAA. The formular for BA in marine regimes simplifies to:

$$\Delta g_B = \Delta g_{FA} - BC_0 \tag{2.8}$$

Finally, it is necessary to consider that BC_0 is a negative value. The satellite-derived Free-Air Anomaly (McAdoo and Laxon, 1997) and the derived Bouguer Anomaly are imaged in figure 13.

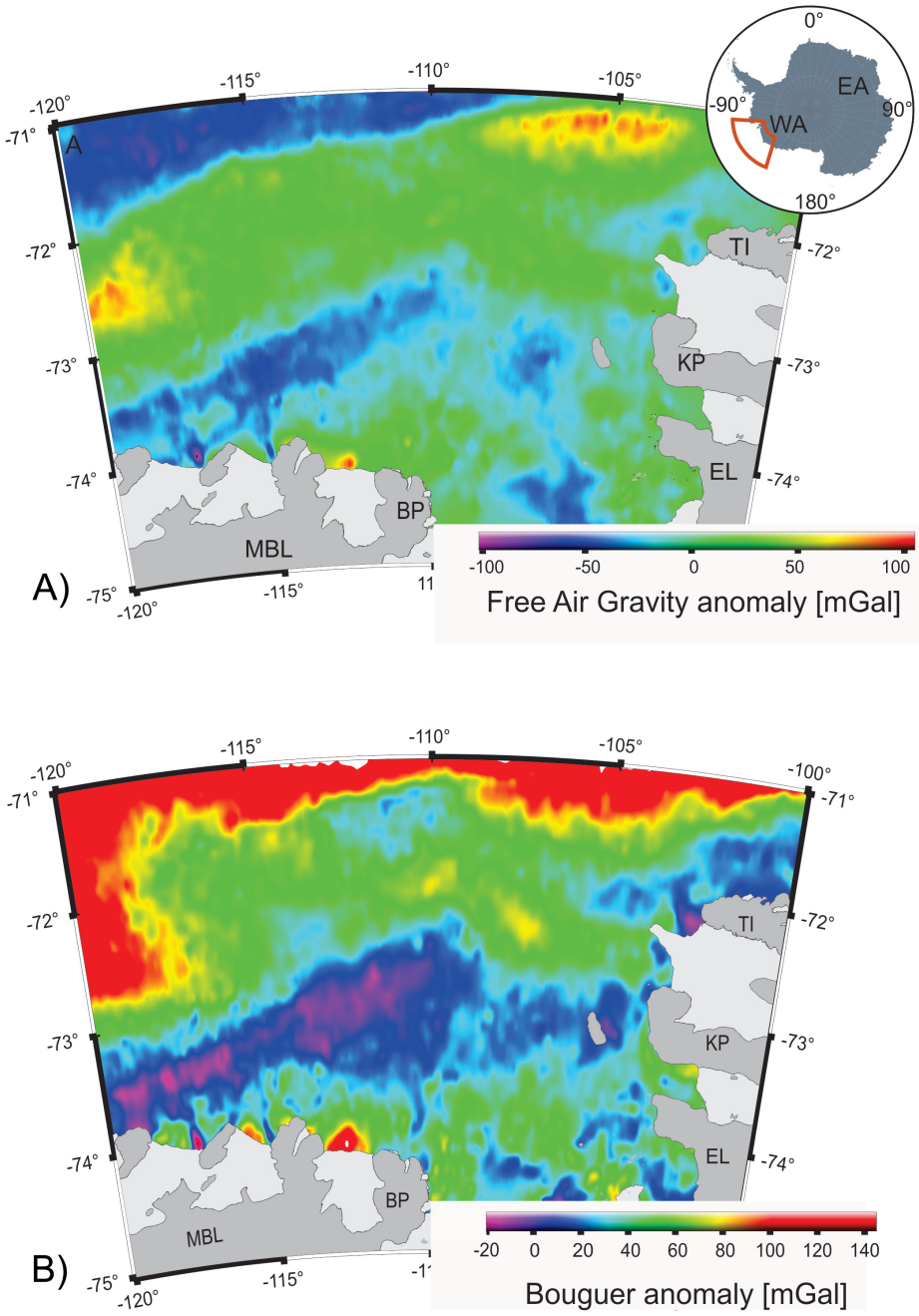

Figure 13: A) Satellite derived Free-Air anomaly in *mGal* (McAdoo and Laxon, 1997). B) Derived Bouguer anomaly in *mGal*. Abbreviations are: BP: Bear Peninsula, MBL: Marie Byrd Land, EL: Ellsworth Land, TI: Thurston Island, KP: King Peninsula.

2.2.2 Magnetic data

The magnetic data which I use in this study were also aquired during the two *RV Polarstern* expeditions ANT-XXIII/4 in 2006 and ANT-XXVI/3 in 2010. The data were collected with a Caesium-vapour magnetometer sensor towed by a 30 m long cable under a BO-105 Helicopter. Additionally, ship-borne magnetic data were continuously recorded with two 3-component fluxgate magnetometer sensors which are mounted on the crows nest. The profile grid of the magnetic measurements are shown in figure 14. A detailed description of the experiment, the processing steps and gridding is documented in the publication of Gohl et al. (2013a) and the cruise reports of the expeditions ANT-XXIII/4 in 2006 and ANT-XXVI/3 in 2010.

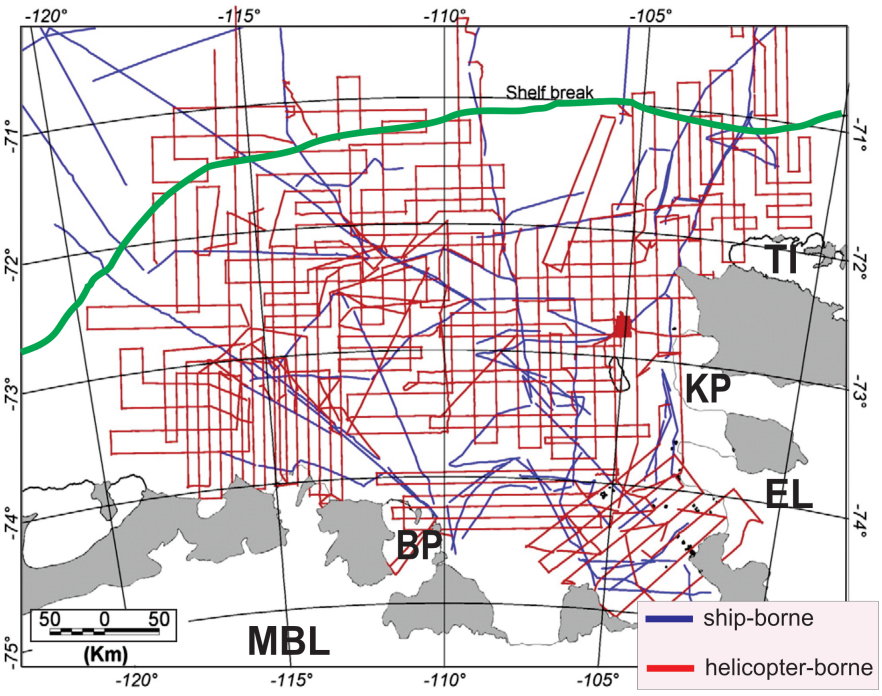

Figure 14: Map with combined helicopter-borne (red lines) and ship-borne (blue lines) magnetic tracks of both RV Polarstern expeditions in 2006 and 2010, which are included in the preparation of the magnetic anomaly grids. The irregular line geometry is due to opportunistic surveying. The green thick line shows the shelf break of the Amundsen Sea Embayment. MBL: Marie Byrd Land, BP: Bear Peninsula, KP: King Peninsula, EL: Ellsworth Land, TI: Thurston Island. Modified after Gohl et al. (2013a).

The magnetic anomaly grid of the Amundsen Sea Embayment (Gohl et al., 2013a) with a grid cell size of 5 km is shown in figure 15 and images clearly the dominance of long-wavelength anomalies over the middle and outer shelf. In contrast, the inner shelf of the ASE is dominated by short-wavelength anomalies.

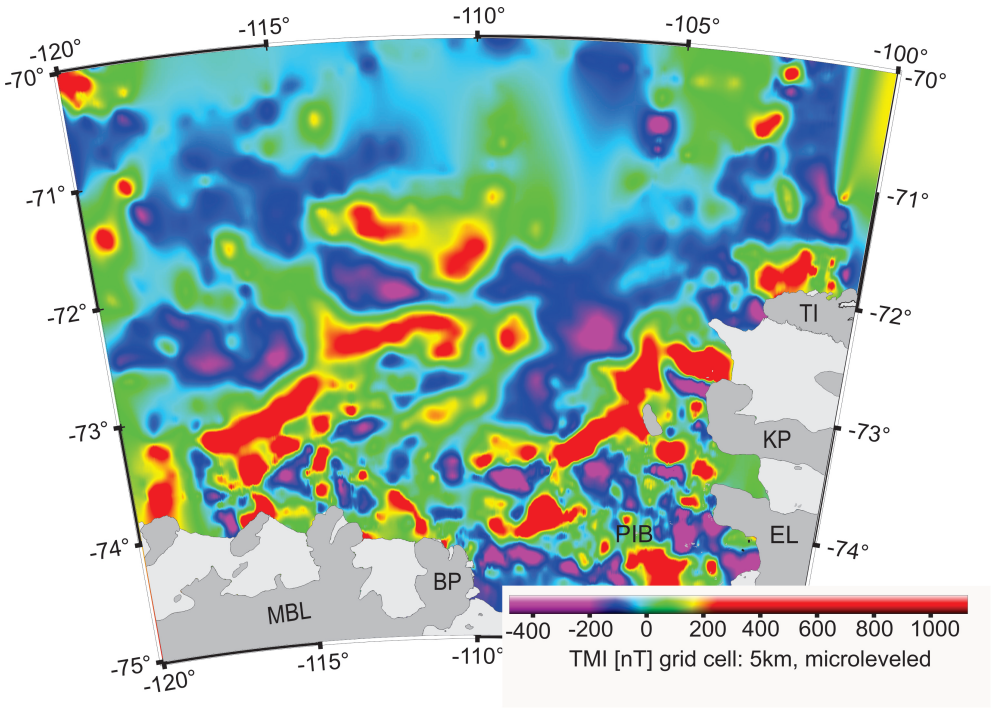

Figure 15: Map with major magnetic anomalies indicating magmatic and tectonic features (Gohl et al., 2013a). Abbreviations are: TMI: Total magnetic intensity, BP: Bear Peninsula, MBL: Marie Byrd Land, EL: Ellsworth Land, TI: Thurston Island, KP: King Peninsula, PIB: Pine Island Bay.

2.3 Spectral analysis

Spectral analysis of potential field data enables to estimate mass anomaly depths of layer boundaries in the subsurface of the earth. The method is based on calculation of the energy spectrum of a potential field to estimate the mean depth of layer boundaries of significant density contrast. The method was initially developed for magnetic data (Spector and Grant, 1970) and was updated for gravimetric data (Dorman and Lewis, 1970; Karner and Watts, 1983). In the following, I present the derivation of Karner and Watts (1983).

The method requires nearly horizontal bounding layers with significant density contrast $\Delta\rho$ in a mean depth d and can be desribed by a laterally varying relief

$t(x)$ (Fig.16).

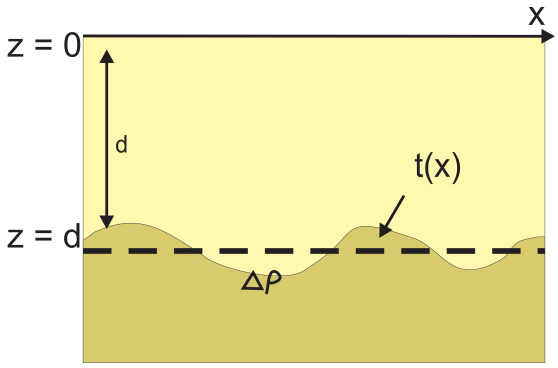

Figure 16: Schematic vertical layer of the crust

.

The boundary between the two layers has a subsurface topography $t(x)$ in a mean depth d. The density contrast at this boundary is $\Delta\rho$ (Fig. 16). The calculation of the gravimetric effect $\gamma(x)$ of the boundary then results from a Fourier Transformation of $\gamma(x)$ to $\Gamma(k)$ and $T(k)$. The gravity effect of the density contrast at the surface ($d = 0$) is:

$$\Gamma(k) = 2\pi G \Delta\rho e^{-kd} T(k) \tag{2.9}$$

In this equation k defines the wavenumber and G the gravity constant. The equation represents the first order derivation of the Taylor series in the spectrum space and bases on the calculation of the gravity effect of undulating layers in the subsurface after Parker (1972). The multiplication with e^{-kd} results in an upward field continuation of the gravity effect of a mass anomaly in the subsurface to the surface. The energy spectrum $\Gamma(k)$ is then the square of the amplitude spectrum of equation 2.9 (e.g. Buttkus, 2000):

$$|\Gamma(k)|^2 = 4\pi G^2 \left|\Delta\rho^2 e^{-2kd} T(k)\right|^2 \tag{2.10}$$

This equation decribes the energy spectrum of the gravity effect of a single layer in the subsurface. Karner and Watts (1983) used a statistical approach to derive

the energy spectrum from equation (2.10). They considered that the boundary in the subsurface as an amount of several mass anomaly bodies which are distributed over a depth range $d \pm \Delta d$. The Energy spectrum of these bodies is then defined as mean energy spectrum $\langle |\Gamma(k)^2| \rangle$ which requires that $\Delta\rho$, d and $T(k)$ are linearly independent in the vector space.

$$|\Gamma(k)|^2 = 4\pi G^2 \Delta\rho^2 e^{-2kd} |T(k)|^2 \tag{2.11}$$

The exponential term in equation 2.11 can be written as:

$$e^{-2kd} = \frac{sinh(2k\Delta d)}{k} e^{-2k\bar{d}} \tag{2.12}$$

In this equation $\bar{d}$ represents the mean depth of the mass anomaly. Applying the logarithm on both sides of equation 2.12 reveals a quasi-linear relationship between the natural logarithm of the mean energy spectrum and the wavenumber.

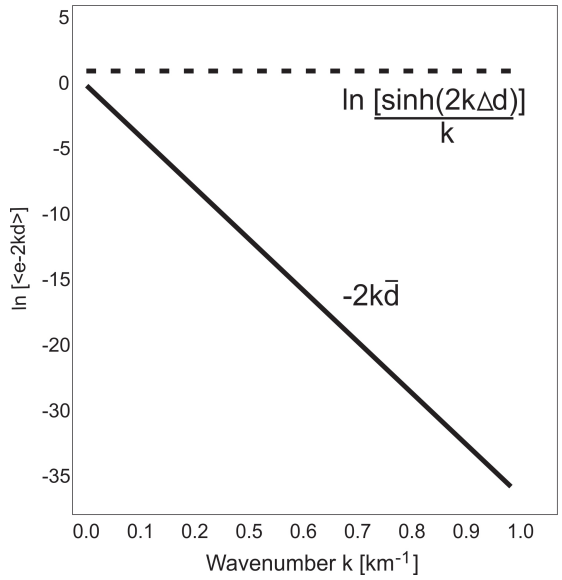

Figure 17: Influence of the different terms in equation 2.12

For my model calculation, I assume a mean mass anomaly depth of 25 km and a subsurface topography undulation of 12.5 km. The second part $ln\left[\frac{sinh(2k)}{k} e^{-2k\bar{d}}\right]$ is constant (Fig. 17)

2.4 Potential field modelling

Potential field modelling has been a standard technique in geophysics for several decades. In general, forward modelling refers to the process of calculating a model response given from a physical model. The aim of potential field modelling is to set profile-based or area-based geophysical data into a regional geological context. The goal of potential-field data is to provide contraints on the distribution of geological rock properties in the subsurface. Magnetic data for example are typically useable in regions where metamorphic and igneous rocks are common and they have proven vital for understanding the structure and age of the subsurface. The interpretation of potential field data, regardless if gravity or magnetic, is highly ambiguous. L. L. Nettleton emphased in 1942:

Unless certain controls other than the gravity and magnetic data are available, the inherent ambiguties of the physically possible distribution of material which can produce the observed effects make accurate calculations meaningless even though the geophysical data may be of any desired precision.

Therefore it is indispensable to include additional informations to constrain the model. For a better understanding which contraints can be placed, I briefly consider the geological controls on these contraints.

In gravity and magnetic modelling, three geophysical rock parameters control the model: 1st.: The density, 2nd.: The magnetic susceptibilty and 3rd.: The remanent magnetisation. These parameters are controlled by the original lithology, the metamorphic and metasomatic mineral assemblages and the structural evolution. After Clark (1997), the lithology controls the density and magnetic properties via the mineralogy. In other words, individual lithologies may comprise a remanent or anisotropic magnetisation that can also be affected by metasomatism or de-

formation. Metasomatism and metamorphism alter the mineralogy regionally or locally. Finally, tectonic and tectono-magmatic processes change the position and orientation of rocks and hence, influence the strucutral evolution of the area. The combination of all three factors lead to the predefined geophysical rock properties.

For potential field modelling, I use the software IGMAS (Götze et al., 1988). To calculate the gravity or magnetic effect of a subsurface body such as an intrusion, the IGMAS algorithm uses triangulated polyhedra built from a set of polygons which were orientated in parallel vertical cross sections. The triangulation between these vertical planes (Fig. 18 and Fig. 22) is done automatically during the modelling procedure.

2.4.1 Gravity modelling

To set-up a starting model, I use all results described above and in chapters 4, 5 and 6 to constraint the model geometries. Afterwards, I define the density of each layer and mass anomaly body in the starting model. Furthermore, as measured P-wave velocities in the crust and the sediments are available, a relationship between the velocity and the density is needed. However, many velocity-density relationships have been presented by different authors for sedimentary, igneous, magmatic and metamorphic rocks (e.g. Nafe and Drake, 1963; Barton et al., 1986; Christensen and Mooney, 1995). I use the velocity-depth distribution of Barton et al. (1986) to calculate sediment and crustal densities.

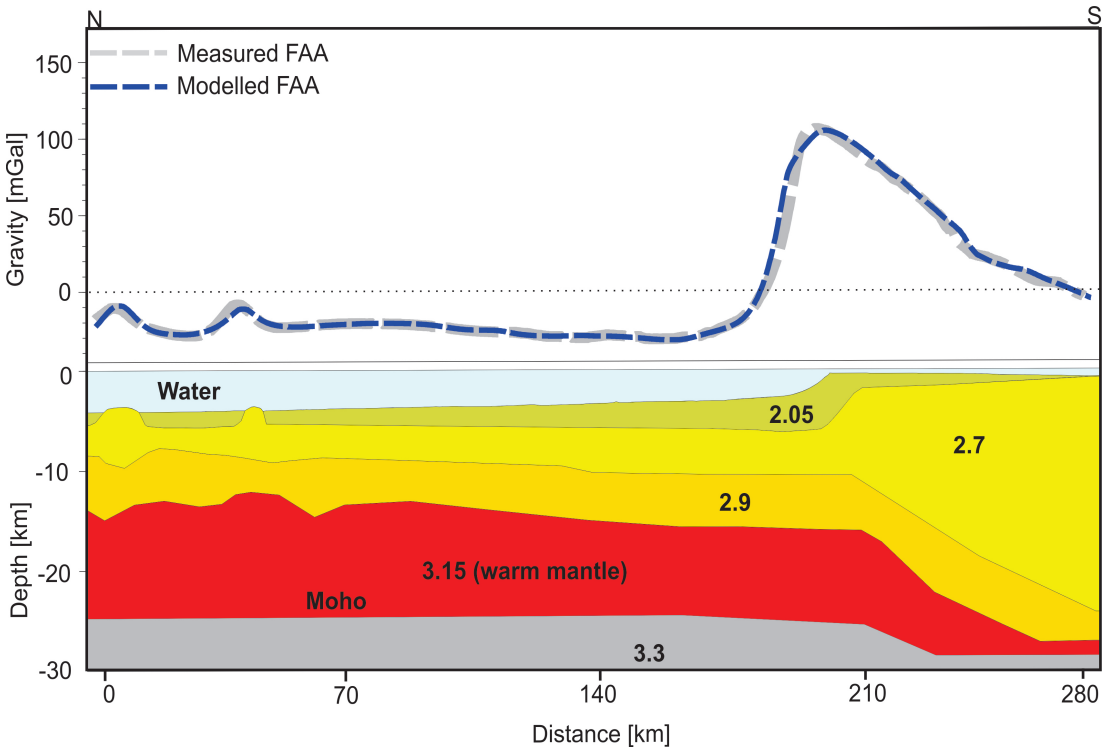

Figure 18: Example layer of a 2D gravity model. Densities are given in $10^3 kg/m^3$.

2.4.2 Magnetic modelling

For magnetic modelling (Fig. 22), knowledge of the magnetic inclination, the magnetic declination and the background reference field is necessary (Götze et al., 1988). The used background reference field of 52000 nT (Fig. 19), the magnetic declination of 30° (Fig. 20) and the inclination of -65° (Fig. 21) were derived from Maus et al. (2010). Further, I use depth estimates based on spectral analysis of the magnetic anomaly data to constraint an initial 3D magnetic anomaly model (see chapter 5). Finally, I use results of an Euler deconvolution (Gohl et al., 2013a) to locate the tops and edges of magnetic bodies in the subsurface.

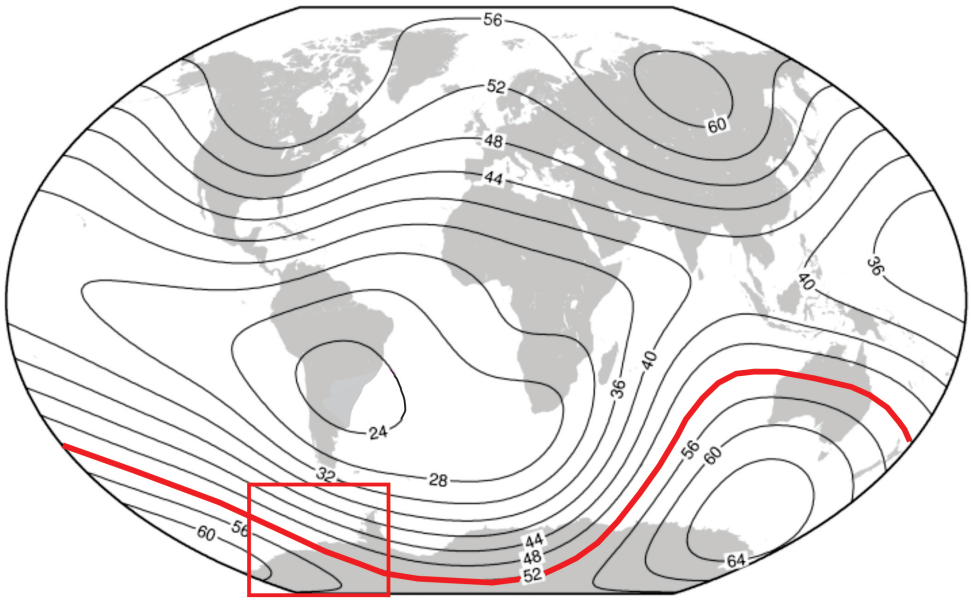

Figure 19: Total magnetic background field in 2010 after Maus et al. (2010). Values are given in 10^3 nT. Red frame marks the area of interest.

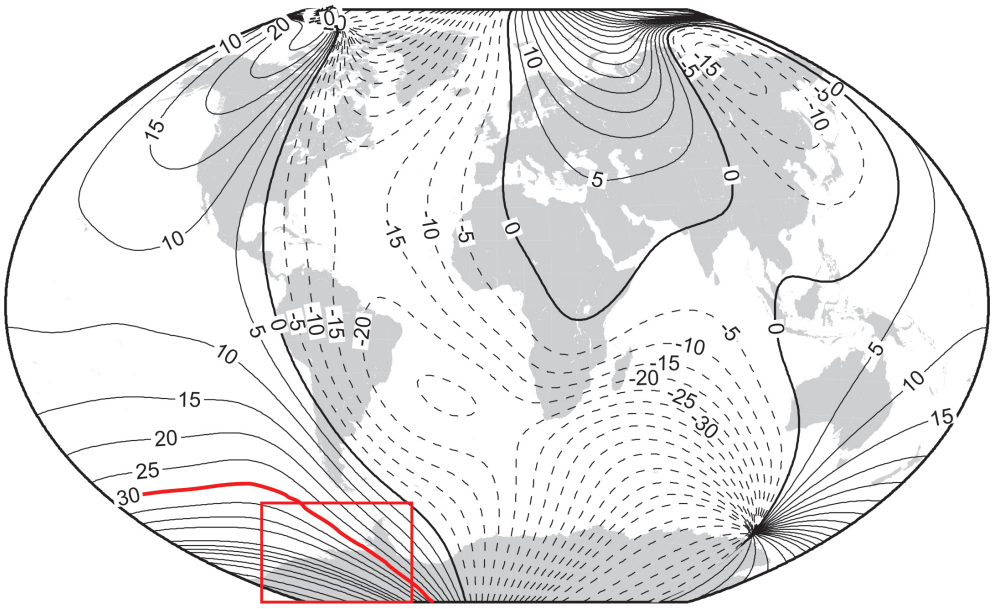

Figure 20: Magnetic declination in 2010 after Maus et al. (2010). Values are given in degree [°]. Red frame marks the area of interest.

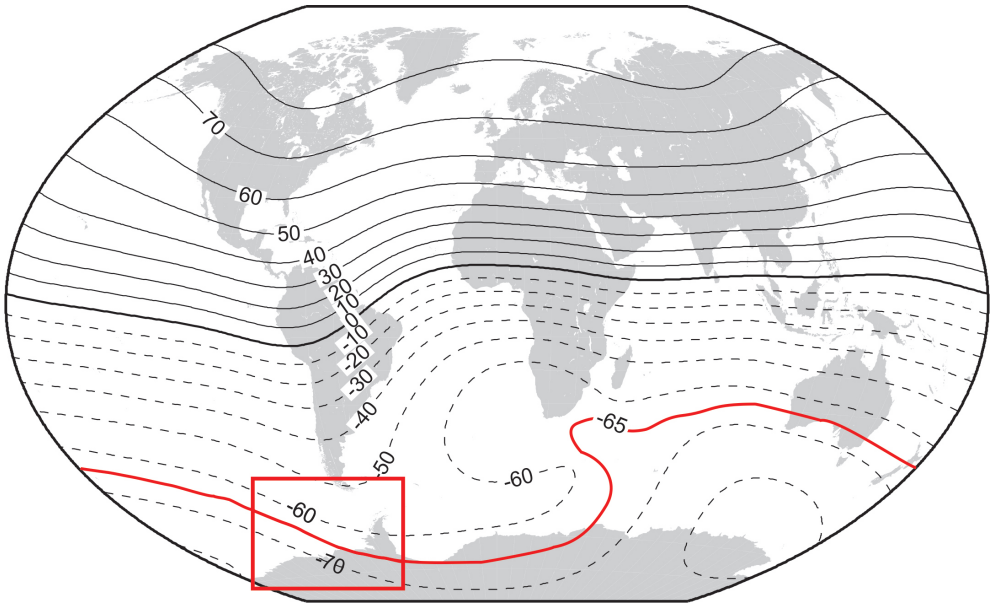

Figure 21: Magnetic inclination in 2010 after Maus et al. (2010). Values are given in degree [°]. Red frame marks the area of interest.

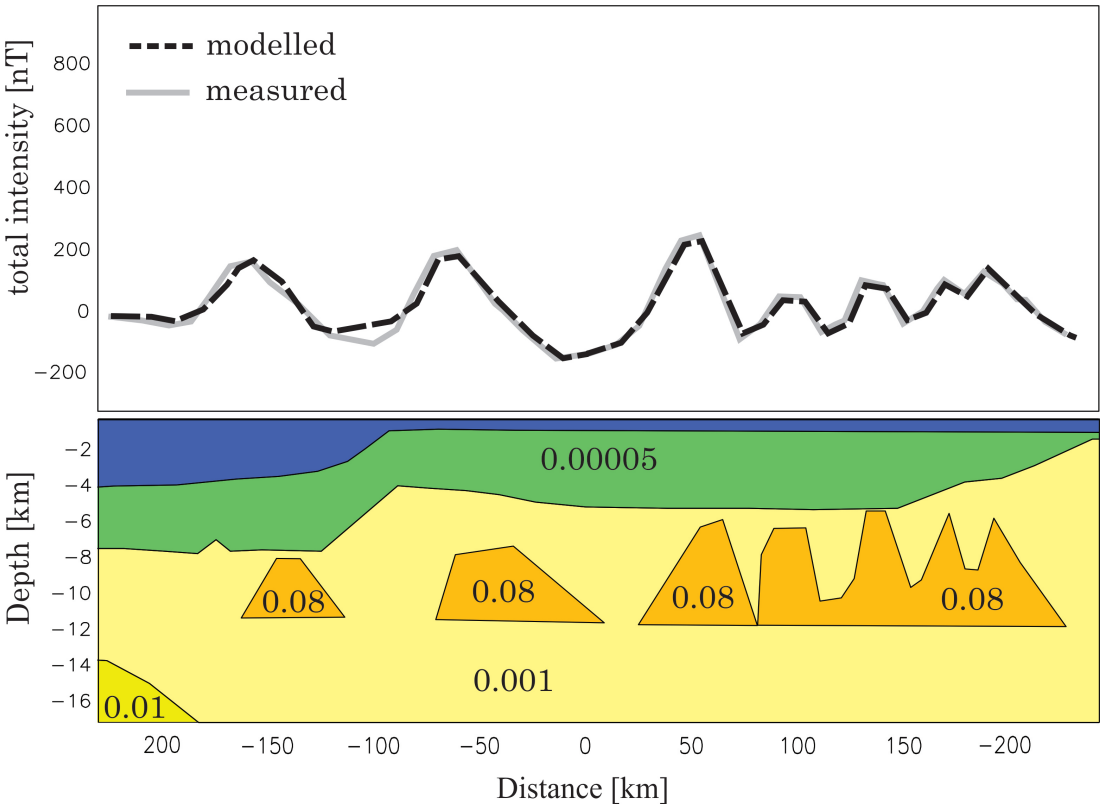

Figure 22: Example layer of a 2D magnetic model. Susceptibility values are given in SI.

2.5 Elastic thickness estimation

An additional parameter which characterizes the nature and evolution of the lithosphere is the effective elastic thickness (Te). The parameter Te can be used to give an idea of the so-called lithospheric rigidity of the lithosphere. The flexural rigidity of the crust is an important parameter in the reconstruction of the formation history of basins, as it controls the subsidence in response to topographic load. I calculate Te via the flexural response of the lithosphere to sedimentary or topographic loading under the assumption that it behaves like an elastic plate with the thickness Te in (Watts, 2001).

However, as temperature is considered to be a controlling parameter on lithospheric strength, the flexural rigidity of the lithosphere might be expected to increase with time since rifting of part of the lithosphere and so can be used to determine the rifting process. For example, young rifts such as the East African or Ethiopian rifts (e.g. Pérez-Gussinyé et al., 2009) are characterized by a marginal elastic thickness (0-10 km).

I used the software LITHOFLEX to obtain an estimate of flexural rigidity in the ASE (Braitenberg et al., 2007). A detailed describtion of the software is given in the publication of Braitenberg et al. (2007) and in chapter 5. The software uses the convolution approach with analytical flexure response functions (Wienecke et al., 2007) or a numerical approach (Braitenberg et al., 2002). I invert the flexural rigidity of the lithosphere of the ASE in order to match the known loads derived from seismic reflection measurements with the crustal thickness model derived from forward gravity modelling. By this procedure, it is possible to divide the lithosphere into different tectonic areas such as rift-related structures or rift systems.

3 Contributions to Scientific Journals

The crustal structure and tectonic development of the continental margin of the Amundsen Sea Embayment, West Antarctica: Implications from geophysical data

Thomas Kalberg and Karsten Gohl

Geophysical Journal International (2014), **198**(1), p.327-341
doi: 10.1093/gji/ggu118

In this paper, we present a P-wave velocity-depth model and two distinct 2D density-depth models along with multichannel seismic reflection data collected in the Amundsen Sea Embayment. The models show that the crust of the embayment is stretched and of continental affinity of about 10-14 km thickness at the continental rise which thickens up to as much as 28 km beneath the inner shelf. We interpret the homogenous crustal architecture of the continental rise, including horst and graben structures as an indication for that wide-mode rifting affected the entire region. A high-velocity layer of variable thickness beneath the margin conicides with a proposed magma flow along the base of the crust from beneath eastern Marie Byrd Land to the Marie Byrd Seamounts. Seaward-dipping reflectors indicate some degree of volcanism in the area after break-up. Gravity anomaly data indicate several phases of fully developed and failed rift systems, including a possible branch of the West Antarctic Rift System.

I calculated the P-wave velocity and the 2D gravity models and I wrote the manuscript. Karsten Gohl supervised the work and was the Chief Scientist during the expeditions ANT-XXIII/4 in 2006 to the Bellingshausen and Amundsen Sea and ANT-XXVI/3 in 2010 again into the Amundsen Sea Embayment.

Rift processes and crustal structure of the Amundsen Sea Embayment, West Antarctica, from 3D potential field modelling

Thomas Kalberg, Karsten Gohl, Graeme Eagles and Cornelia Spiegel
Submitted to Marine Geophysical Research (2015)

We present a 3D gravity and a 3D magnetic model of the Amundsen Sea Embayment based on satellite derived free-air gravity anomaly and a compiled magnetic grid. Further, we present results of an effective elastic thickness estimation of the crust in the Amundsen Sea Embayment. Together with crustal thickness estimated based on power spectral analysis of the gravity and magnetic data, we used a set of seismic reflection profiles in the embayment as constraints for the potential field modelling. The results of modelling were used to derive maps of the sediment thickness, the basement structure and the Moho. The models reveal several tectonic lineaments and shows rift basins within the middle and inner shelf of the Amundsen Sea Embayment. Estimates of the elastic lithospheric thickness provide further constraints on the geodynamic and tectono-magmatic evolution of the Amundsen Sea Embayment.

I calculated the 3D gravity and the 3D magnetic model. Further, I calculated the spectral analysis and the flexural rigidity and I wrote the manuscript. Karsten Gohl, Graeme Eagles and Cornelia Spiegel supervised the work. Karsten Gohl was the Chief Scientist during the exepeditions ANT-XXIII/4 in 2006 to the Bellingshausen and Amundsen Sea and ANT-XXVI/3 in 2010 again into the Amundsen Sea Embayment.

Crustal structure and sedimentary architecture in Wrigley Gulf / Marie Byrd Land, West Antarctica: Implications for the tectonic evolution and environmental changes from geophysical observations

Thomas Kalberg and Karsten Gohl

To be submitted to Marine Geophysical Research (2015)

A seismic reflection transect from the continental rise onto the shelf in Wrigley Gulf off Hobbs Coast was used to image the sedimentary architecture and the basement morphology offshore western Marie Byrd Land. Together with seismic data from the neighbouring western Amundsen Sea Embayment, the eastern Ross Sea and onshore receiver function results south of central Marie Byrd Land, we calculated 4 distinct 2D gravity models based on ship-borne free-air gravity data along the seismic transect. The data infer Pratt-type compensated stretched continental or transitional crust which is underlain by a low-density upper mantle. A near sea- level break-up between New Zealand and West Antarctica and uplift of Marie Byrd Land thereafter is probable. Furthermore, the seismic reflection data from the continental rise and the inner shelf image changes in the reflection character which in turn represent changing environmental conditions during deposition and episodes of alternating major ice sheet advance and retreat that can be correlated to environmental changes.

I processed and interpreted the seismic reflection profile, the 2D gravity models and I wrote the manuscript. Karsten Gohl supervised the work and was the Chief Scientist during the exepedition ANT-XXVI/3 in 2010 into the Amundsen Sea Embayment.

4 The crustal structure and tectonic development of the continental margin of the Amundsen Sea Embayment

Thomas Kalberg and Karsten Gohl

Dept. of Geosciences

Alfred Wegener Institute Helmholtz-Centre for Polar and Marine Research

Am Alten Hafen 26

27580 Bremerhaven

submitted to Geophysical Journal Internationalat 19th June 2013

accepted at 23th March 2014

published at 20th May 2014

4.1 Summary

The Amundsen Sea Embayment of West Antarctica represents a key component in the tectonic history of Antarctic-New Zealand continental break-up. The region played a major role in the plate-kinematic development of the southern Pacific from the inferred collision of the Hikurangi Plateau with the Gondwana subduction margin at approximately 110-100 Ma to the evolution of the West Antarctic Rift System. However, little is known about the crustal architecture and the tectonic processes creating the embayment. During two RV Polarstern expeditions in 2006 and 2010 a large geophysical dataset was collected consisting of seismic- refraction and reflection data, ship-borne gravity and helicopter-borne magnetic measurements.

Two P-wave velocity-depth models based on forward travel-time modelling of nine ocean bottom hydrophone recordings provide an insight into the lithospheric structure beneath the Amundsen Sea Embayment. seismic reflection data image the sedimentary architecture and the top-of-basement. The seismic data provide constraints for 2D gravity modelling, which supports and complements P-wave modelling. Our final model shows 10 - 14 km thick stretched continental crust at the continental rise that thickens to as much as 28 km beneath the inner shelf. The homogenous crustal architecture of the continental rise, including horst and graben structures are interpreted as indicating that wide-mode rifting affected the entire region.

We observe a high-velocity layer of variable thickness beneath the margin and related it, contrary to other "normal volcanic type margins", to a proposed magma flow along the base of the crust from beneath eastern Marie Byrd Land - West Antarctica to the Marie Byrd Seamount province. Furthermore, we discuss the possibility of upper mantle serpentinization by seawater penetration at the Marie

Byrd Seamount province. Hints of seaward-dipping reflectors indicate some degree of volcanism in the area after break-up. A set of gravity anomaly data indicate several phases of fully developed and failed rift systems, including a possible branch of the West Antarctic Rift System in the Amundsen Sea Embayment.

4.2 Introduction

Studying the lithospheric architecture of the Amundsen Sea Embayment (ASE) of West Antarctica (Fig. 23) provides constraints on tectono-magmatic reconstructions of the West Antarctic continental margin and the embayment itself from Paleozoic to Cenozoic times. Improved knowledge of the structure and development of the lithosphere is the key to unravelling the evolution of the West Antarctic continental margin and the corresponding landscapes. The area experienced a number of key events during the tectonic history of the southern Pacific, including the inferred collision of the Hikurangi Plateau with the Gondwana at approximately 110 - 100 Ma subduction margin (Davy and Wood, 1994; Mortimer et al., 2006) to the evolution of the West Antarctic Rift System.

A number of plate-kinematic reconstructions are centred on the region, most recently by Eagles et al. (2004a) and Wobbe et al. (2012), but suffer from a lack of information about the deep crustal structure of the West Antarctic continental margin. The ASE also experienced a number of magmatic events from mid-Mesozoic to Late Cenozoic times (Wobbe et al., 2012). Analysis and modelling of magnetic data provides a first insight into the basement structure of the ASE shelf and implies that the present day basement morphology of the ASE shelf may control the dynamic behaviour of grounded parts of the West Antarctic Ice Sheet (WAIS) (Gohl 2012, Gohl et al., 2013a). An improved understanding of the tectono-magmatic processes and of the formation of basement ridges and sedimentary basins provides further constraints on paleo and modern ice sheet

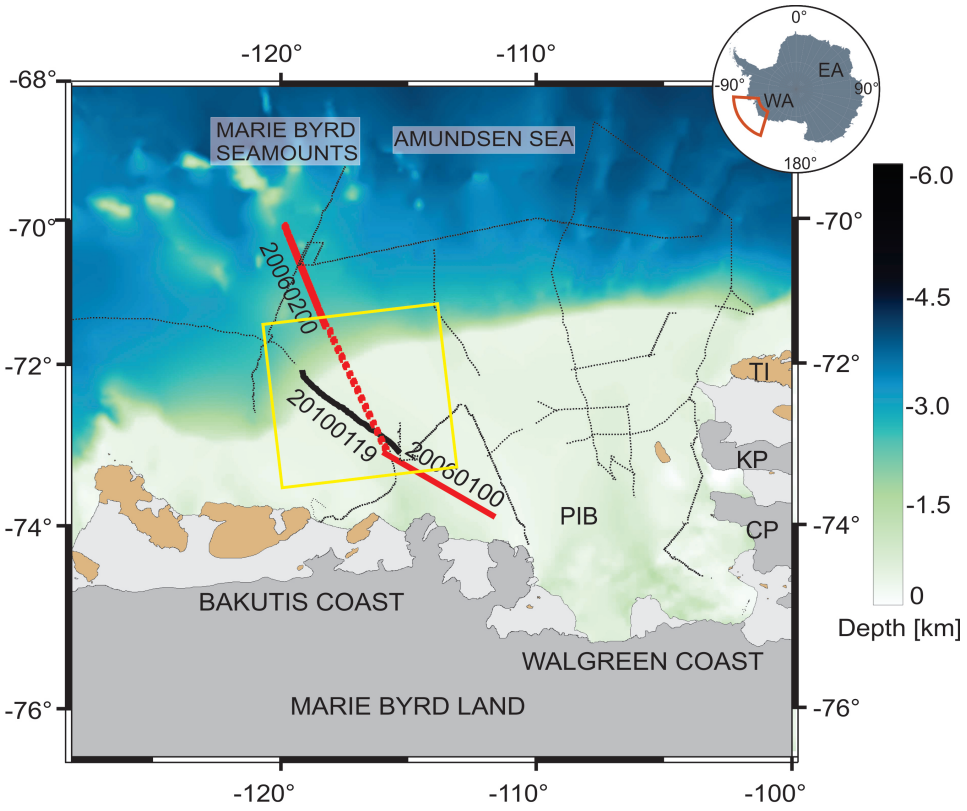

Figure 23: Bathymetric map of the Amundsen Sea Embayment after Nitsche et al. (2013) showing the locations of two OBH profiles and corresponding multi-channel seismic reflection profiles (thick black lines). The red dashed line marks the interpolated profile AWI-100/200, connecting the profiles AWI-20060100 and AWI-20060200. Thin dotted black lines mark other seismic reflection profiles. The thin yellow frame shows the window which was used for the spectral analysis. TI is Thurston Island, PIB is Pine Island Bay, KP is King Peninsula, CP is Canisteo Peninsula.

dynamics as demonstrated in Bingham et al. (2012) or Smith et al. (2013).

This study presents a combination of geophysical data from the ASE, which were collected to study the lithospheric architecture and tectono-magmatic evolution of the West Antarctic continental margin. At first, we present and highlight the results of each individual dataset. A continental rise-to-shelf seismic reflection transect provides constraints on the top- of-basement morphology and sedimentary architecture of the margin. Two deep crustal seismic refraction and wide-angle reflection profiles are used to derive velocity-depth profiles. Supported by a spectral analysis of gravity data, two different continuous 2D forward gravity models place constraints on the crustal architecture and formation of the continental margin and shelf of the ASE.

Following this, we propose a new integrated model of the tectonic evolution of the margin of the ASE. With this model we attempt to reconstruct the tectono-magmatic development of this margin from its break-up from New-Zealand as early as 90 Ma (Wobbe et al., 2012) to the Present which further supports boundary conditions for ice-sheet modelling attempts in this part of West Antarctica.

4.3 Tectonic and geological background

The tectonic development of the Pacific margin of West Antarctica since Late Cretaceous times consisted of several distinct phases (Fig. 24). The southwestward propagation of rifting and break-up began with the separation of Chatham Rise from the Amundsen Sea margin of eastern Marie Byrd Land as early as 90 Ma and continued around 83 Ma with the break-up of Campbell Plateau from central Marie Byrd Land (e.g. Mayes et al., 1990; Bradshaw et al., 1991; Larter et al., 2001; Eagles et al., 2004a, Wobbe et al., 2012).

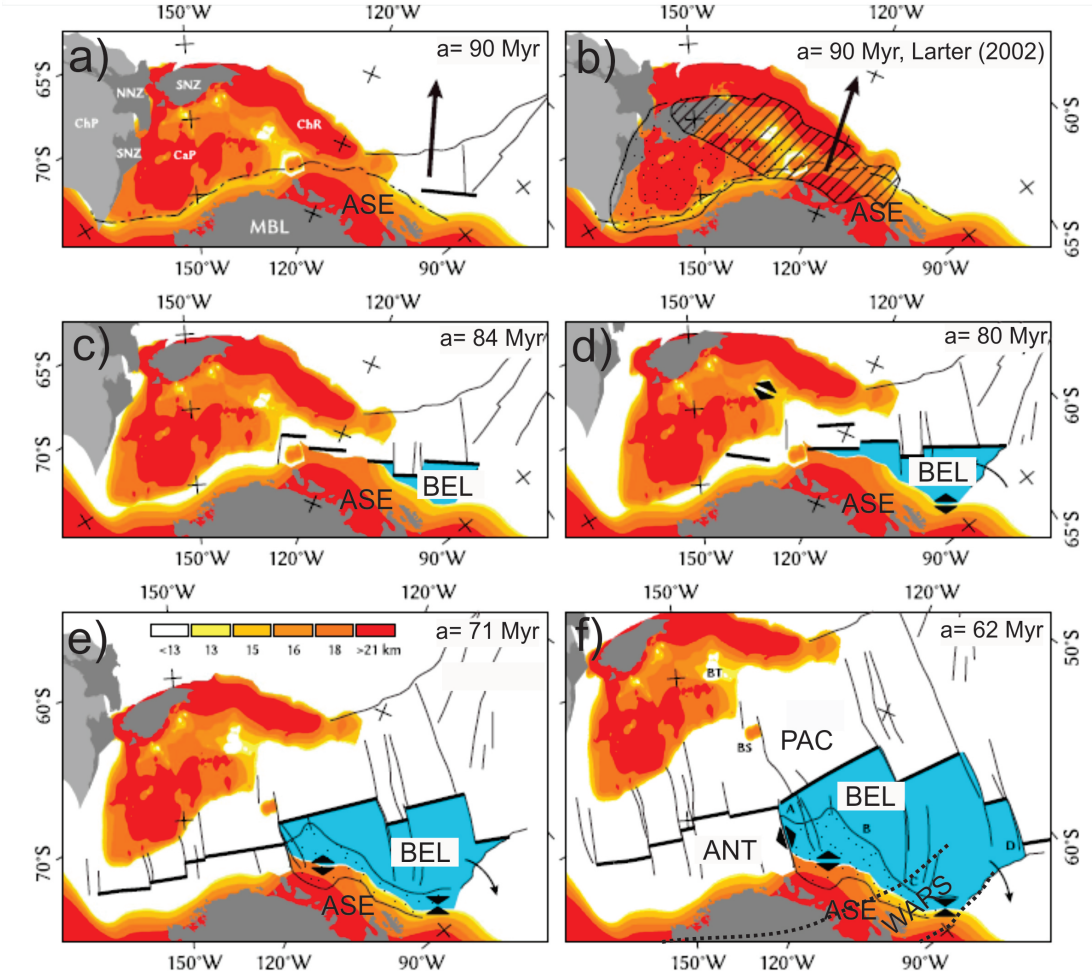

Figure 24: Pre-rift reconstruction model of distinct tectonic phases from the late Cretaceous to early Paleocene of the Amundsen Sea Embayment including Chatham Rise (striated) and Campbell Plateau (stippled) modified after Wobbe et al. (2012) (Fig. 24 a, c-f) using the rotation parameters of Wobbe et al. (2012) and Grobys et al. (2008). Fig. 24b shows configuration using the rotation parameters from Larter et al. (2002). The black arrows in Figure 24a and 24b show the direction of movement of the Bellingshausen Plate. Thin black lines show fracture zones, thick black lines show mid ocean ridge segments. Thin black dashed line show suspected rift arm of the West Antarctic Rift System. Stippled area in Fig. 24e and 24f shows oceanic crust which was formed along the Bellingshausen Plate margin. The colour scale in Fig. 24e shows the crustal thickness after modelling results of Wobbe et al. (2012)

From about 80 Ma, the Bellingshausen Plate started acting as an independently rotating plate, and continued to do so until about 61 Ma (e.g. Larter et al., 2002; Eagles et al., 2004a, b). Its incorporation into the Antarctic Plate occurred as part of a major plate reorganisation in the South Pacific (Cande et al., 2000). Kipf et al. (2014) postulated that at around 65-56 Ma, the Marie Byrd Seamounts were formed from magmatic material that was transported from beneath the West Antarctic continental crust by a so-called continental insulation flow.

The eastern shelf, which contains Pine Island Bay, has been suggested by Dalziel and Elliot (1982), Storey (1991) and Grunow et al. (1991) as the site of a Paleozoic-Mesozoic crustal boundary zone between the Marie Byrd Land block in the west and the Thurston Island crustal block in the east, whose apparent paleomagnetic polar wander paths differ.Recent analysis of magnetic and seismic data from the ASE shelf show that tectonic lineaments and sedimentary sub-basins cross the shelf of which some may be related to a branch of the eastern West Antarctic Rift System (Gohl et al., 2013a, b). Apatite-He age trends, derived from rock samples of the eastern Pine Island Bay, infer rift-related block faulting indicating that the present glacially formed Pine Island Trough may have originated from tectonic activity as part of the West Antarctic Rift System (Lindow et al., 2011). Different thermal signatures of the Mt. Murphy area and its neighbouring areas indicate a major fault system which was active during or after Oligocene (Lindow et al., 2011).

Latest geological studies in Marie Byrd Land show Cretaceous multistage rifting phases and strike slip faulting superimposed by transtension (Siddoway, 2008). Gravity data, receiver-function analysis of teleseismic earthquakes and geological analysis suggest that the submarine plateaus of New Zealand and conjugate Marie Byrd Land consist both of thinned continental crust of only 25-28 km thickness (Llubes et al., 2003; Luyendyk et al., 2003; Winberry and Anandakrishnan, 2004;

Grobys et al., 2009). In the ASE, gravity modelling showed the crust of the inner to middle shelf to be of 24 to 28 km thickness. Moreover, it seems that the ASE was affected by magmatic intrusions interpreted from distinct zones of anomaly patterns and lineaments which can be associated with three major tectonic phases (Gohl et al., 2007, 2013a, b).

Jordan et al. (2010) calculated a Moho depth of about 19 km under the Byrd Subglacial Basin and the newly identified Pine Island Rift based on gravity inversion. Additionally, Bingham et al. (2012) also inferred crustal thinning leading to 25-21 km thick crust beneath the Ferrigno rift and the adjacent Siple Trough region.

4.4 Seismic experiment

The seismic dataset presented in this study consist of two deep-crustal seismic refraction profiles and a suite of multichannel seismic reflection profiles (Fig. 23), that were acquired during RV Polarstern expeditions ANT-XXIII/4 in 2006 and ANTXXVI/3 in 2010. The seismic source used for both refraction and reflection recordings of the profiles AWI-20060100 and AWI-20060200 consisted of 8 G-Guns (68.2 liters in total) and a Bolt air gun (32 liters). The shot interval of 60 s corresponded to an average shot spacing of 150 m. Additionally, seismic reflection profile AWI-20100119 was acquired with 3 GI-Guns, fired every 10 s (Gohl et al., 2013b). The multi-beam bathymetry was measured with the Hydrosweep DS-III system.

4.4.1 Seismic reflection data

We mapped the top-of-basement along the refraction profiles AWI-20060100 and AWI-20060200, in coincident seismic reflection data (Fig. 25). These were acquired by using a 600 m long analogue streamer with 96 channels. The data were recorded with a sampling interval of 4 ms. The data gap between the seismic reflection profiles AWI-20060100 and AWI-20060200 (Fig. 25) was bridged with the nearest seismic reflection profile AWI-20100119 (Fig. 25) in order to generate an almost continuous transect. Data processing comprised CDP sorting with binning of 100 m, owing to the long shot interval for the profiles AWI-20060100 and AWI-20060200 and 25 m for the profile AWI-20100119, bandpass filtering of 10-200 Hz and a detailed velocity analysis followed by stacking and poststack migration.

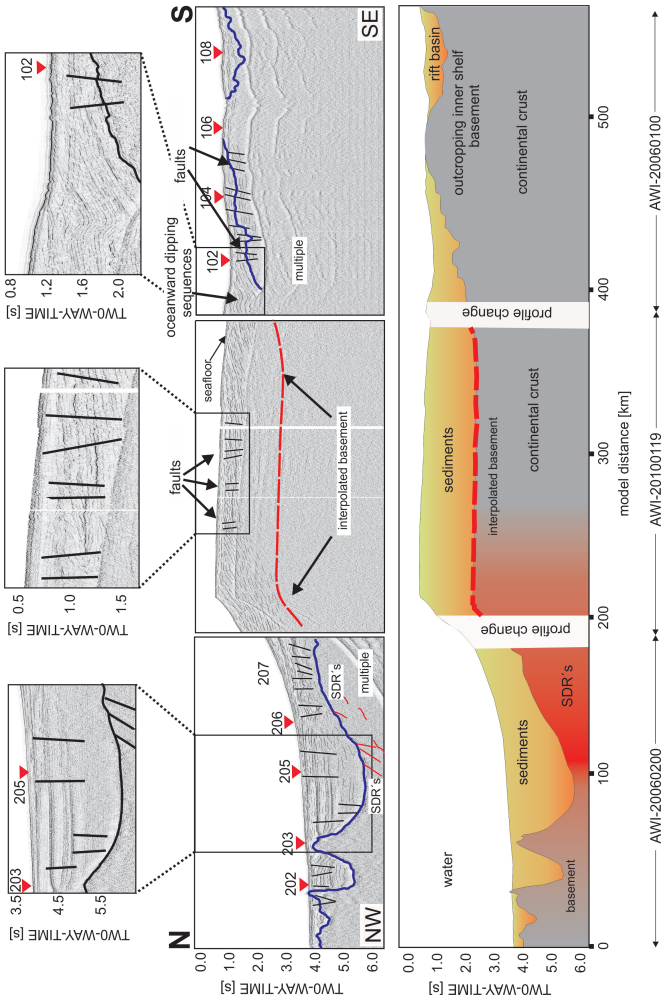

Figure 25: Compilation, line drawing and interpretation of seismic-reflection profiles AWI-20060100, AWI-20060200 and AWI-20100119 across the continental margin of the Amundsen Sea Embayment. The thick blue line indicates the interpreted top-of-basement. The dashed red line shows the interpolated top-of-basement based on a spectral analysis of free-air gravity data. The thin black lines within the sedimentary layer indicate unconformities, horst and graben and rift structures. Numbers including red triangles show the position of the OBH stations along the transect. The red lines indicate SDR - seaward dipping reflectors.

Attempts to suppress the shallow-water multiples on the shelf (Fig. 25) using techniques such as FK-filtering, Radon-transformation and predictive deconvolution produced minimal improvements due to the limited streamer length. Multiple suppression yielded, however, better results with the data of profile AWI-20100119 (Gohl et al., 2013b). We composed the three seismic reflection profiles into a single projected seismic transect (Fig. 25). On the continental rise, the reflection data show stratified sediments to a two-way-time of 2.5 s (around 3 km depth) in the deepest basins. Below the sediments, the rise is dominated by seamounts of the Marie Byrd Seamount province.

We observe indications of normal faults and horst and graben structures within the continental rise sediments. At the foot of the slope, some reflections beneath the top of the acoustic basement are reminiscent of the seaward-dipping reflectors (SDR) known for many passive continental margins of volcanic type. The top basement reflector disappears south of profile distance 160 km (AWI-20060200) (Fig. 25) and beyond which strong seafloor multiples on the shelf and the slope mask deeper signals.

The seismic shelf records show that the basement is exposed on the inner shelf of the ASE (Fig. 25). Sediment sequences beneath the middle shelf dip seawards at 0.5°, and at 1.5° beneath the inner shelf. The outer shelf is dominated by large progradational sedimentary wedges (Gohl et al., 2013b).

4.4.2 Seismic refraction data and traveltime modelling

Due to sea-ice coverage, and in order to minimize the risk of instrument loss, only 9 ocean bottom hydrophone (OBH) systems were deployed along the 165 km long profile AWI-20060100, with a regular interval of 18 to 19 km (Fig. 25). Four of the systems (OBH 102, 104, 106 and 108) recorded usable data. Along the 171 km long profile AWI-20060200 (Fig. 25), seven OBH systems were deployed with the same spacing between the Marie Byrd Seamount province and the foot of the continental slope (Fig. 25). Only five of these recorded usable data (OBH 202, 203, 205, 206 and 207).

The raw OBH data were merged with the navigation data and then converted to SEG-Y format. The exact position of the OBH stations on the seafloor along the tracks were relocated by using direct P-wave arrivals. A bandpass filter of 4-20 Hz was applied to the seismic traces for reducing high and low frequent noise from the seismic signal.

We identify coherent P-wave phases of up to 120 km source-to-receiver offset at some stations (Fig. 26). All records show good-quality refracted P-wave phases from the crust (Pc1 and Pc2 phases) (Fig. 26), some recordings contain high-amplitude wide-angle Moho reflections (PmP-phase) and intracrustal reflections (PcP -phase) as well as low-amplitude refracted phases from the upper mantle (Pn-phase). The Moho was identified as velocity contrast between the crustal layer and the upper mantle at velocities higher than 8.0 km/s.

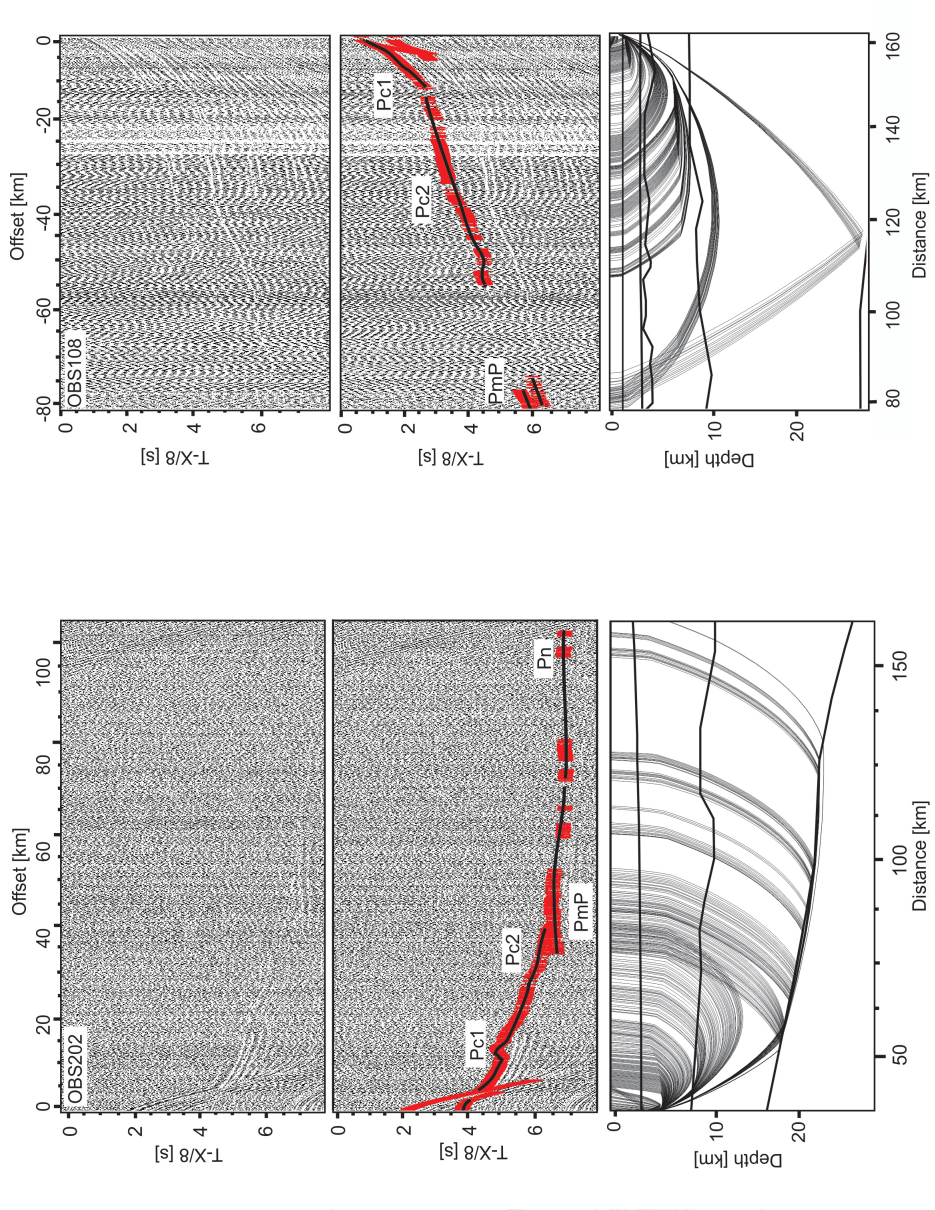

Figure 26: Top panel: part of seismic section from OBS 202 and 108, both plotted with a reduction velocity of 8 km s-1 and a bandpass filter of 4-20 Hz. Middle panel: Same section with modelled phases (black lines) and picked signals (red bars with bar length representing the pick uncertainty). Bottom panel: Ray tracing results with ray coverage in the P-wave velocity model.

We assigned a picking uncertainty of 150 ms to all P-wave arrivals. The travel-time inversion software RAYINVR (Zelt and Smith, 1992) was then used for ray-tracing to forward model the travel-time branches, by applying a layer-stripping procedure from top to bottom. This was followed by a travel-time inversion for fine-tuning the model parameters.

For the lower crust a resolution between 0.5 and 0.6 is reasonable at the shelf edge and continental rise, where 0 means no ray coverage and 1.0 represent maximum ray coverage (Fig. 29). Hence, the resolution of our P-wave models is the better in the upper and lower crust and the ray coverage is the densest at the middle section of both OBH profiles. Limited offsets lead to a lack of Pn- and PmP phases recordings at the ends of the profiles. The velocity distribution is laterally homogenous within the entire crust.

The velocity-depth model of profile AWI-20060200 (Fig. 28A) consists also of a sedimentary layer, upper and lower crustal layers underlain by an upper mantle layer. Sediment velocities range from 1.7 to 2.5 km/s in the upper part to 3.5 km/s in the deepest basin. The depth to basement increases slightly towards the shelf. Two basement highs separate the area into three distinct areas (Fig. 28A, B). In satellite-altimetry data (McAdoo and Laxon, 1997), these highs correspond to circular features south of the Marie Byrd Seamount province. They probably therefore represent buried seamounts of the province. The northernmost area is around 30 km wide and 1.0 - 1.5 km thick.

A second area in the middle part of the profile is 25 km wide and filled with sedimentary rocks of around 1.8 km thickness. At the southern flank of the profile the largest basin is 120 km wide and the sediments are up to 2.1 km thick. The upper crust thickens slightly from 3 km in the north to 6 km at the southern profile end. P-wave velocities in the upper crust range from 5 to 6 km/s. The lower crust also thickens slightly southward, from 7 km in the northern ASE to around 13 km towards the shelf. The crust-mantle boundary (seismic Moho) can be identified at a depth of 14 km in the north, which increases to 23 km near the foot of the continental slope. Lower crustal velocities range from 6 km/s at the top of the layer to 7 km/s at its base in the north and 7.7 km/s in the south. The seismic Moho can be recognised at the base of the lower crustal high-velocity layer by upper mantle velocities larger than 8 km/s.

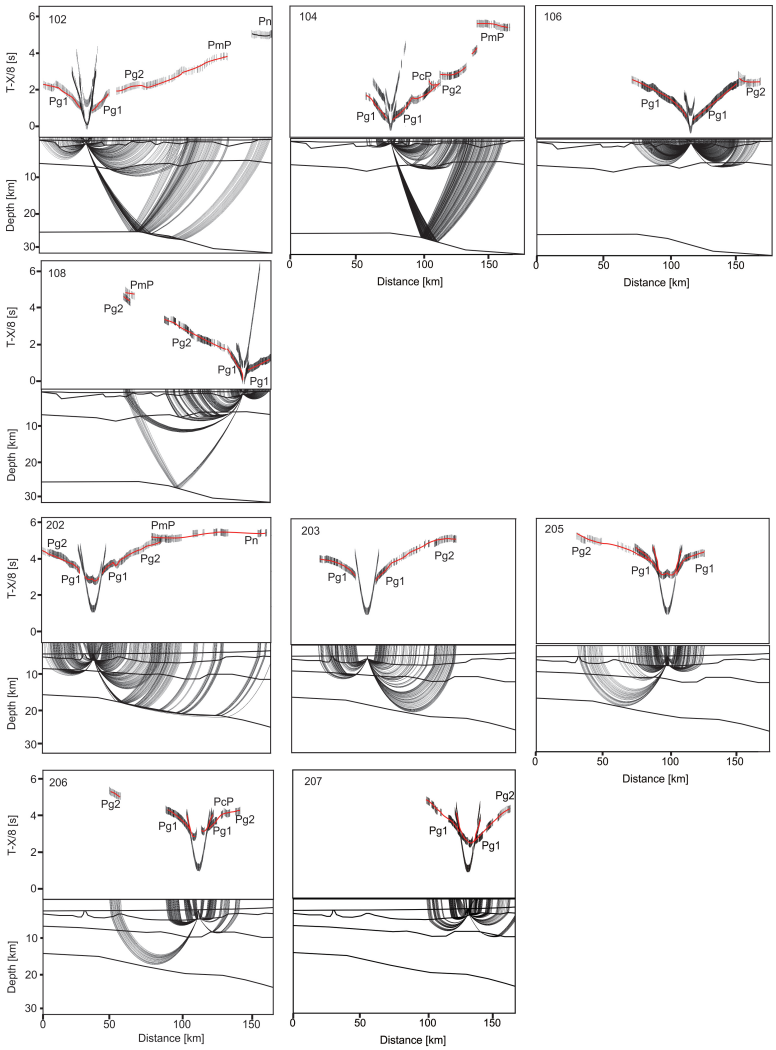

Figure 27: Comparison of picked and computed travel time branches from the P-wave velocity models for each OBH station combined with the corresponding ray path. Depth is annotated in km, the sections are plotted with a reduction-velocity T-X/8 in (s). The error bars indicate observed picking times and the size of the bars corresponds to the picking uncertainty. Solid red lines show the calculated travel times. Near-offset phases (Psed, direct waves) are not annotated. Position of each OBH along the profiles is shown in figure 25.

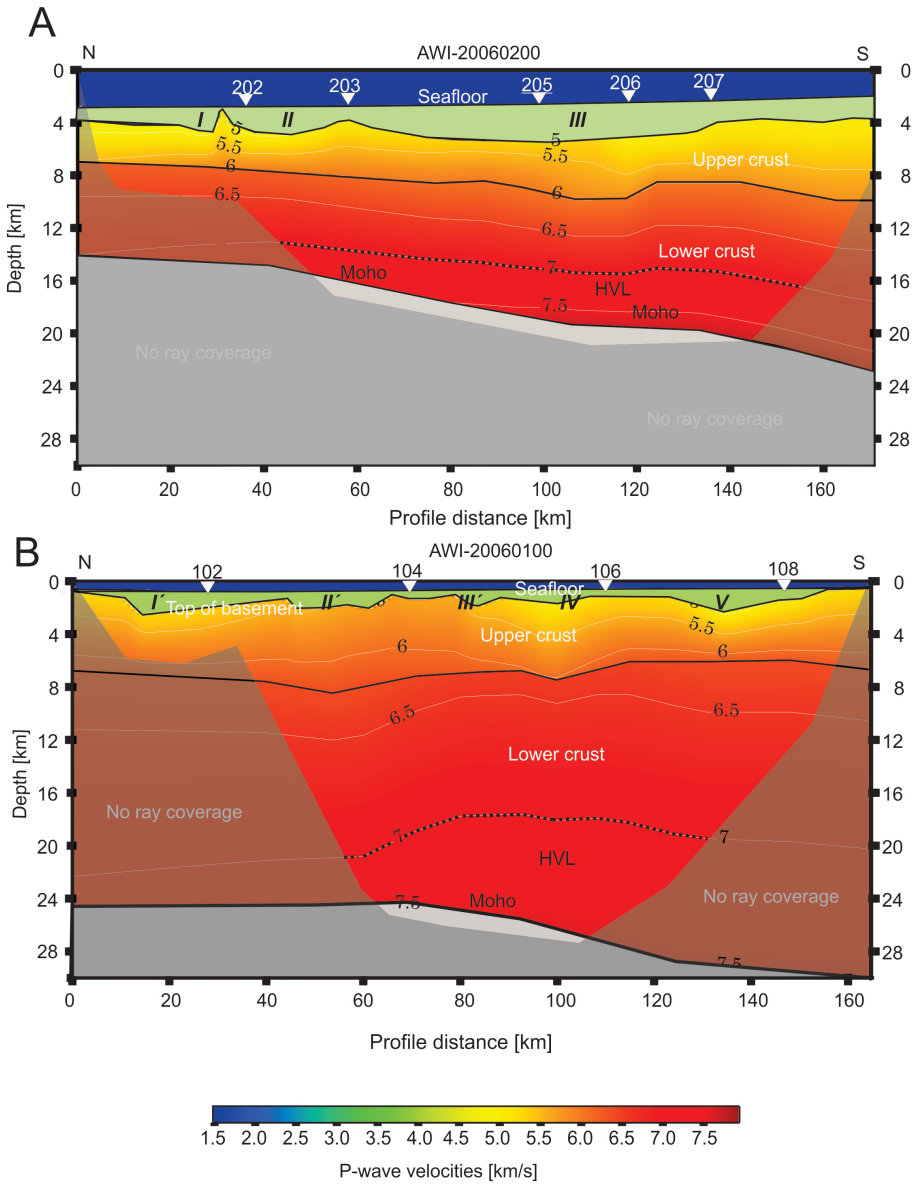

Figure 28: Final P-wave velocity models of the seismic refraction profiles. B: AWI-20060100 (bottom) and A: AWI-20060200 (top). The models are overlain by a semi-transparent mask showing areas without ray coverage. Numbers and triangles show the OBH stations along the profiles. I, II, III and I', II', III', IV and V label sedimentary basins along the profiles.

The data of OBH profile AWI-20060100 (Fig. 28B) were inverted to yield a 2D velocity-depth model that comprises a sedimentary layer, and upper and lower crustal layers underlain by the uppermost mantle. We identify five distinct sedimentary basins with variable (0.7 km -1.5 km) fill thickness and velocities ranging between 1.7 km/s and 3 km/s. The upper crust is between 4.1 and 6.3 km thick with P-wave velocities ranging from 5 km/s to 6.2 km/s. The lower crustal thickness increases southward from 14 km in the north to 24 km beneath the inner shelf. Velocities in this layer range between 6.2 km/s and 7.1 km/s in northern part and between 7 to 7.6 km/s in the southern part. The seismic Moho was identified at depths between 25 and 30 km. Similar ss on profile AWI-20060200, the seismic Moho is identified at the base of the lower crustal high-velocity layer.

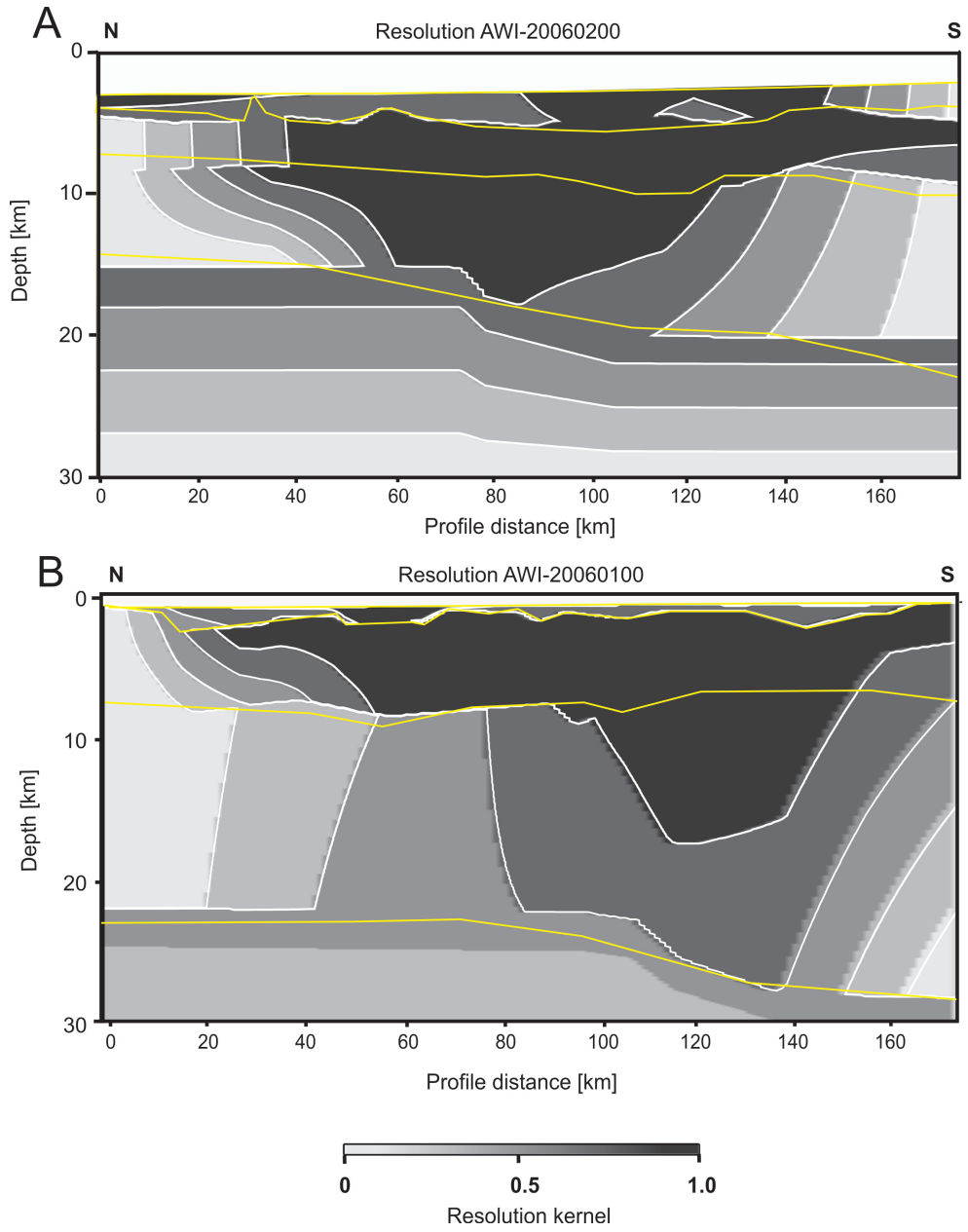

Figure 29: Resolution values of the two seismic travel-time inversion models for the P-wave velocity -depth models B: AWI-20060100 (bottom) and A: AWI-20060200 (bottom). The grey shading corresponds to the resolution value. Resolution values of greater than 0.5 indicate a moderate to good resolution. The yellow lines show the layer boundaries from the corresponding velocity-depth model. Contour lines are plotted at an interval of 0.2.

4.5 Gravity anomalies and modelling

The interpretation and modelling of potential field data is carried out to investigate regional geological issues and to highlight deep and shallow crustal anomalies as well as basin structures. A joint interpretation of profile-based seismic data with free-air gravity anomaly (FAA) (Fig. 30A) and Bouguer anomaly (BA) (Fig. 30B) grids sets the seismic data into a regional geological context. We calculated the BA of the area between 75°S to 71°S and 100°E to 120°E by using the satellite derived FAA of McAdoo and Laxon (1997), the latest bathymetry grid of Nitsche et al. (2013) (Fig. 23) and a Bouguer reduction density of 2670 kg/m^3.

Additionally, we used the spectrum of the gravity data to fill the data gap between the seismic refraction profiles AWI-20060100 and AWI-20060200, which exhibits a prominent gravity anomaly high. This high is similar to those observed close to various shelf breaks worldwide, which can be related to various density contrasts including those resulting from crustal thinning, thick accumulations of sediments, and magmatic underplating (Watts and Fairhead, 1999). However, in order to calculate the depths of significant density interfaces in our data gap, we applied the power spectral analysis based on the method of Spector and Grant (1970) to the FAA of McAdoo and Laxon (1997).

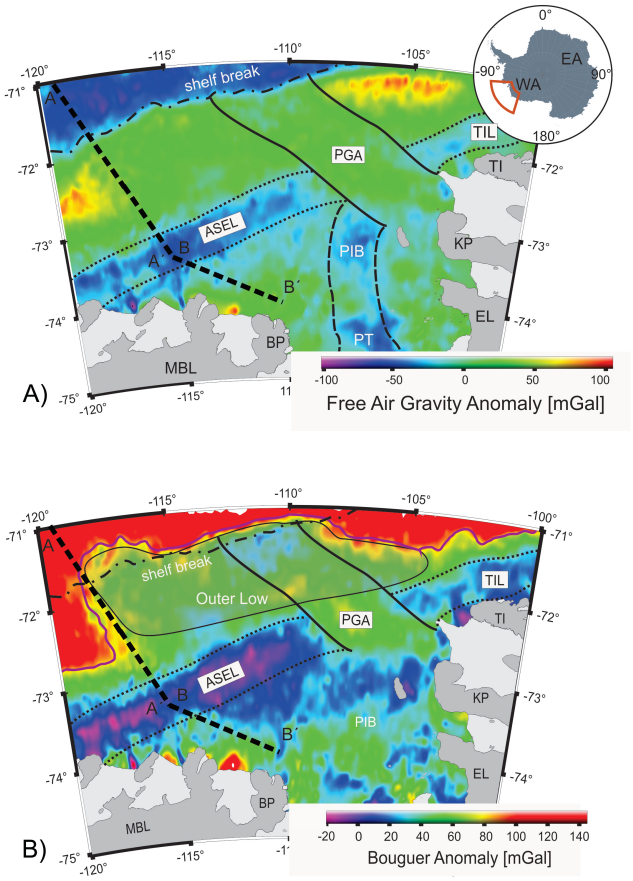

Figure 30: Compilation of gravity data. Fig. 30A maps the satellite-derived free-air gravity anomaly of the Amundsen Sea Embayment (McAdoo and Laxon, 1997). The thin black dotted and continues lines mark prominent gravity anomalies along the middle and outer shelf of the Amundsen Sea Embayment. Figure 28B images the calculated Bouguer Anomaly. The framed semi-transparent area beneath shelf break shows a prominent low (Outer Low). The thick black dotted line marks the 2D gravity rise-to-shelf model transect (Fig. 32). Abbreviations are: ASEL-Amundsen Sea Embayment Low, TIL-Thurston Island Low, PGA-Peacock Gravity Anomaly, PT-Pine Island Trough, BP-Bear Peninsula, MBL- Marie Byrd Land, EL is Ellsworth Land, TI is Thurston Island, KP is King Peninsula.

The method was developed for magnetic data and adapted for gravity data by Karner and Watts (1983). The method is based on the assumption of geological interfaces that are essentially horizontal with some small relief. With this assumption, the power spectrum of a group of prismatic sources distributed over the subsurface topography reveals a quasi-linear relationship between the power spectral density (PSD) and the wave number kr. In a plot of the natural logarithm of the FAAs power spectrum against kr, a set of distinct linear segments is related to the mean anomalies of the mass anomaly. The slope of a linear segment multiplied by -0.5 yields the mean depth to its source. The window used for the spectral analysis covers an area of 200 km^2 and is a compromise between uniform size and area (Fig. 23). The chosen area should contain provinces of uniform geology, but on the other hand should be large enough to resolve longer wavelengths and therefore greater depths.

4.5.1 Satellite-derived free-air gravity anomaly

The FAA of the outer shelf is dominated by two highs of up to 80 *mGal* which correspond to the bathymetrically elevated Western and Eastern Outer Banks (Gohl et al., 2013b). Over the middle shelf area, we identify a major WSW-ENE trending negative anomaly with a minimum of -70 *mGal* and name it the Amundsen Sea Embayment Low (ASEL). This anomaly is interrupted by the so-called Peacock Gravity Anomaly (PGA) that is northwest-southeast orientated (Eagles et al., 2004a) and which continues to Thurston Island (TI) as the Thurston Island Low (TIL). Pine Island Bay (PIB) is divided by the north-striking glacial Pine Island Trough (PIT) with a gravity low of -50 *mGal* (Fig. 30A).

4.5.2 Satellite-derived Bouguer anomaly

The gravity effect of topography and bathymetry is removed from the FAA to generate the BA such that only information on rock density variations is retained. At long wave-lengths, the transition from oceanic to continental crust can be clearly identified from a pronounced southward decrease of the BA from 140 to 40 *mGal* (Fig. 30B). The inner shelf is characterized by shorter wavelength anomalies of between 0 and 70 *mGal* whereas the outer shelf shows predominantly long wavelength anomalies of between -20 and 70 *mGal*, that correlate with bodies identified in a recent magnetic analysis of the ASE (Gohl et al., 2013a). We also identify a significant BA high larger as 60 *mGal* in the PIB region.

As in the FAA, the ASEL and TIL appear as a WSW-ENE trending low dominating the middle shelf (Fig. 30B) which is interrupted by a positive WNW trending anomaly of up to 70 *mGal* corresponding to the PGA. The outer shelf area is dominated by a major gravity low which we name the Outer Low. The boundary between the outcropping basement in the south and the sedimentary

basin on the shelf corresponds to a change in the BA from 0 to 50 $mGal$. At least a prominent BA high up to 60 $mGal$ over the PIB can be identified.

4.5.3 Spectral analysis results

Spectral analysis for the gap between the two seismic refraction profiles (Fig. 23) reveals two distinct linear segments for which linear regressions suggest a deeper and a shallower interface (Fig. 31). The choices of endpoints for the linear regression were made by visual inspection. The slope of the low-frequency (deeper) segment A corresponds to a mass anomaly depth of 22 ± 2 km whereas the slope of high-frequency (lower) segment B corresponds to an anomaly depth of about 4 ± 2 km. The uncertainty of the depths of the interfaces is controlled by the sampling interval of the spectral analysis and can be estimated to be around 2 km for crustal depths (Cianciara and Marcak, 1976).

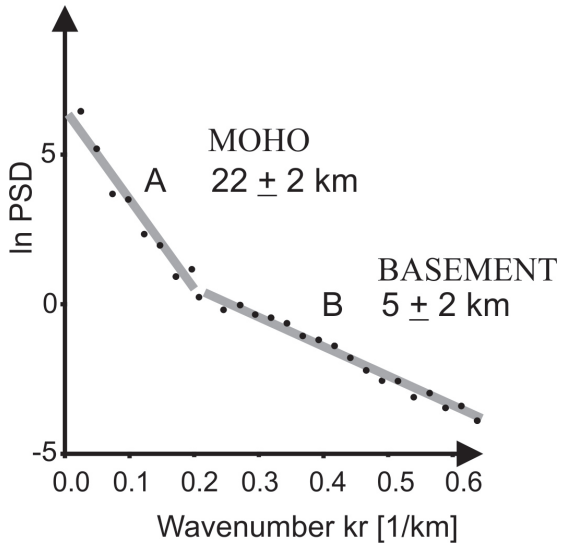

Figure 31: Spectral analysis of the satellite-derived free-air gravity anomaly of McAdoo and Laxon (1997). The natural logarithm of the energy spectra (PSD) in $mGal/km$ is plotted against the wave number in km^{-1}. The black dots show the values of the energy spectra and the grey line is the result of a linear regression for the depth estimation. The slope of the regression line corresponds to the anomaly mass depth. Anomaly mass depth is presented in km. Line A show the low frequency area (wave-number lower than 0.1 km^{-1}) and line B the high-frequency area.

4.6 Ship-borne gravity data and 2D modelling

4.6.1 Data processing and description

Shipborne gravity data were collected continuously along all profiles with a KSS-31 sea gravimeter at a sampling interval of 1 s. The raw data were corrected for instrument drift during the cruise by using reference measurements in Punta Arenas, Chile. We reduced the data to FAA with respect to the GRS80 gravity model using a standard processing procedure (Torge, 1989), including an Eötvös correction calculated with the ships navigation. The around 200 km wide data gap between profiles AWI-20060100 and AWI-20060200 was filled using the free-air gravity data of McAdoo and Laxon (1997).

The gravity anomaly decreases linearly from model distance 0 to 150 km from -10 $mGal$ to -70 $mGal$ (Fig. 32). Two short wavelength undulations of a few $mGal$ in the north correlate with the buried seamounts in the seismic data (Fig. 25). Across the shelf edge, the FAA increases up to 50 $mGal$ at profile distance 250 km. This gravity high is similar to other observations at various shelf breaks, named the "sedimentation anomaly" according to Watts and Fairhead (1999). If a 2D model profile is oriented perpendicular to the shelf break the density contrast between the sediments and the water is sufficient to model the anomaly. As our profile runs more or less perpendicular to the shelf edge (Fig. 23), it is likely that a 3D effect of the shelf break contributes to the upward anomaly. Over the middle shelf, the FAA reaches a local minimum of -50 $mGal$ at 400 km profile distance and increases up to 20 $mGal$ towards the inner shelf.

4.6.2 2D Density-depth modelling

We used the software IGMAS (Götze et al., 1988) to model a composite FAA transect. To calculate the 2D gravity effect of a mass anomaly, the IGMAS algorithm uses triangulated polyhedra built from a set of polygons defined in parallel vertical cross sections. The triangulation between these vertical planes is done automatically during the modelling procedure. We defined polygons using ship-borne bathymetry data, seismic refraction and seismic reflection data along profiles AWI-20060100, AWI-20060200 and AWI-20100119, and the results of the spectral analysis in order to setup a starting model. The model geometries at the ends of the profiles were edited to account for the regional gravity field.

To simplify the model, we combined all observed sedimentary units into one layer and calculated an average density of 2050 kg/m^3 using the velocity-density relationship of Nafe and Drake (1963). As the observed P-wave velocities of the crust indicate continental affinity along the modelled profile (Christensen and

Mooney, 1995) we used the velocity-density relationship of Barton et al. (1986) to define upper-crust density of 2650 kg/m^3 and a lower-crust density of 2800 kg/m^3. Finally, we modelled the observed high-velocity layer with a density of 3150 kg/m^3, also after Barton et al., (1986). The uppermost mantle was modelled with a density 3300 kg/m^3. During the modelling procedure, we compared the density with results of the P-wave velocity-depth models and adjusted every layer boundary to obtain a best fit between the measured and modelled anomaly by varying the crustal geometry as little as possible.

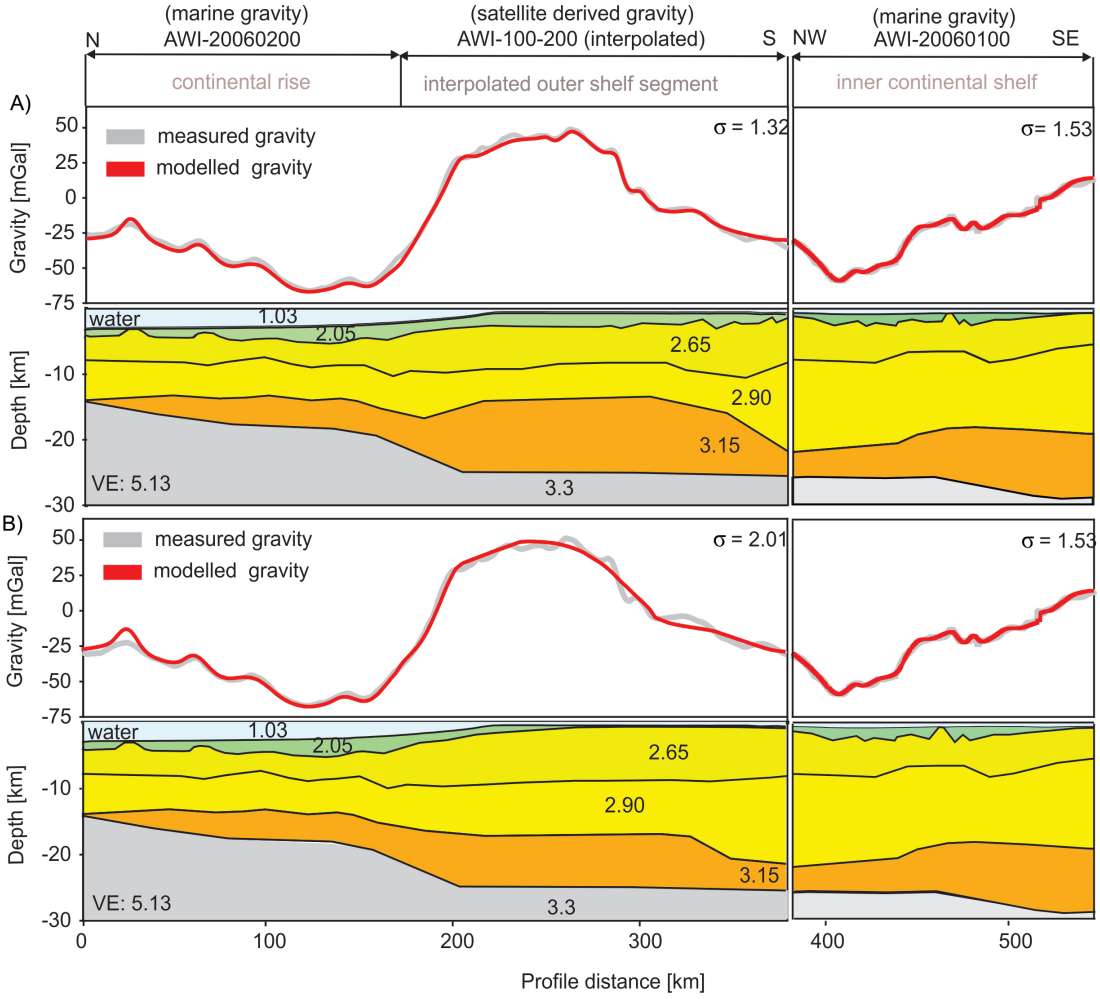

Figure 32: Two different 2D forward gravity models of the seismic refraction profiles AWI-20060100 and AWI-20060200. The data gap between the two seismic refraction profiles was bridged with satellite-derived gravity data from McAdoo and Laxon (1997) and modelled using constraints from spectral analysis of the satellite-derived gravity data of McAdoo and Laxon (1997) and the adjacent seismic reflection profile AWI-20100119 (Fig. 25). Bathymetric surface is after Nitsche et al., (2013). Density values are given in $10^3 kg/m^3$.

Owing to the inherently non-unique testimony of gravity signals, we present two models that each explain the observed anomaly (Fig. 32). The standard deviation between the measured and modelled FAA in model A is 1.53 $mGal$ along profile AWI-20060100 and 1.32 $mGal$ along profile AWI-20060200 including the interpolated part. With model B, these values are 1.53 and 2.01 $mGal$. In general, the correspondence between the velocity-depth and density-depth models is acceptable. In its central part (Fig. 32) the model suffers from the absence of seismic reflection data and a velocity-depth model. We constrained the range of models applicable to this part using the results of the power-spectral analysis of its FAA field. As noted above, this part of the profile crosses the gravity high of the Western Outer Bank (Gohl et al., 2013a).

In model A, the sedimentary layer is up to 3 km thick, consistent with the power spectral analysis. The top-of-basement interface is rough south of the gravity high at profile distance of 300-370 km. The Moho steps down from a depth of about 22 to 27 km between profile distance 170 - 200 km, again consistent with the power spectral analysis, and remains at this depth until after profile distance 400 km, where it is constrained once again by refraction results on profile AWI-20060100. With these layers, it becomes necessary to model the gravity high as the signal from a 10 km high bulge in the high-density/high-velocity layer of the lowermost crust between profile distance 210 - 370 km. In model B, the high can be explained by thinning of the sedimentary layer between profile distance 170 - 250 km, and its absence between profile distance 250 - 370 km, although this latter depiction is not consistent with the power spectral analysis. The high-density layer is 4-7 km thick with no significant bulge.

4.7 Discussion

4.7.1 Crustal structure

The FAA predominantly reflects the seafloor topography (Fig. 30A), whereas the BA portrays density and thickness variations of the lithosphere, including the gradual negative gradient that indicates the transition from continental to oceanic crust (Fig. 30B). However, our transect lies mostly within the interpreted continental crust. The Outer Low of the ASE shelf correlates with an elevated basement identified in seismic reflection data from the ASE, named the Western Outer Bank (Gohl et al., 2013b). Contrary to the FAA, the corresponding BA signal reaches into the continental rise indicating that its source is not topographic. The corresponding BA signal is probably the gravimetric signal of a thicker continental sliver generated during the Cretaceous extension that led to the separation of West Antarctica and Zealandia.

We subdivide the crust of the ASE into an upper crust, a lower crust and a high-velocity lowermost crustal layer. The average upper crustal P-wave velocity of around 5.5 km/s along the entire transect is typical of uppermost continental crust (Christensen and Mooney, 1995) (Fig. 28). The absence of any P-wave velocity or density variations below the two Marie Byrd seamounts indicates that these basement highs consist of similar material as the surrounding crust. The northern end of profile AWI-20060200 is less certain due to the lack of ray coverage and reversed records.

In general, the lower crustal P-wave velocities and densities are greater than expected for normal continental crust indicating a more mafic crustal composition (Christensen and Mooney, 1995). Between model distances 180 to 380 km, our models are not constrained by deep seismic data. However, based on the gravity spectral analysis and an adjacent seismic reflection profile, we argue that

the sedimentary layer and the upper and lower crust have architectures similar to those beneath the continental slope and the inner shelf. The modelled rougher basement explains the high-frequency variations of the FAA. In Model A the estimated depth to top basement fits better to the flanking seismically constrained profiles than Model B, suggesting that its geometry is more appropriate to describe the ASE.

4.7.2 High-velocity layer

Traveltime modelling reveals P-wave velocities of 7.0 to 7.6 km/s in the lower crust along both seismic refraction profiles corresponding to densities between 3140 to 3160 kg/m^3 in the gravity models (Barton et al., 1986). These densities differ significantly from those expected for normal upper mantle density (3300 kg/m^3) or for normal lower continental crust (Anderson, 1989). The maximum 10 km thickness of this layer is comparable to the thickness of high-velocity bodies known from other extended and volcanic type continental margins like the East Greenland continental margin (Voss et al., 2007) or its conjugate Vøring margin offshore mid-Norway (Mjelde et al., 2002). In these settings, the high-velocity bodies are interpreted as underplating of gabbro by accumulation of magma at the Moho during extension.

By analogy, therefore we propose that the high-velocity layer beneath the ASE may represent widespread magmatic underplating (Fig. 32) indicating that the margin is of volcanic-type rather than of magma-poor type (Mutter et al., 1984). Hints of SDRs farther north reinforce the notion that the break-up process between greater New Zealand and West Antarctica was accompanied by magmatism. Grobys et al. (2009) interpret the observed high-velocity body of the conjugate southern Bounty Trough off eastern New Zealand as a mafic body intruded into the lower and upper crust and its high-velocity zone, as possible underplating at

the base of the crust. However, the continental margins of eastern Zealandia, the Chatham Rise and the Campbell Plateau are not characterised well enough to match the categories of volcanic or non-volcanic type margins due to the lack of deep crustal data.

If the SDRs found along line AWI-20060200 (Fig. 25) of the Amundsen Sea do not find a counterpart on the New Zealand margin, the Amundsen Sea SDRs may be sequences of post-break-up volcanic phases. A study of the Southeast Greenland margin of Hopper et al. (2003) reports volcanic seaward dipping reflectors on oceanic crust, 180 km seaward of the continent-ocean-boundary which suggests that SDRs are not necessarily related to initial break-up.

Kipf et al. (2014) propose the generation of magma from partial melting of upper mantle rocks convecting as part of a so-called continental insulation flow on the basis of HIMU-type magmatic rocks (high time-integrated 238U/204Pb) from beneath the Marie Byrd Land to the present day Marie Byrd Seamount province between Late Cretaceous and Paleocene. They suggested the upwelling arm of the convection cell exists beneath Marie Byrd Land at the present day. This hypothesis suggests an alternative source of gabbroic lower crust on the ASE shelf, in direct proximity to the Marie Byrd Land Seamount province.

However, if the bulge would be constituted by gabbroic melt, the expected density would be around 2800 kg/m^3, which is significant lower than the observed 3150 kg/m^3.In the end the density of the HVL is too high for magma of Phanerozoic origin. On the other hand, the occurrence of cumulated layers could significantly rise the density of the material.

4.7.3 Serpentinization

An alternative explanation for the HVL is serpentinization of mantle material (e.g. Carlson and Miller, 2003). Serpentinized peridotite can have velocities and densities similar to those of lower continental crust (Biollot et al., 1992). Serpentinite was observed along many non-volcanic passive margins such as the West Iberian margin (Boillot and Winterer, 1988, Whitmarsh and Sawyer, 1996) or the Newfoundland margin (Reid, 1994). Biollot et al. (1992) suggested that the formation and accretion of serpentinite beneath the crust may play a role in areas of rifted continental margins.

However, in these settings serpentinisation requires the penetration of seawater downward via faults, and low-angle detachment surfaces. Another possibility is via deep hydrothermal circulation. Hydrothermal activity was observed at intraplate volcanoes such as the Lo-'ihi volcano (Malahoff et al., 2006). The Marie Byrd Seamount province is identified as a system of intraplate volcanoes (Kipf et al., 2014). Hence, the crust of this area has a potential for seawater penetration.

Serpentinization is a gradual process creating no clear boundary between unaltered peridotite and serpentinized mantle material. Magma-poor margins are often characterized by an increasing P-wave velocity from the crystalline basement to the mantle without a clear Moho response due to serpentinized mantle material (Minshull, 2009). At the West Iberian margin, the absence of clear Moho reflections were interpreted as the result of partial serpentinized mantle peridotite (Chian et al., 1999).

Mjelde et al. (2002) discussed the possible occurrence of serpentinized mantle in combination with magmatic underplating along the Vøring volcanic passive margin offshore mid-Norway. The observation of clear Moho reflections was the

key argument for favouring the underplating hypothesis (Mjelde et al., 2002). We modelled the observed HVL with a density of 3300 kg/m^3 and hence, of significant higher density than the average density of serpentinite at this depth (Christensen, 1996). We therefore imply a continental margin that is likely more influenced by magmatism than undercrusted by serpentinite.

4.7.4 Tectono-magmatic evolution

The seismic reflection data of the ASE reveal dipping lowermost strata on the inner ASE shelf, which may represent the earliest sedimentary rocks in the Amundsen Sea (see also Gohl et al., 2013b). We interpret the different northward dipping sedimentary reflectors as probable results of different extensional phases during the formation of the area. Normal faults indicate crustal extension affected the area. The present-day crustal architecture beneath the shelf infers wide-mode rifting such as observed in the Basin and Range Province of western North America (Hamilton, 1987) rather than narrow-mode rifting such as the east African Rift System (e.g. Ebinger et al., 1989, Buck et al., 1991; Rosenbaum et al., 2002) but the existence cannot be excluded from our data.

Horst and graben structures are a further indication that the region evolved by wide-mode rifting (Buck et al.,1991). Fault-like structures on the shelf may represent block-faulting during early stage and aborted rifting. The BA of the ASE shelf (Fig.30B) shows several pronounced local highs and lows suggesting a pattern of rift basins and intervening highs. It is possible to speculate that the basins in the ASE (Fig. 25) are related to the pre-break-up dextral transtensional strain known from western MBL (Siddoway et al., 2008) which is a hint for activity of the WARS affecting the entire ASE. A southward decrease of the BA with a gradient of about 1.5 $mGal\ km^{-1}$ may also indicate that the crust was affected by rifting. The WSW-ENE trending ASEL and TIL strike parallel

to the Pacific Antarctic Ridge in the north and the Bentley Subglacial Trough in the south and where our model crosses the ASEL it shows a thinned, 20 km thick continental crust.

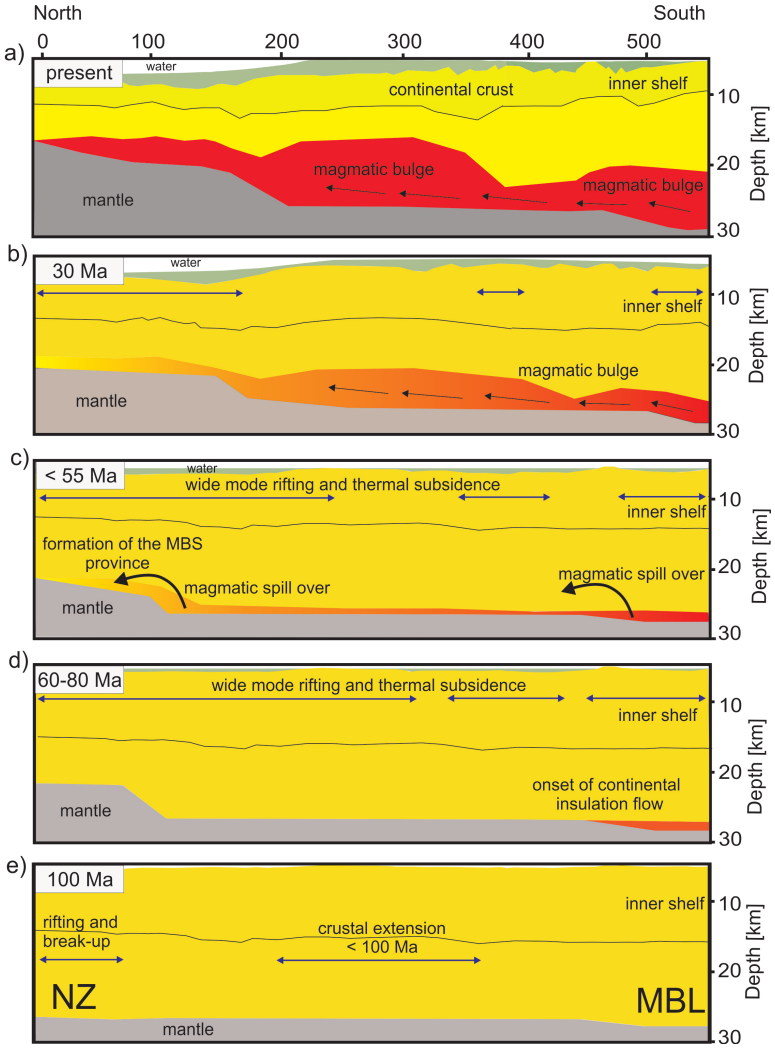

Figure 33: (a) interpreted 2D gravity model based on the seismic refraction profiles AWI-20060100 and AWI-20060200. The top-of-basement was mapped by using the seismic reflection profiles AWI-20060100, AWI-20060200 and AWI-20100119. The black arrows show the flow direction of the inferred continental insulation flow (Kipf el al., 2012, 2014) from beneath Marie Byrd Land to the Marie Byrd Seamount Province. The blue arrows represent extensional rifting. The slides (b) to (e) show schematically the tectono-magmatic development of the margin from break-up of New Zealand and West Antarctica to Oligocene. Abbreviations are: MBL is Marie Byrd Land, NZ is New Zealand.

We interpret these observations as a record of a multi-stage initial Cretaceous wide-mode rifting event and thermal subsidence that followed the eventual successful break-up Zealandia from Antarctica. Our data show evidence for crustal extension connected to activities of the WARS since Cretaceous that resulted in the abandonment or evolution of a young-stage wide rift zone in favour of a fully developed extended continental margin and mature oceanic crust. It is possible that this rifting is connected to the well documented distributed Cenozoic extension superposed by narrow mode extensional events within the eastern Ross Sea sector of the WARS and the onshore parts of the ASE (Luyendyk et al., 2003; Davey et al., 2006; Jordan et al., 2010). However, the absence of implications for narrow-mode rifting in the offshore part of the ASE is not in conflict with this interpretation.

The orientation of lineaments in potential field data infer that these rifting events continued to affect the ASE after break-up from Zealandia, becoming a site for Bellingshausen-West Antarctic and East Antarctic-West Antarctic plate divergence in Paleocene and Oligocene times (Eagles et al., 2004a; Gohl et al., 2013a). Figure 33 presents a schematic tectono-magmatic reconstruction of the continental margin segment sampled by our model from late Cretaceous break-up of New Zealand and West Antarctica until Oligocene times (Fig. 33 e to b) and the present-day configuration (Fig. 33a). Fig. 33e shows the possible lithospheric configuration during or short before break-up between New Zealand and West Antarctica at around 100 Ma.

The crustal architecture was homogenous along the entire profile. At this time, extension may starts between Zealandia and West Antarctica. Mukasa and Dalziel (2000) inferred subduction-related I-type magmatism occurred at least until 94 $\pm$ 3Ma (U-Pb zircon date) from the Walgreen Coast - eastern MBL (Fig. 23) to western Pine Island. Fig 33d. shows the possible configuration during onset of

wide-mode rifting between 60 to 80 Ma. We infer the onset of magmatism at this time based on magmatic flow estimations as discussed above. Fig. 33c images ongoing magma flow, the occurrence of the Marie Byrd Seamount province which was accompanied by thermal subsidence of the paleo shelf of the ASE. The time slice shown in Fig. 33b illustrates the lithospheric configuration during 30 Ma. Ongoing magma accumulation was accompanied by tectonic rifting. At least Fig. 33a illustrates the present day configuration. The reconstruction is based on the crustal architecture of our gravity and seismic model (Fig. 32b). The basin development we illustrate at the top surface of our transect is based on a schematic back-strippe reconstruction applied for the ASE shelf by Gohl et al. (2013b).

Due to the absence of evidence for a volcanic extended margin south of Zealandia, we prefer to explain the magmatic underplating as a product of partial melting during convective mantle flow set up by long-lived continental insulation. There are no robust constraints about the timing of this flow but Kipf et al. (2014) propose the formation of the Marie Byrd Seamounts to be in Early Cenozoic (56 Ma). With respect to the present-day distance of around 800 to 1000 km between the central Marie Byrd Seamount province and coast of eastern Marie Byrd Land (Fig. 23) and an average convective velocity of around 1-5 cm/a (Schubert et al., 2001), the onset of magma flow may have occurred around 10 m.y. earlier at about 65 Ma. This is consistent with a suspected major plate reorganisation in the South Pacific in Paleocene (Cande et al., 2000).

Further, the assumed increasing magmatic activity beneath the ASE shelf shown in Fig. 33b at about 30 Ma correlates with the emplacement age of the Dorrel Rock intrusive complex in Marie Byrd Land (Rocchi et al., 2006) implying that a major or several single magmatic events related to multi-stage tectonic activity affected the Amundsen Sea margin. Additionally, the observation of different thermal signatures in the Mt. Murphy area of western Marie Byrd Land, which

indicate a major fault system and which was active during or after the Oligocene (Lindow et al., 2011) is an implication for tectonic activity in this region. We interpret this as a further indication that tectonic and magmatism were coupled processes during the Oligocene and are related to the active branch of the WARS in the ASE (Gohl et al., 2013 a,b).

Following the recent hypothesis of Kipf et al. (2014) we infer that the magmatic bulge at the Moho discontinuity was the result of a long-distance magma flow which reached the Moho, grew continuously and then spilled over (Fig. 33). This magma bulge is likely to be responsible for the Outer Low in the BA and the corresponding elevated top-of-basement which is identified in seismic data (Gohl et al., 2013b). It seems reasonable, that the accumulation of magmatic material at the Moho cause uplift of the overlying structures (Brunov et al., 2005).

4.8 Conclusion

Geophysical data from the ASE provide new insights into the lithospheric architecture and tectono-magmatic development of this continental margin. Two deep crustal seismic profiles image the crustal and upper mantle structure of parts of the continental rise, slope and shelf. A continuous rise-to-shelf 2D gravity model supports and expands on the velocity-depth models and enables the interpretation of a tectono-magmatic history for the ASE margin from its break-up with Zealandia to the present and indicating a margin-wide process of magmatic underplating. The main findings are summarized as follows:

1. The geophysical data image the upper and lower crust and reveal a high-velocity layer at the base of the lower crust beneath the shelf. The crust is 10 - 14 km thick at the continental rise and up to 29 km thick beneath the inner shelf. Seismic refraction data reveal P-wave velocities between 7.1 and 7.6 km/s in the high-velocity layer indicating a margin-wide process of

magmatic underplating whose thickness varies up to a maximum 10 km.

2. 2D gravity modelling supports the hypothesis of a magmatic layer beneath the shelf and is consistent with the velocity-depth model. Indications of seaward-dipping reflectors in the seismic data suggest that break-up between greater New Zealand and West Antarctica may have been accompanied by magmatism not necessarily related to initial break-up.

3. Following the interpretation of Kipf et al. (2014), the high-velocity layer can be related to the Marie Byrd Seamount Province as product of a continental insulation flow which transported mantle material from beneath West Antarctica to the present day Marie Byrd Seamount Province. The onset of the magma flow in the Paleocene, which is maybe mantle originated, correlates with a major plate reorganisation in the South Pacific (Cande et al., 2000). Magma accumulation at the base of the crust seems to be responsible for the elevated basement beneath the outer shelf of the Amundsen Sea Embayment. The absence of a gradational transition between the velocity body, normal upper crustal seismic velocities and a significant higher density of the observed HVL suggest that serpentinized mantle not is present beneath the ASE.

4. The crustal architecture, sedimentary setting and potential field data from the ASE indicate its formation during crustal extension. The constant crustal thickness and horst and graben structures suggest that this process was an expression of wide-mode rifting. Geophysical data show early stage, fully developed and failed initial rifting structures within the ASE suggesting a late active branch or integrated feature of the West Antarctic Rift System.

5 Rift processes and crustal structure of the Amundsen Sea Embayment, West Antarctica, from 3D potential field modelling

Thomas Kalberg[1], Karsten Gohl[1], Graeme Eagles[1] and Cornelia Spiegel[2]

1. Dept. of Geosciences

Alfred Wegener Institute Helmholtz-Centre for Polar and Marine Research

Am Alten Hafen 26

27580 Bremerhaven, Germany

2. University of Bremen, Dept. of Geosciences, Bremen, Germany

Submitted to Marine Geophysical Research 25th April 2015

Revision received with minior revisions 24th June 2015

5.1 Abstract

The Amundsen Sea Embayment of West Antarctica is of particular interest as it provides critical geological boundary conditions in better understanding the dynamic behavior of the West Antarctic Ice Sheet, which is undergoing rapid ice loss in the Amundsen Sea sector. One of the highly debated hypothesis is whether this region has been affected by the West Antarctic Rift System, which is one of the largest in the world and the dominating tectonic feature in West Antarctica. Previous geophysical studies suggested an eastward continuation of this rift system into the Amundsen Sea Embayment.

This geophysical study of the Amundsen Sea Embayment presents a compilation of data collected during two RV Polarstern expeditions in the Amundsen Sea Embayment of West Antarctica in 2006 and 2010. Bathymetry and satellite-derived gravity data of the Amundsen Sea Embayment complete the dataset. Our 3D gravity and magnetic models of the lithospheric architecture and development of this Pacific margin improve previous interpretations from 2D models of the region.

The crust-mantle boundary beneath the continental rise and shelf is between 14 and 29 km deep. The imaged basement structure can be related to rift basins within the Amundsen Sea Embayment, some of which can be interpreted as products of the Cretaceous rift and break-up phase and some as products of later propagation of the West Antarctic Rift System into the region. An estimate of the flexural rigidity of the lithosphere reveals a thin elastic thickness in the eastern embayment which increases towards the west.

The results are comparable to estimates in other rift systems such as the Basin and Range province or the East African Rift. Based on these results, we infer an arm of the West Antarctic Rift System is superposed on a distributed Cretaceous

rift province in the Amundsen Sea Embayment. Finally, the embayment was affected by magmatism from discrete sources along the Pacific margin of West Antarctica in the Cenozoic.

5.2 Introduction

Knowledge of the present architecture of the Pacific margin of West Antarctica (WA) is essential for improved plate kinematic and tectonic reconstructions of the Amundsen Sea Embayment (ASE) (Fig. 34). The embayment experienced processes that formed the southern Pacific starting with the inferred collision of the Hikurangi Plateau with the Gondwana subduction margin at approximately 110-100 Ma (Davy and Wood, 1994; Mortimer et al., 2006) and continuing until the evolution of the West Antarctic Rift System (WARS).

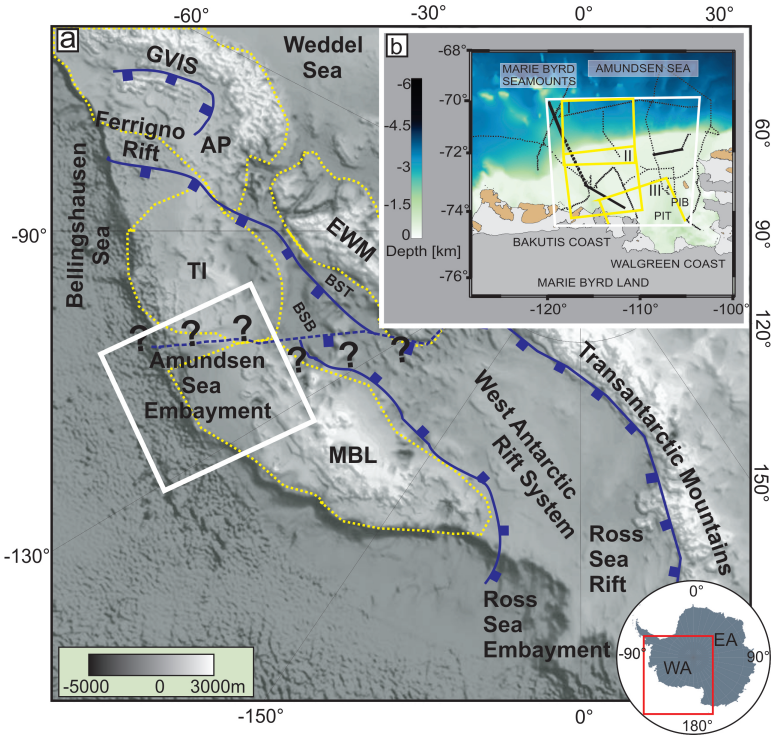

Figure 34: (a) Topographic map of West Antarctica showing the regional setting derived from BEDMAP2 (Fretwell et al., 2013). Tectonic blocks (Dalziel and Elliot, 1982) are marked in yellow-dotted areas: EWM Ellsworth-Whitmore Mountains, TI Thurston Island, AP Antarctic Peninsula, MBL Marie Byrd Land. Rift structures such as the West Antarctic Rift System, Ferrigno Rift (FR) and George IV Sound (GIVS) are indicated with blue lines. The dotted blue line shows a possible extension of the West Antarctic Rift System branch into the Amundsen Sea Embayment. (b) Overview bathymetric map of the Amundsen Sea Embayment after Nitsche et al. (2007, 2013) showing the locations of three seismic refraction profiles (thick black lines) (Kalberg and Gohl., 2014) and seismic reflection profiles (thin dotted black lines). Yellow frames show the areas used for the spectral analysis of the magnetic and gravity anomaly data. The white frame shows the area within which our potential field data are modelled. PIB is Pine Island Bay, PIT is Pine Island Trough, BSB is Bentley Subglacial Basin and BST is Bentely Subglacial Trench.

Additionally, as tectonic processes can influence the variation of environmental conditions (Hay, 1996), understanding the region's tectonic history may help constrain models and concepts for Cenozoic global cooling and Antarctic glaciation (De Conto and Pollard, 2003; Coxall et al., 2005). For example, there is an increasing interest in the geomorphological evolution of the ASE and the controls it exerted on the dynamics of the West Antarctic Ice Sheet (WAIS) (e.g. Bell et al., 1998; Studinger, 2001, Dalziel et al., 2001). In addition, detailed knowledge of the lithospheric development may provide constraints on key geological parameters to estimate geophysical proxies such as geothermal heat flux (Shapiro and Ritzwoller, 2004).

The influence of plate tectonic processes on the evolution of the cryosphere has been studied in other regions of Antarctica such as the Scotia Sea, just north of the Antarctic Peninsula (Lawer et al., 2011; Eagles and Jokat, 2014). However, knowledge of the tectonic development and continental lithospheric structure in West Antarctica is based mostly on geophysical studies in the Ross Sea (Cooper et al., 1991; Trey et al., 1999; Luyendyk et al., 2001, Luyendyk et al., 2003), Marie Byrd Land (LeMasurier and Landis, 1996; Winberry and Anandakrishnan, 2004; LeMasurier, 2008) and the Pine Island Glacier region (Jordan et al., 2010). These regions are characterized by thinned continental crust with an average thickness of 21 km to 25 km. Numerous fault-bounded basins in the Ross Sea sector comprise the well-known West Antarctic Rift System (WARS). Further east, a crustal thickness of 21 km under the Bentley Subglacial Trench suggests intra-continental extension there too (Winberry et al., 2004).

Recent studies of the ASE presented by Weigelt et al. (2007), Gohl et al. (2007, 2013a,b), Wobbe et al. (2012) and Kalberg and Gohl (2014) reveal the ASE to be underlain by multi-staged rifted, extremely stretched and magmatically-underplated continental crust which is overprinted by several tectonic lineaments.

The data have been interpreted to indicate a set of rift basins that formed as a prolongation of the WARS into the ASE (Gohl et al., 2007; Gohl et al., 2013a,b; Kalberg and Gohl, 2014). The ASE seems to have evolved by wide-mode rather than narrow-mode rifting (Kalberg and Gohl, 2014). The modelled magmatic underplating can be related to a continental insulation flow, which transported magmatic material from beneath the crust of Marie Byrd Land to the Marie Byrd Seamount province offshore (Kipf et al., 2014; Kalberg and Gohl, 2014).

Eagles et al. (2009) suggested extensional branches of the WARS were active around Alexander Island and in George VI Sound (GVIS), to the NE of the ASE, in the period 34-26 Ma. Additionally, recent studies of Bingham et al. (2012) showed that the Ferrigno Rift, inland of the ASE and GVIS (Fig. 34) was affected by crustal thinning that they attributed to the same causes as the WARS. Contrary to the Ross Sea and the Amundsen Sea sectors of the WARS, there seems to be no evidence for widespread Cenozoic magmatism around the Ferrigno rift region (Bingham et al., 2012). In great contrast, Granot et al (2013) calculated Euler rotation parameters that infer these eastern reaches of the WARS would have worked in plate convergence.

Plate kinematic reconstructions of the southern Pacific realm and the West Antarctic margin (e.g. Larter et al., 2002; Eagles et al., 2004; Wobbe et al., 2012) explain reasonably well the general break-up and ocean drifting process between New Zealand and West Antarctica but suffer from sparse information on the regional tectonic architecture of the ASE lithosphere which was a key region for the initiation of rifting and break-up.

This study presents a spatial insight into the lithospheric architecture of the Pacific margin of WA in the ASE between 120°W and 104°W and between 70°S and 74°S using a detailed 3D gravity and magnetic model supported by seis-

mic constraints. The models image the basement morphology, regional crustal thickness, and the distribution of magmatic bodies and magmatic zones in the embayment. A joint interpretation reveals several tectonic lineaments and shows rift basins within the middle and inner shelf of the ASE. Estimates of the elastic lithospheric thickness provide further constraints on the geodynamic evolution of the ASE.

5.3 Geological background

The tectonic blocks of West Antarctica (Dalziel and Elliot, 1982) are separated from the tectonically contrasting East Antarctic cratons and mobile belts by the Transantarctic Mountains and the WARS, which is one of the world largest continental rift systems (Fig. 34). The structural composition of the WARS is comparable to other major continental rift zones such as the East African Rift or the Basin and Range Province (Behrendt et al., 1991; Tessensohn and Wörner, 1991; LeMasurier and Landis, 1996; LeMasurier, 2008).

The ASE was formed as consequence of the Late Cretaceous break-up of the former Gondwana supercontinent blocks of West Antarctica and greater New Zealand (e.g. Eagles et al., 2004a; Wobbe et al., 2012). The evolution of the Pacific margin of WA since that time included several distinct tectonic phases (Fig. 35). South-westward propagation of rifting and break-up started with the separation of Chatham Rise from the eastern MBL margin as early as 90 Ma and continued to around 83 Ma with the break-up of Campbell Plateau from central Marie Byrd Land (e.g. Mayes et al. 1990; Bradshaw et al., 1991; Larter et al., 2001; Eagles et al., 2004a, Wobbe et al., 2012).

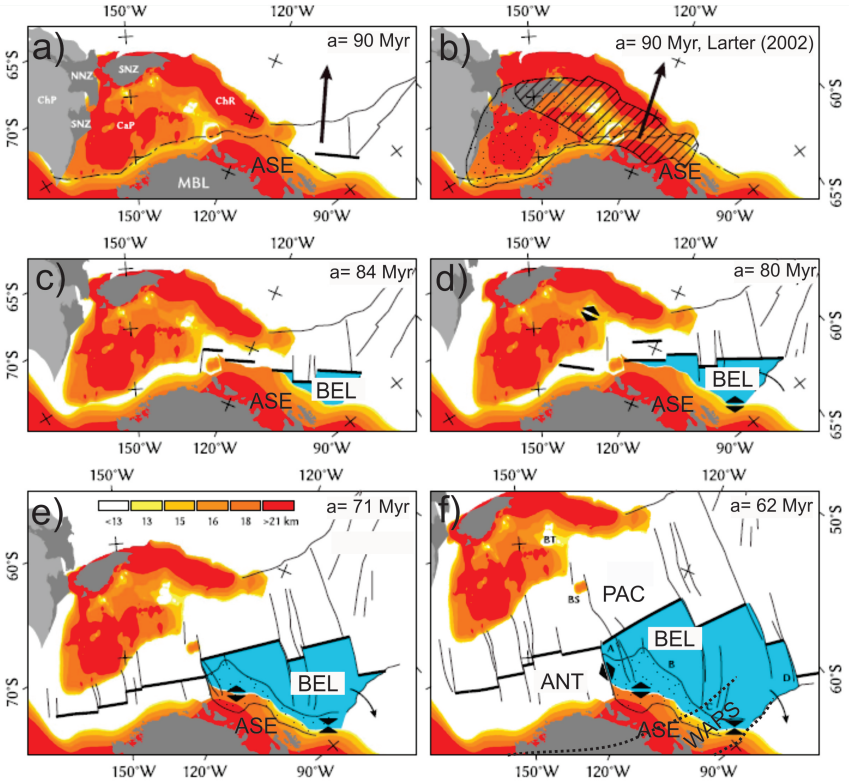

Figure 35: Schematic plate-tectonic reconstruction model of distinct tectonic phases in the SW Pacific from Late Cretaceous to early Paleocene (modified after Wobbe et al., 2012) using rotation parameters of Grobys et al. (2008) and Wobbe et al. (2012) in (a) and (c-f), and rotation parameters of Larter et al. (2002) in (b). The black arrows in (a) and (b) show the movement direction of the Bellingshausen Plate. Thin black lines show fracture zones, thick black lines show mid ocean ridge segments. The thin black dashed line indicates the presumed eastern rift branch of the West Antarctic Rift System (Gohl et al., 2013a,b). Dotted area in (e) and (f) shows oceanic crust which was formed along the Bellingshausen Plate margin. (e) includes the crustal thickness scale of Wobbe et al. (2012). Abbreviations are: ANT West Antarctic plate, BEL Bellingshausen plate, BS Bollons Seamount, BT Bounty Trough, CaP Campbell Plateau, ChP Challenger Plateau, ChR Chatham Rise, MBL Marie Byrd Land, NNZ North Island of New Zealand, PAC Pacific plate, SNZ South Island, ASE Amundsen Sea Embayment, WARS West Antarctic Rift System and ASE is Amundsen Sea Embayment.

From about 80-79 Ma, the Bellingshausen Plate began acting as an independent tectonic plate, and continued to do so until about 61 Ma (e.g. Larter et al., 2002; Eagles et al., 2004a,b). Its incorporation into the Antarctic Plate at this time occurred as part of a major plate reorganisation in the South Pacific (Cande et al., 2000). Based on Ar-Ar dating of dredged rocks, Kipf et al. (2014) postulated that at about 65-56 Ma the Marie Byrd Seamounts were formed from magmatic material that was transported from beneath the West Antarctic continental crust by a continental insulation flow.

The eastern shelf of the ASE has been suggested as the site of a Paleozoic-Mesozoic crustal boundary between the Thurston Island crustal block in the east and the MBL block in the west, whose apparent paleomagnetic polar wander paths differ significantly (Dalziel and Elliot, 1982; Storey, 1991; Grunow et al., 1991). Müller et al. (2007) considered that the WARS east of the Ross Sea started acting in dextral strike-slip or extensional motion east of the ASE between chrons 21 and 8 (48-26 Ma.). They postulated that this motion was connected to a Pacific-Phoenix-East Antarctica triple junction at the southwestern Bellingshausen Sea margin via the Bentley Subglacial Trench (Fretwell et al., 2013) and the Byrd Subglacial Basin.

Moho depth estimates under the Byrd Subglacial Basin and the Pine Island Rift reveal crust of only 19 km thickness (Jordan et al., 2010). An estimate of the region's flexural rigidity suggests an effective elastic thickness of just 5 km in the same area (Jordan et al., 2010). These results infer continental thinning in this part of WA, which Jordan et al. (2010) interpreted to have been achieved by distributed Cretaceous rifting followed by Cenozoic narrow-mode rifting. Crustal thickness estimates based on receiver functions reveal a crustal thickness of about 17 km in parts of the western WARS (Chaput et al., 2014). Recent analyses of geophysical data from the ASE shelf show that sedimentary sub-basins and tec-

tonic lineaments cross the shelf, some of which can be related to an eastern branch of the WARS (Gohl et al., 2013a,b; Kalberg and Gohl, 2014). A continuous 2D continental rise to shelf gravity model shows 12-29 km thick continental crust that seems to have been thinned during wide-mode rifting (Kalberg and Gohl, 2014).

Recent Apatite-He age trends derived from rock samples of the eastern Pine Island Bay infer rift-related block faulting (Lindow et al., 2011). In this context, it seems likely that the topographic depression of the present glacially-formed Pine Island Trough on the eastern ASE shelf may have originated by extensional tectonic activity related to development of the WARS. West of Pine Island Bay, thermochronological analysis of the Mt. Murphy block and its neighbouring areas reveals a history of differential burial and uplift that is interpreted in terms of Oligocene motions on a major fault system (Lindow et al., 2011).

5.4 Data acquisition and processing

5.4.1 Database

The gravity data comprise the satellite-derived Free-air gravity anomaly (FAA) from McAdoo and Laxon (1997) (Fig. 36c). We calculated the Bouguer anomaly (BA) (Fig. 36c) based on the FAA and the bathymetric grid of Nitsche et al. (2007, 2013), using a Bouguer reduction density of 2670 kg/m^3. Figure 36c shows a magnetic anomaly grid of the ASE (Fig. 36c). Gohl et al. (2013a) describe the experimental setup, data processing and gridding procedure from helicopter and shipborne magnetic data collected during two RV Polarstern expeditions in 2006 and 2010, and go on to interpret the grid with the help of a set of 2D forward models.

We constrained the crustal thickness and density distributions in our gravity model by using the results of published seismic reflection data and forward modelling of three seismic refraction profiles (Nitsche et al., 2000; Lowe and Anderson, 2002; Gohl et al., 2007; Uenzelmann-Neben et al., 2007; Weigelt et al., 2009, 2012; Uenzelmann-Neben and Gohl, 2012, 2014; Gohl et al., 2013b; Hochmuth and Gohl, 2013; Kalberg and Gohl, 2013; Gohl et al., 2013b; Kalberg and Gohl, 2014). Where no deep crustal seismic data are available, we used the results of a power spectral analysis of the gravity and magnetic data.

5.4.2 Data description

Free-air anomaly:

The FAA of the outer shelf is dominated by two gravity highs of up to +80 $mGal$ corresponding to the bathymetrically elevated Eastern and Western Outer banks (Gohl et al., 2013b) (Fig 36a). A characteristic feature of the middle shelf area is a major WSW-ENE trending negative anomaly with a minimum of -70 $mGal$, named the Amundsen Sea Embayment Low (Kalberg and Gohl, 2014). This anomaly is interrupted by the prominent northwest-southeast trending Peacock Gravity Anomaly (Cunningham et al., 2002) and continues north of Thurston Island as the Thurston Island Low (Kalberg and Gohl, 2014). Pine Island Bay at the inner shelf is divided by the north-striking glacial Pine Island Trough with a gravity low of -50 $mGal$.

Bouguer anomaly:

The gravitational influence of the bathymetry can be removed from the FAA by calculating the BA such that only the effects of rock density variations in the subsurface are retained. The inner shelf of the ASE is dominated by short wavelength anomalies of between 0 and +70 $mGal$ whereas the outer shelf shows predominantly long wavelength anomalies between -20 $mGal$ and +70 $mGal$ that

correlate with bodies modelled in recent magnetic data collected in the ASE (Gohl et al., 2013a). As in the FAA, the Amundsen Sea Embayment and Thurston Island lows (Kalberg and Gohl, 2014) appear as a WSW-ENE trending anomaly that dominates the middle shelf (Fig. 36b) and is interrupted by the positive Peacock Gravity Anomaly. The outer shelf area is dominated by a major Outer Low (Kalberg and Gohl, 2014) of up to +80 $mGal$. The boundary between the outcropping basement of the inner shelf and the sedimentary basin of the middle and outer shelf (Gohl et al., 2013a,b) corresponds to a step in the BA from 0 $mGal$ to +50 $mGal$.

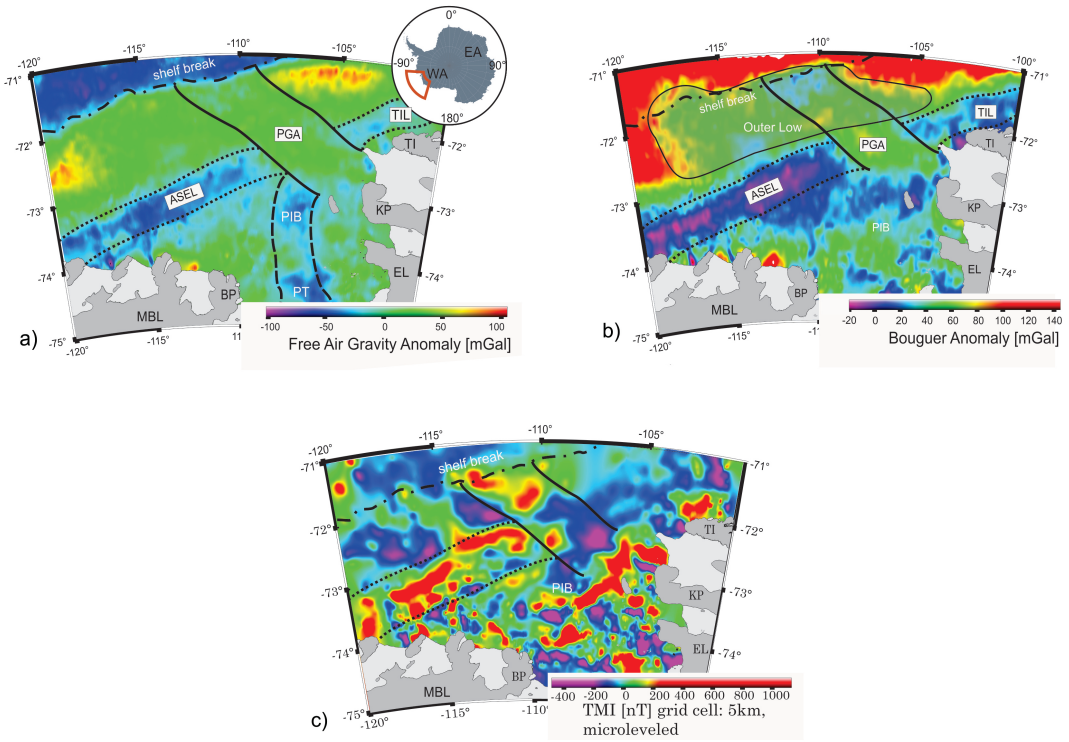

Figure 3

Figure 36: Compilation of gravity and magnetic data. Fig. 36a maps the satellite-derived free-air gravity anomaly of the Amundsen Sea Embayment (McAdoo and Laxon, 1997). The thin black dotted and continues lines mark prominent gravity anomalies along the middle and outer shelf of the Amundsen Sea Embayment. Figure 36b maps the calculated Bouguer Anomaly. The framed semi-transparent area beneath shelf break shows a prominent low (Outer Low). Figure 35c shows the magnetic anomaly map of the ASE (Gohl et al., 2013a). Abbreviations are: ASEL-Amundsen Sea Embayment Low, TIL-Thurston Island Low, PGA-Peacock Gravity Anomaly, PT-Pine Island Trough, BP-Bear Peninsula, MBL- Marie Byrd Land, EL is Ellsworth Land, TI is Thurston Island, KP is King Peninsula and PIB is Pine Island Bay.

Magnetic data:

The outer and the middle shelf areas of the ASE shelf are dominated by long wavelength NW-SE trending magnetic anomalies (Fig. 36c) which crossing the Peacock Gravity Anomaly (Fig. 36a and 36b). Recent studies have related these anomalies to fault-bounded basins formed by rift processes that occurred before break-up as early as 100 Ma and during break-up between 90 and 83 Ma (Gohl, 2012; Wobbe et al., 2012; Gohl et al., 2013a). The inner shelf shows predominately short wavelength anomalies (Fig. 36c). The transition from long to short wavelength magnetic anomalies is interpreted to be the signature of a boundary between sediment-covered basement and outcropping basement (Gohl et al., 2013a) (Fig. 36c).

5.5 Spectral analysis

As directly measured crustal thickness is only available from two seismic refraction profiles in the western ASE (Kalberg and Gohl, 2014) (Fig. 34b), we use spectral analysis of the potential field data to derive crustal thicknesses for the entire embayment. We calculated the depth of interfaces with significant density and susceptibility contrast by using a power spectral analysis of the FAA and the magnetic data. This method was initially developed for magnetic data (Spector and Grant, 1970) and upgraded for gravity data (Dorman und Lewis, 1970; Syberg, 1972; Karner und Watts, 1983).

The power spectral analysis is based on the assumption that the source of an anomaly field can be regarded as a collection of flat-topped prisms of different heights below the measurement surface. With this assumption, the natural logarithm of the power spectrum of the field should portray a set of linear facets when plotted against wave number (kr). The gradients of the facets can be used to interpret the mean depths to the sources.

We chose three sub-areas for the power spectral analysis. Ideally, the chosen areas should contain provinces of relatively uniform geology, but should also be large enough to resolve longer wavelengths and, therefore, greater target depths. Hence, the chosen window size of 200 km^2 is a result of a compromise for these considerations. The analysed areas cover the continental slope and rise (I) as well as the middle (II) and inner shelf area (III) (Fig. 33b). The uncertainty of the depth calculation is controlled by the sampling resolution and can be estimated to be around 2 km (Cianciara and Marcak, 1976). Studinger (2001) showed that the information contents in the low-frequency parts of the spectra of satellite-derived and aero-gravity data are comparable, and thus that the differences between crustal thickness estimates based on the two sources are negligible.

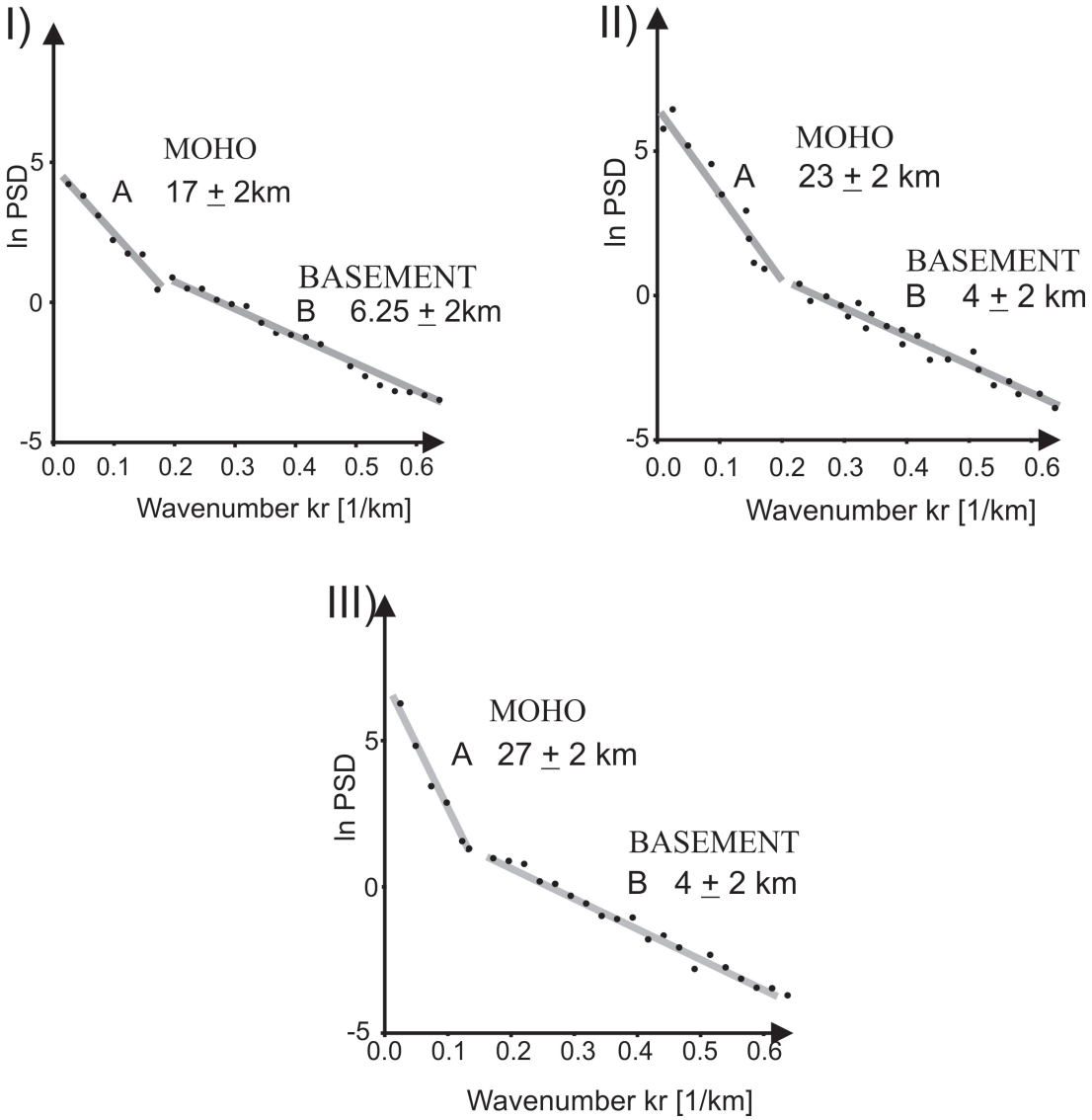

Figure 37: Power spectrum analysis of free-air gravity data of McAdoo and Laxxon (1997) (Fig. 36a). I, II and III are plots of the natural logarithm of the radially averaged power spectra (PSD) as a function of radial wave number kr. Plots I-III correspond to divisions shown in figure 34b. The black dots show the values of the energy spectra and the grey lines are the result of a linear regression for the depth estimation. Anomaly mass depth is presented in km. Mean depth to anomaly mass depth are estimated from the slope of the corresponding PSD's are shown.

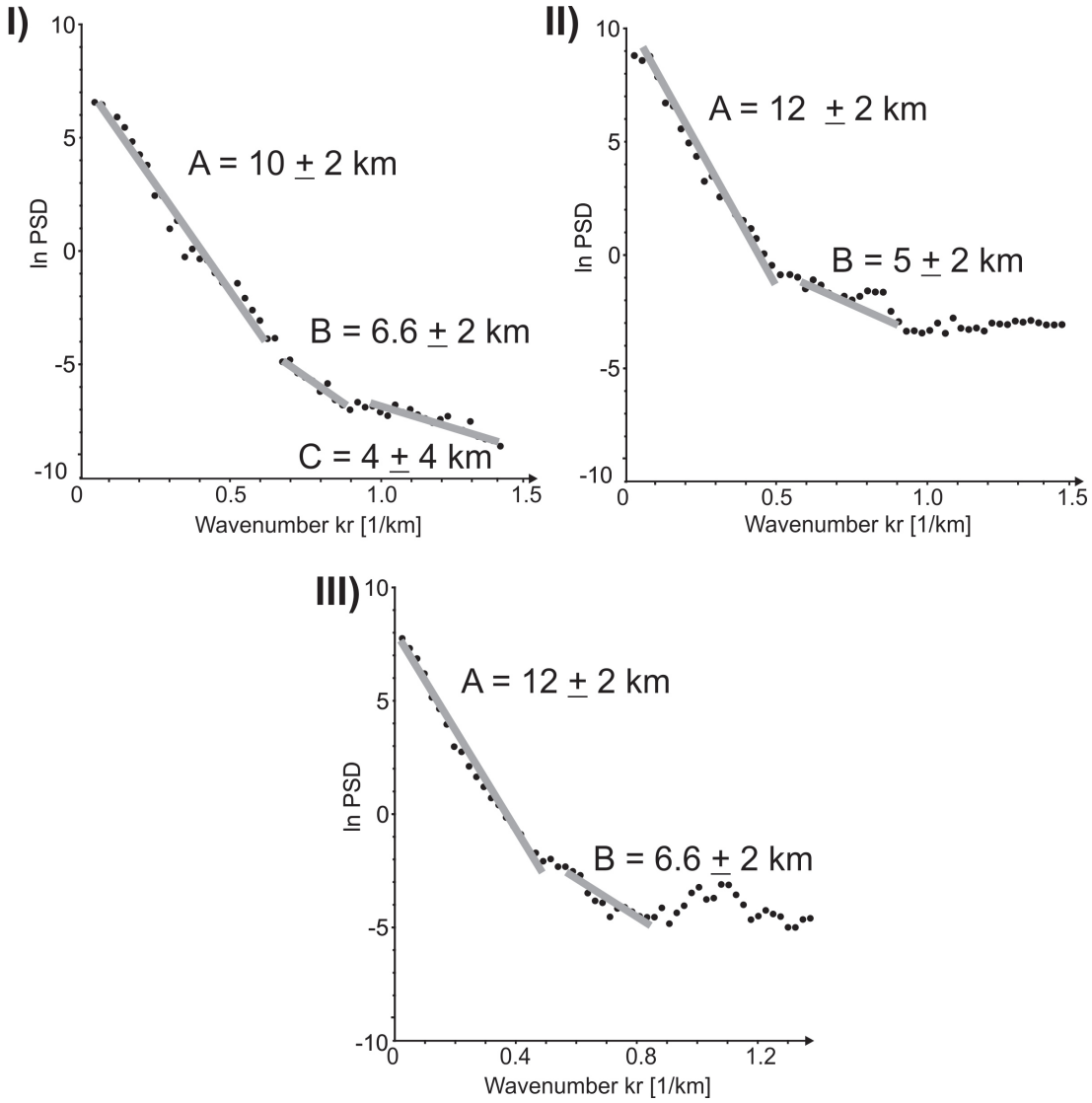

Figure 38: Power spectral analysis of magnetic data (Fig. 36c). I, II and III are plots of the natural logarithm of the radially averaged power spectra (PSD) as a function of radial wave number kr. Plots I-III correspond to divisions shown in figure 34b. The black dots show the values of the energy spectra and the grey lines are the result of a linear regression for the depth estimation. Anomaly mass depth is presented in km.

The results of the power spectral analysis are presented in Figures 37 and 38. At first glance, it is evident that the crustal thickness estimates based on the power

spectral analysis and the crustal thickness derived from seismic refraction data (Kalberg and Gohl, 2014) are comparable. The power spectral analyses of the FAA in all three sub-areas show two linear segments corresponding to distinct density interfaces (Fig. 37). At the Nyquist wave number (0.50 km^{-1}), the power spectrum flattens out in the high-frequency domain and gives way to white noise. Spectral analysis of Gohl et al. (2013a) magnetic anomaly grid of the ASE reveal three linear segments in all three areas (Fig. 38). Similar to the gravity data, the power spectral analysis of the magnetic data flattens out at high frequencies and gives way to white noise at a Nyquist wave number of 0.80 km^{-1}.

5.6 Potential field modelling

We used the potential field forward modelling software IGMAS (Götze et al., 1988) to calculate the 3D effects of anomalous bodies in the subsurface. The gravity or magnetic effect is calculated for a set of triangulated polyhedrons generated from polygons drawn along parallel vertical cross-sections. Density or magnetic susceptibility values are then assigned to each of these polygons. Our starting model comprises 22 parallel vertical planes, which are orientated from north to south and cross the shelf break of the ASE. The spacing between each pair of 500 km long planes is 25 km. The modelled area presented in this study covers an area of 275000 km^2 between 70°S and 74°S and between 104°W and 120°W (Fig 34b). To avoid edge effects, the flanking planes (planes 1 and 22) are modelled at distances of 1000 km eastward and westward of the region.

5.6.1 Density-depth modelling

To simplify our starting model, we treated all the sedimentary units as a single layer with an average density of 2050 kg/m^3. We used a maximum model depth below sea-level of 30 km. P-wave velocities of the crystalline crust in the ASE infer continental affinity (Kalberg and Gohl, 2014). We used the velocity-density relationship for continental crust of Barton et al. (1986) for calculating crustal densities based on the seismic refraction data. The upper-crustal density was 2650 kg/m^3 and the lower-crustal density was 2800 kg/m^3. Further, we modelled an intracrustal layer based on latest seismic refraction observations in the Embayment with a density of 3150 kg/m^3 (Kalberg and Gohl., 2014) as well as magmatic intrusive bodies with a moderate high density of 3000 kg/m^3. Finally, the uppermost mantle was modelled with a density of 3300 kg/m^3.

The standard deviation between the observed (Fig. 39a) and modelled FAA (Fig. 39b) is 6.78 $mGal$ for the entire ASE. Differences between the modelled and the measured FAA can be explained by out-of-plane effects and edge effects at the shelf edge. Uncertainty of 100 kg/m^3 for the density of the high-density body infers an uncertainty of 1 km in crustal thickness. The depth of the Moho below sea-level increases from 14 km at the continental rise to 29 km at the inner shelf of the ASE (Figs. 40, 41 and 42a). Above this, the entire ASE is underlain by a high-density lower crust of thickness varying between 1 and 10 km, from north to south (Fig. 40).

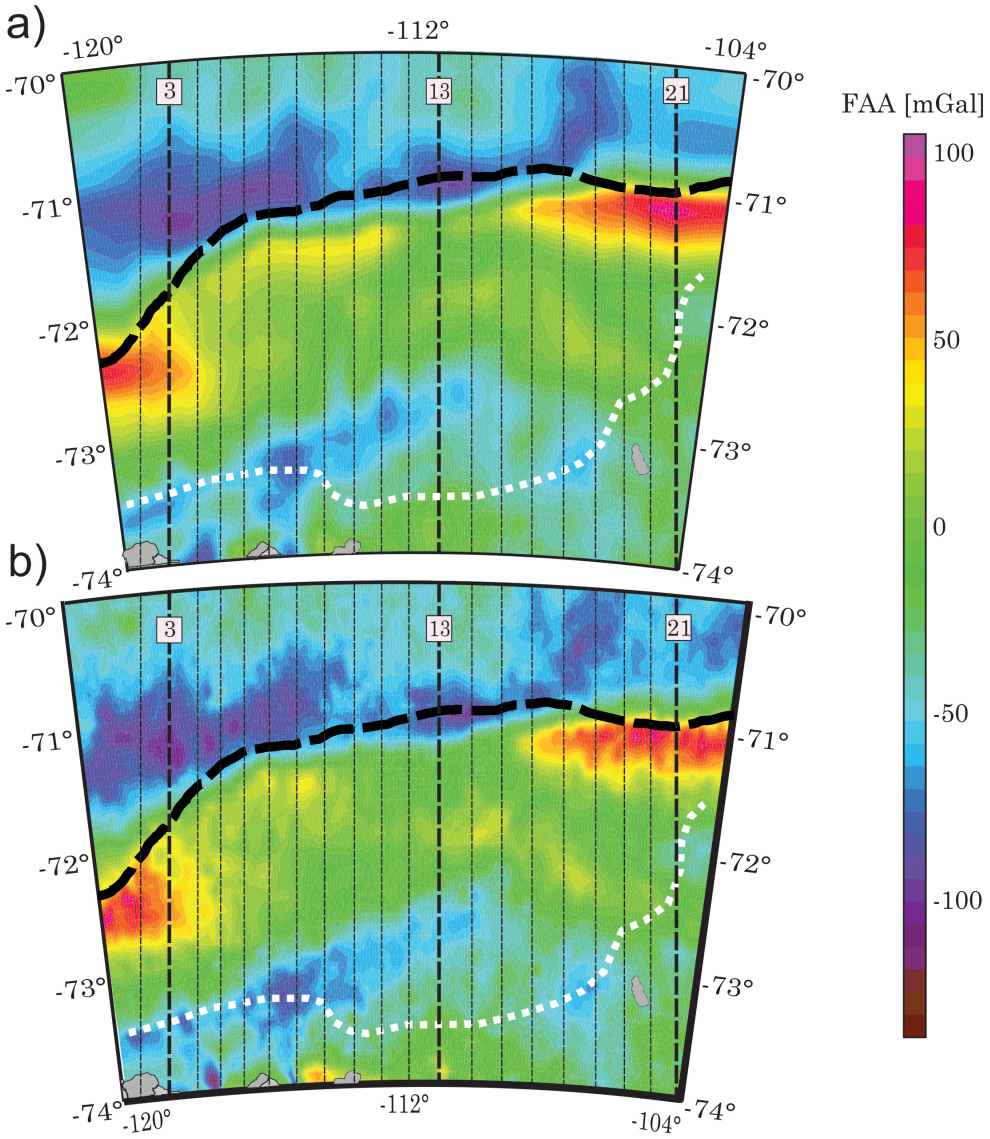

Figure 39: Figure 39a maps the modelled free-air gravity anomaly of the Amundsen Sea Embayment. Fig. 39b images the measured free-air gravity anomaly (McAdoo and Laxon, 1997). The three vertical thick black dashed lines show the position of three example vertical layers 3, 13 and 21 which are shown in Fig. 40. Thin dashed vertical black lines show the position of all other model layers which are shown in Fig. 41. The thick black dashed line image the shelf break and the dashed white line shows outcropping basement (Gohl et al., 2013a,b).

At the continental rise in the eastern embayment, we modelled the top of basement at 7.5-9.0 km to be covered by 1.0-4.5 km of sedimentary rocks. This geometry is confirmed in seismic and bathymetric data (Fig. 42b) (Gohl et al., 2013a,b; Kalberg and Gohl, 2014; Nitsche et al., 2007, 2013). The outer shelf of the western embayment is characterized by shallower basement at 4 to 5 km depth beneath the Western Outer Bank (Gohl et al., 2013b). Seismic data confirm the model depiction of a shallower level basement over parts of the shelf edge of the eastern embayment (Fig. 39b; Hochmuth and Gohl, 2013). The model shows NE-SW trending basins crossing the central and eastern parts of the middle shelf, filled with 6 km or more of sediments (Fig. 39b). South of these basins, the top-of-model-basement is only very shallowly buried or exposed (Fig. 39a and b), as can be observed or inferred in seismic and magnetic data (Gohl et al., 2013a,b).

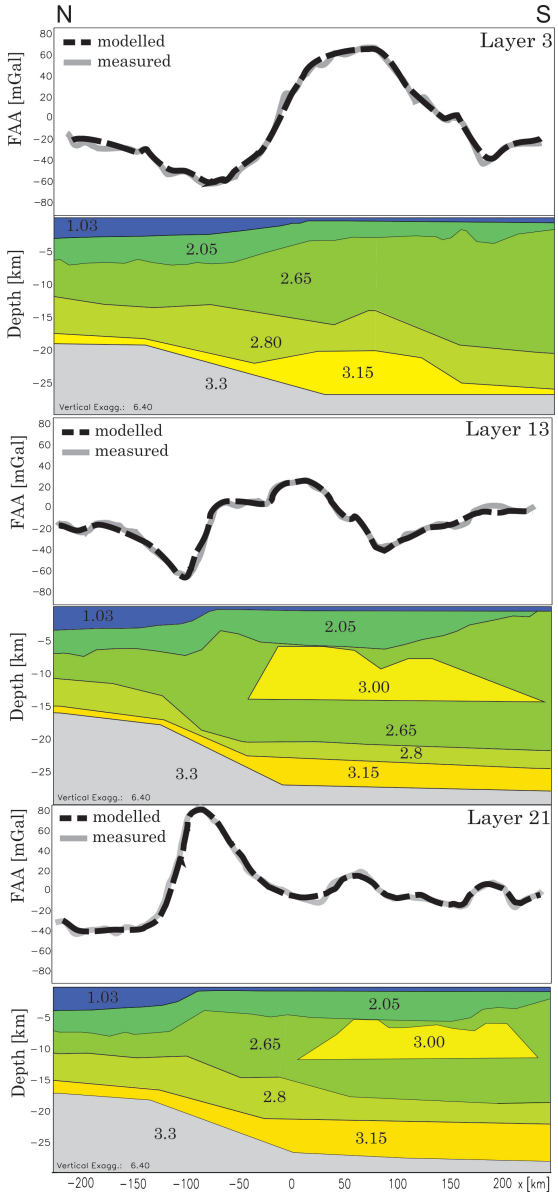

Figure 40: 2D forward gravity models of the example layers 3, 13 and 21. Database is the satellite-derived gravity data from McAdoo and Laxon (1997), crustal informations derived from a spectral analysis of the satellite-derived gravity data of McAdoo and Laxon (1997) and a previous 2D model in the western embayment (Kalberg and Gohl, 2014). Bathymetric surface is after Nitsche et al., (2013). Density values are given in $10^3 kg/m^3$.

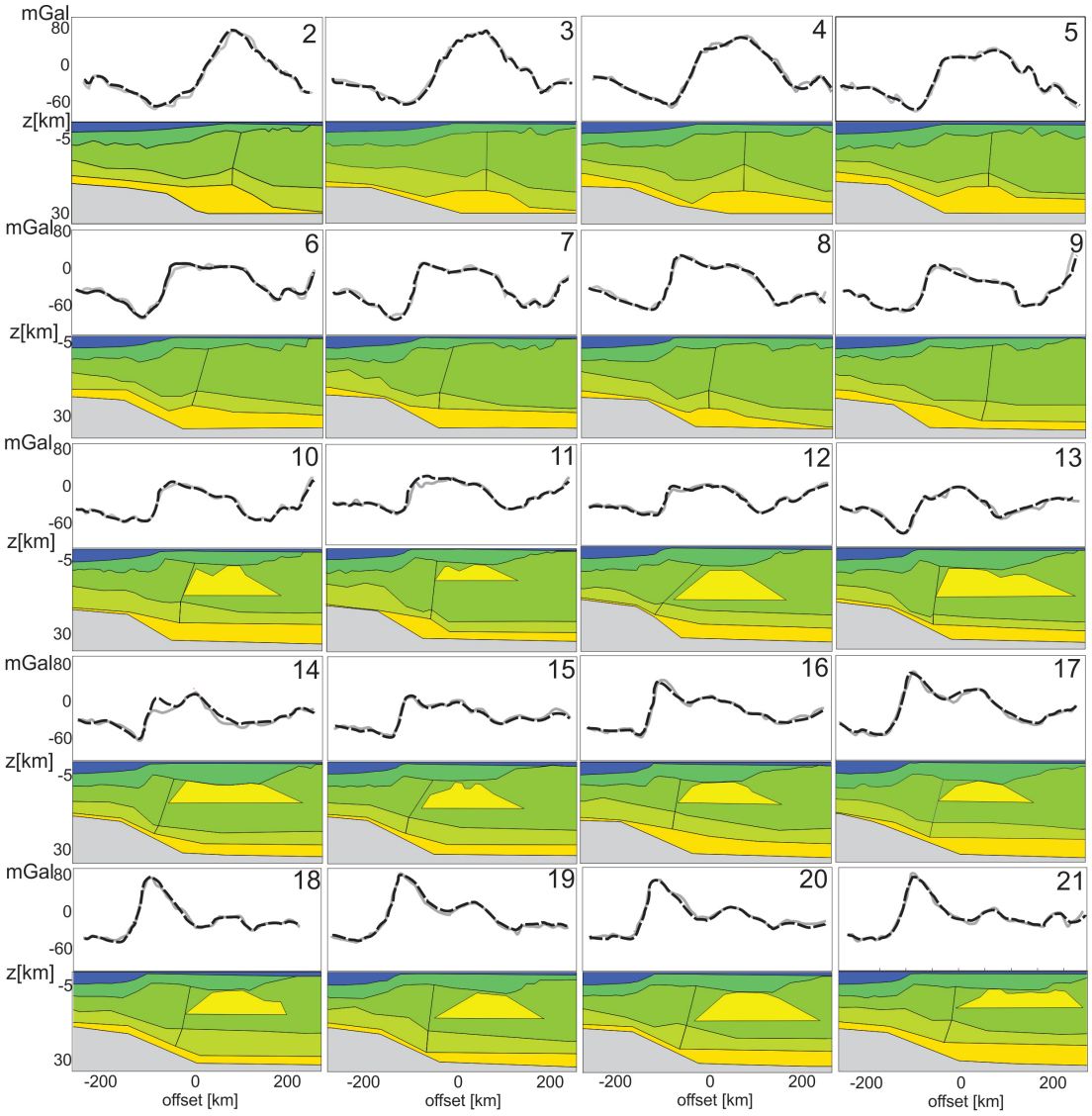

Figure 41: 2D forward gravity modelling results of all layers. Database and density-colour codification is the same as for the three example layers in fig. 40.

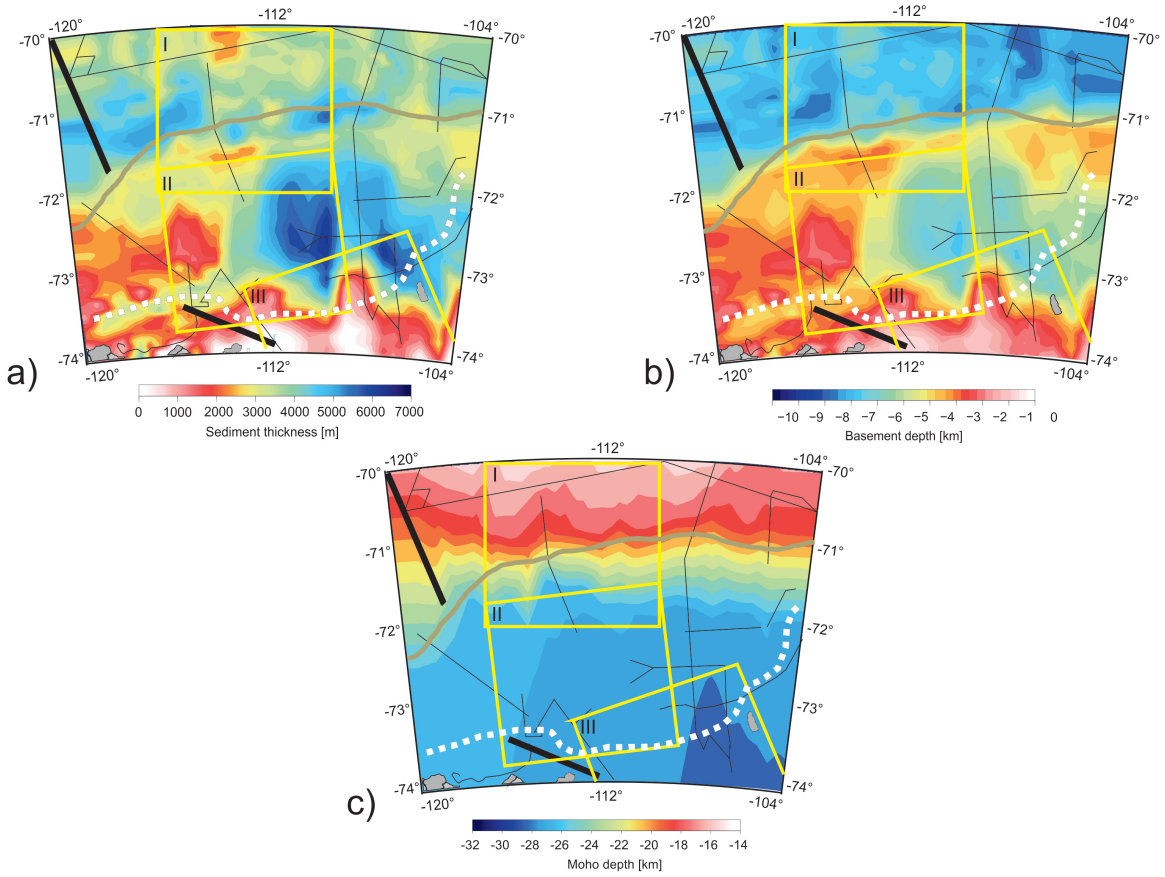

Figure 9

Figure 42: Features derived from 3D forward gravity modelling. a) sedimentary thickness map of the Amundsen Sea Embayment. b) crustal thickness in the ASE. c) Moho depth. Thin black lines illustrate multi-channel seismic reflection profiles and the two thick black lines show deep crustal seismic refraction profiles in the western embayment (Kalberg and Gohl, 2014). The three yellow frames show the windows I-III which were used for spectral analysis of the magnetic and gravity data (Fig. 34b). The thick white dotted line shows the northerly limit of outcropping or shallow basement as interpreted from magnetic anomalies (Gohl et al., 2013a,b).

5.6.2 Magnetic modelling

Magnetic modelling used a magnetic declination of 30°, an inclination of -65° and a 52000 nT background reference field (Maus et al., 2010). Depth estimates based on spectral analysis of our magnetic anomaly data provided constraints for an initial 3D magnetic anomaly model. Further, results of an Euler deconvolution (Gohl et al., 2013a) were used to locate the tops and edges of magnetic sources. The Euler deconvolution suggests the tops of distinct source bodies may be found at depths of 7 km below sea-level on the outer and the middle shelf, but that the tops of inner shelf source bodies may be much shallower (Gohl et al., 2013a). The maximum model depth was fixed at 16 km in view of an estimated Curie depth of 16 km beneath the central ASE shelf (Denk, 2011). Above this, the top of basement was estimated from seismic data (Weigelt et al., 2009, 2012; Gohl et al., 2013b; Kalberg and Gohl., 2014).

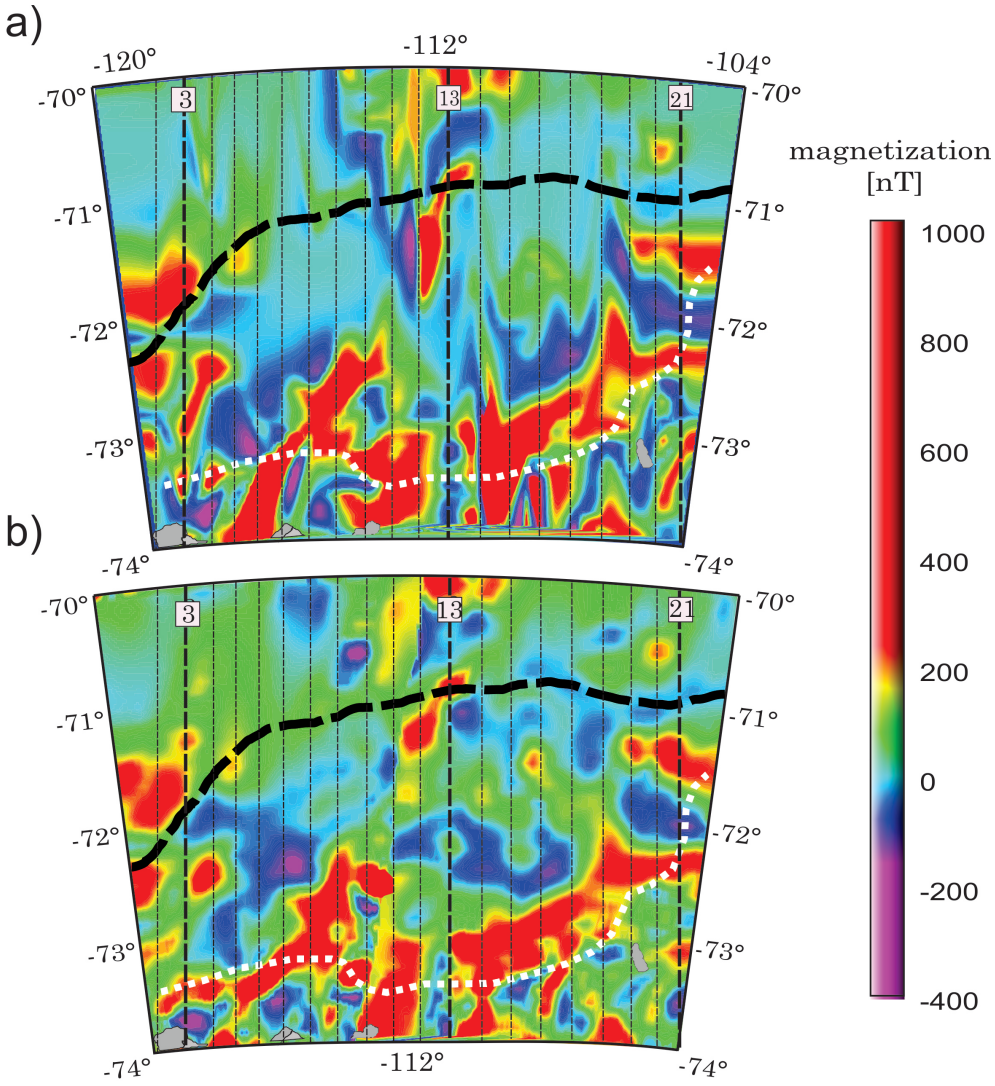

Figure 43: Figure 43a shows the modelled magnetic anomaly map of the Amundsen Sea Embayment. Fig. 43b images the measured magnetic anomaly map (Gohl et al., 2013a). The three vertical black dashed lines show the position of the three example slices 3, 13 and 21 which are shown in Fig. 44 and the thin dashed lines show the locations of all other slices. The thick black dashed line images the shelf break and the thick white dashed line marks the outcropping basement (Gohl et al., 2013a,b).

Although the magnetic susceptibilities of different rock types can vary by several orders of magnitude, it is possible to use them to distinguish generally between sedimentary (0.000005 SI), mafic (0.0001-0.13 SI) or felsic (0.0001-0.02 SI) rock compositions (Domack et al., 1992; Sanger and Glen, 2003). In our model, we used susceptibilities of 0.000005 SI for the sedimentary layer, 0.001 SI for the crystalline continental crust, and 0.08 for mafic intrusive bodies. The standard deviation between the measured (Fig. 43a) and modelled total anomaly field (Fig. 43b) is 50.8 nT which corresponds to a model error of about 3.5 percent. As for the gravity model, differences between the modelled and the measured magnetic anomalies can be explained by out-of-plane and edge effects of intrusive bodies.

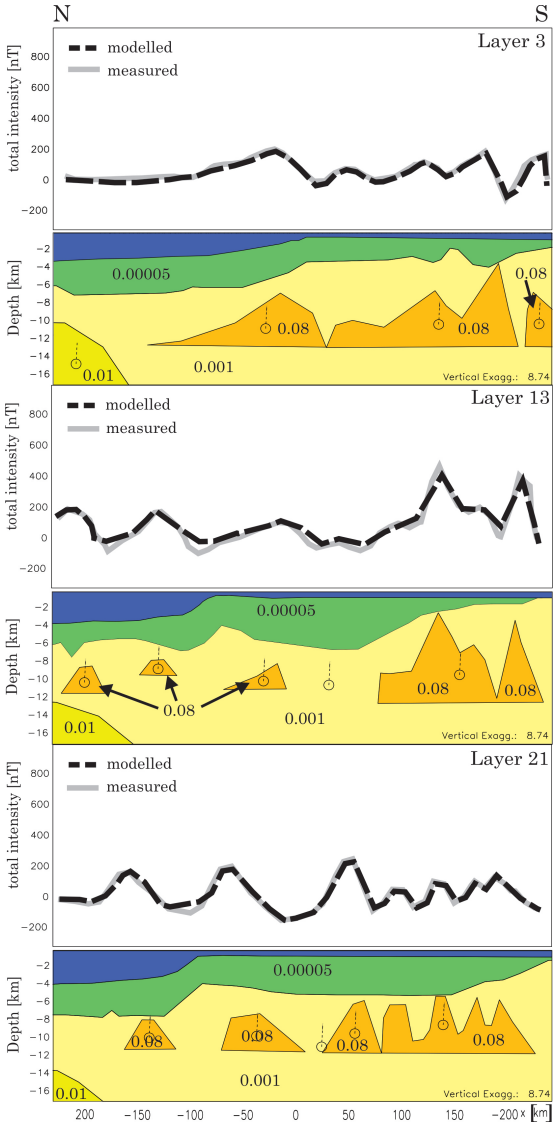

Figure 44: 2D forward magnetic models of the example layers 3, 13 and 21 (Fig 43). Database is the measured magnetic anomaly map of the ASE from Gohl et al. (2012), mass anomaly depth estimations derived from a power spectral analysis of the magnetic data (Fig. 36c) and a previous 2D magnetic model in the western embayment (Gohl et al, 2012). Bathymetric surface is after Nitsche et al., (2013) and the basement structure was derived from seismic observations. Susceptibility values are given in SI.

For simplicity, and given the lack of independent constraints, we used a single susceptibility value for all intrusive bodies in the embayment. Below the outer and middle shelf, most of the source bodies are deep-seated, whereas intrusions below the inner shelf top close to the seafloor. In contrast to the gravity modelling, the basement morphology has no significant influence on the long wavelength magnetic anomaly field. Magnetic anomalies associated with the basins of the middle and inner shelf of the eastern embayment are modelled by susceptibilities consistent with the presence of mafic intrusions (Figs. 44 and 45). The locations of the strong susceptibilities correlate with modelled high-density bodies in the 3D gravity model (Figs. 40 and 41).

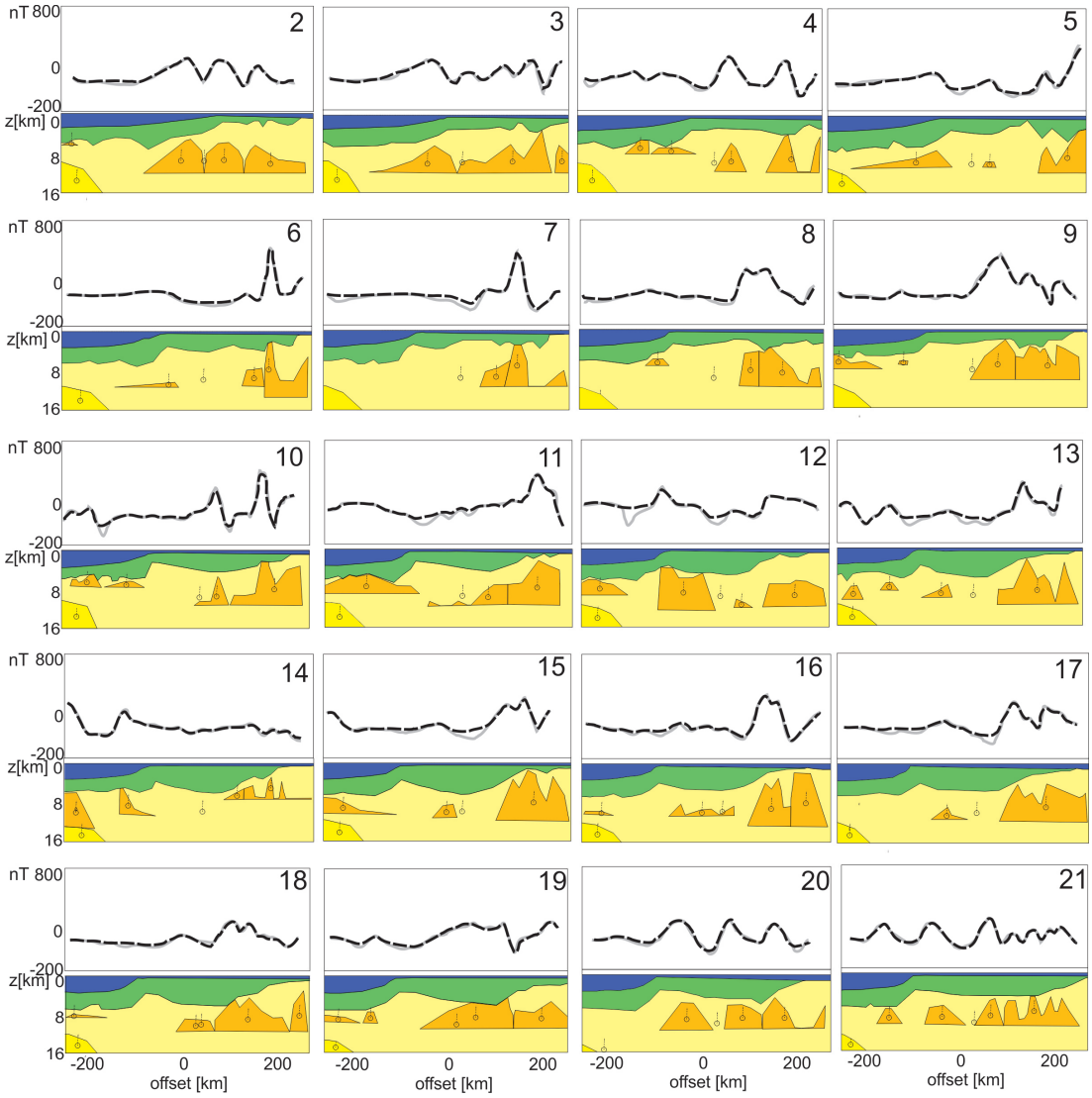

Figure 45: 2D forward magnetic models of all layers. Database and susceptibility-colour codification is similar to the three example layers in fig. 44.

5.7 Elastic thickness estimation

The effective elastic thickness (Te) of the lithosphere gives an idea of lithospheric rigidity, and is calculated via its flexural response to sedimentary or topographic loading under the assumption that this response is like that of an elastic plate with thickness Te (Watts, 2001). As temperature is considered to be a control on lithospheric strength, the flexural rigidity of the lithosphere might be expected to increase with time since rifting of part of the lithosphere and so might be used to determine the rifting process.

We used the software *LITHOFLEX* to obtain an estimate of flexural rigidity in the ASE (Braitenberg et al. 2007). LITHOFLEX provides a suite of utilities to study the isostatic state, rheologic properties and the elastic thickness of the lithosphere. In addition, the program includes a set of utilities that allow forward and inverse calculation of the gravity field. LITHOFLEX requires the crustal load and Moho depth, which are available from our 3D density-depth model (Figs. 40, 41 and 42) and seismic data (Gohl et al., 2013b; Kalberg and Gohl, 2014). The crustal load can be defined by the so-called equivalent topography or rock equivalent topography (RET). RET is a representation of the topography of the Earth that combines ocean water and ice into layers equivalent to the density of topographic rock, while keeping the water and ice masses constant. Hence, RET allows the computation of the gravity effect based on a single constant mass-density layer.

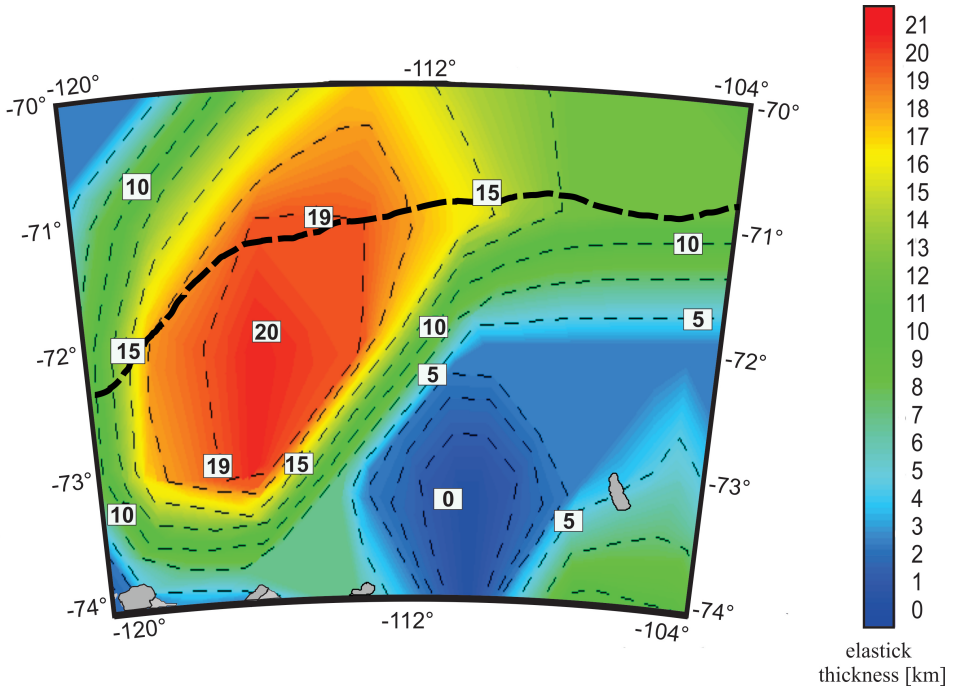

Figure 46: Map of the effective elastic thickness (Te) of the lithosphere of the Amundsen Sea Embayment. Values are given in [km]. Thick black dashed line marks the shelf break.

We calculated RET with LITHOFLEX using the bathymetry of Nitsche et al. (2007; 2013), the water density (1030 kg/m^3) and an average crustal density (2800 kg/m^3) (Kalberg and Gohl., 2014). As the ice sheet in the ASE sector is grounded relatively far inland of the rifted parts of the ASE, we ignore the effect of the ice sheet and argue that this has no significant influence on the isostatic state of the shelf. We calculate the flexural rigidity with respect to the known sedimentary cover and the known crustal thickness. Based on this method, it is possible to divide the ASE into different lithospheric areas, which can be interpreted according to their geological significance. The best fitting lithospheric Te model (Fig. 46) exhibits an elastic thickness increasing from 10 to 15 km in the eastern embayment, from 10 to 20 km in the western embayment and from 0 to 5 km in Pine Island Bay, which is therefore the weakest part of the ASE.

5.8 Interpretation and Discussion

Lithospheric and crustal structure

The transition from oceanic to continental crust can be clearly identified at a gradient towards more positive values beyond the shelf break in the Bouguer anomaly (Fig. 36b). The Outer Low over the Western Outer Bank of the ASE shelf (Fig. 36a) comprises a terrace in this signal and a basement terrace in our gravity model. Unlike in the FAA, the BA signal is not ubiquitous beneath the outer shelf, indicating that its source is not of topographic nature. We interpret it to indicate a buried horst block, possibly a remnant from Cretaceous extension that led to the separation of West Antarctica and Zealandia.

The basement morphology in the ASE is interpreted to be the result of distributed crustal rifting and deformation, leaving a buried network of failed rifts and rift-related accommodation zones (Gohl et al., 2013b; Kalberg and Gohl, 2014). These sedimentary sub-basins of the middle and outer shelf can be related the long tectonic history of the embayment. The basement ridge in the western embayment (Fig. 42b) follows an ENE-WSW trending positive gravity anomaly (Fig. 36a and Fig. 36b) and might be related to uplift over a high-density magmatic layer, possibly a part of a lithospheric mantle, transported from Marie Byrd Land by a postulated continental insulation flow (Kalberg and Gohl, 2014; Kipf et al., 2014) (Fig. 40).

The basement topography of the western embayment (Fig. 42 and 43) may have determined its preglacial geomorphology. We infer that the basement ridges (Fig. 41a) may have set the template for past ice flow trends as has been interpreted for the eastern embayment (Gohl et al., 2013b; Hochmuth and Gohl, 2013). The two deep sub-basins in the eastern embayment also parallel the major glacial troughs such as the Pine Island Trough and Abbot Trough.

The intrusive bodies of moderately high-density (3000 kg/m^3) are interpreted to consist of cumulated gabbro resulting from partial melting of the lithospheric mantle.

The correlation between these high-susceptibility and high-density bodies is better in the eastern than in the western embayment. Only mafic intrusions produce both significant magnetic and positive gravity anomalies (Sterritt, 2006). Hence, we suggest the eastern embayment hosts a greater concentration of mafic intrusions than the western embayment, where intrusions may be of more felsic composition. Thus, the sources of the intrusions are from different fractionation processes of the melt. Mafic intrusions in the eastern embayment can be related to the Dorrel Rock intrusive complex in Marie Byrd Land which is an emplacement of the gabbro from abot 34 Ma (Rocchi et al., 2006), implying that a major magmatic event in late Cenozoic affected the Amundsen Sea margin (Kalberg and Gohl, 2014).

We attribute the felsic intrusions in the western embayment to decompression melting during WARS-related extension (Gohl et al., 2013a,b), the presence of a mantle plume beneath Marie Byrd Land (e.g. LeMasurier and Landis, 1996) or to the large Southwest Pacific Diffuse Alkaline Magmatic Province as postulated by Finn et al. (2005). For example, Trua et al. (1999) proposed that felsic intrusions can be generated by partial melting of gabbroic material followed by low-pressure fractionation. However, a conclusive process cannot be stated based on our data.

Assuming a normal lower continental crustal layer in the Amundsen Sea Embayment, the expected density would be around 2800 kg/m^3. This is significant lower than the observed 3150 kg/m^3 (Kalberg and Gohl, 2014). The density of this observed layer seems to be also too high for magma of Phanerozoic origin but the occurrence of cumulated layers could significantly rise the density of parts of the crustal material. A similar high-density/high-velocity layer of 10-15 km thickness was observed beneath normal continental lower crust of the Ethiopian Rift by Mackenzie et al. (2005). They interpret a density of about 3170 kg/m^3 as a result of Oligocene underplating of mafic material. We infer a similar process of margin-wide magmatism in the embayment (Kalberg and Gohl., 2014), possibly related to a magmatic insulation flow (Kipf et al., 2014).

Te and rifting:

Our calculated lithospheric elastic thickness Te of 0-5 km for the eastern ASE and PIB (Fig. 46) correlates with the NNW-SSE trending thick sedimentary basin in the eastern embayment (Fig. 42; and in Gohl et al., 2013b) and with a small positive Bouguer gravity anomaly (Fig. 36b). Unlike the positive BA associated with sedimentary basins in the Ross Sea Rift, where Te is greater (Karner et al., 2005) therefore, it seems unlikely that the BA could be seen as the consequence of a time lag between mantle uplift during Cretaceous rifting of a weak lithosphere (Te = 0 km), followed much later by regionally-compensated Cenozoic sedimentation over a strengthened lithosphere (Te = 30 km).

Latest gravity inversion results of Cochran et al. (2015) suggest that the ASE shelf has been tectonically inactive since Cretaceous extension and continental breakup. They relate the post-breakup architecture of the embayment and shelf to be the result of subsidence, sedimentation and the advance-retreat cycles of the West Antarctic Ice Sheet. However, our Te estimates are similar to those over young continental rift zones such as the Basin and Range Province (Te =

5km) (Lowry and Smith 1994) or the Afar region, followed by the Main Ethiopian rift (Te = 7km) (Pérez-Gussinyé et al., 2005). We therefore suggest that the low rigidity and the positive Bouguer anomaly of the eastern ASE shelf are signals of fairly recent rift events, possibly related to younger WARS activity (Gohl et al., 2013b) overprinting the Cretaceous extensional phases.

Tectono-magmatic implications:

The lower crust in the Amundsen Sea Embayment with a density that is significantly higher than that of normal lower crust in the region suggests widespread magmatism. This is in agreement with the hypothesis of a continental insulation flow transporting HIMU-like material from beneath western Marie Byrd Land to the Marie Byrd Seamounts at 80-60 Ma (Kipf et al., 2014). Kalberg and Gohl's (2014) schematic tectono-magmatic reconstruction of a 2D continental rise to shelf gravity model is in agreement with this interpretation (Kalberg and Gohl, 2014) which suggests that the continental margin was magmatically underplated. Finn et al. (2005) attributed the Marie Byrd Seamounts to a Southwest Pacific Diffuse Alkaline Magmatic Province, sourced from the mantle over the paleo-Pacific subduction zone that preceded late Cretaceous rifting in the ASE region. This part of the mantle is characterised today by low shear velocities (Schaeffer and Lebedev, 2013) below Marie Byrd Land, the Ross Sea and the ASE.

However, the thickness of the lithosphere, and with it conceivably Te, decreases with increasing geothermal gradient that can result from extension or the advection of anomalously warm material (Ebinger et al. 1999; Buck, 2004). We observe a decrease in Te at the continental rise of the ASE through the middle shelf of PIB which correlates with the slow mantle shear wave velocities (Schaeffer and Lebedev, 2013). Similar observations were also made in the East African and Ethiopian rifts (e.g. Pérez-Gussinyé et al., 2009).

The NNE-SSW striking basin in the eastern embayment coincides well with the low Te values (Fig. 46). We suggest that this basin may have developed as a result of transtensional motion on branch of the WARS. As such, the basin may have a similar origin as the Ferrigno Rift (Bingham et al., 2012) or GVIS (Eagles et al., 2009). If, like in these analogues, the basin lay along part of the West-East Antarctic plate boundary zone and connected with the paleo-subduction zone west of Palmer Land and the Antarctic Peninsula, then it would date from some time soon after the around 61 Ma establishment of the East Antarctic-West Antarctic-Phoenix triple junction south of Peter I island.

5.9 Conclusions

Analyses of geophysical data from the ASE provide new insights into the lithospheric architecture and tectono-magmatic development of this part of the continental margin of West Antarctica. Our 3D gravity model supports and expands on previous 2D velocity-depth and density-depth models (Kalberg and Gohl, 2014) and enables an interpretation of the tectono-magmatic history for the ASE margin from its break-up with Zealandia to the present, indicating a margin-wide process of magmatic underplating. Our 3D magnetic model supports earlier interpretations of distinct magmatic events in the ASE. An estimate of the flexural rigidity completes the interpretation of the tectono-magmatic history. The main findings are summarized as follows:

1. 3D gravity modelling reveals the upper and lower crustal architecture beneath the shelf. The crust is 10 - 14 km thick at the continental rise, and up to 29 km thick beneath the inner shelf. A high-density layer of variable thickness, reaching a maximum of 10 km, is ubiquitous at the base of the lower crust. The high-density layer indicates a margin-wide process of magmatic underplating. The crust is intruded by numerous magmatic bodies.

2. 3D magnetic modelling suggests a set of high-susceptibility bodies that correlate more closely with the modelled magmatic bodies in the eastern embayment than in the western embayment. This suggests magmatic intrusions of more mafic composition in the eastern embayment and material of more felsic composition in the western embayment, and can be interpreted in terms of varying melt sources for the two regions. The mafic intrusions may correlate with the Dorrel Rock intrusive complex in MBL, implying a major magmatic event accompanied the multi-stage tectonic activity that

affected the Amundsen Sea margin during Oligocene. The interpreted felsic intrusions in the western embayment may be attributed to decompression melting during WARS-related extension, to a suspected mantle plume beneath MBL, or to the mantle source of the large Southwest Pacific Diffuse Alkaline Magmatic Province (Finn et al., 2005).

3. Lithospheric rigidity is low (Te of 0 - 5 km) under the Pine Island Bay segment of the eastern Amundsen Sea Embayment and corresponds to a shelf sub-basin observed in seismic records. The low Te supports an interpretation that Cenozoic rifting affected this segment of the ASE.

6 Crustal structure and sedimentary architecture in Wrigley Gulf/Marie Byrd Land, West Antarctica: Implications for the tectonic evolution and environmental changes from geophysical observations

Thomas Kalberg and Karsten Gohl

1. Dept. of Geosciences

Alfred Wegener Institute Helmholtz-Centre for Polar and Marine Research

Am Alten Hafen 26

27580 Bremerhaven, Germany

To be submitted to Marine Geophysical Research in September 2015

6.1 Abstract

Marie Byrd Land, West Antarctica, is characterized by higher topography than its surrounding area, which can be related to the presence of an anomalous underlying mantle. The temporal and spatial distribution of this mantle anomaly and its influence on the geomorphological development of the West Antarctic continental margin and the entire South Pacific have been subject of vigorous debates. During the RV Polarstern cruise ANT-XXVI/3 (2010), a geophysical dataset was collected offshore Marie Byrd Land consisting of seismic reflection data, ship-borne gravity and bathymetry data in order to study the regions sedimentary and the crustal structure and their implications for uplift of the Marie Byrd Land margin.

Sediment sequences of alternating reflectivity at the continental rise and on the shelf indicating changes in climate conditions during deposition and distinct tectonic events after break-up. A larger inclination angle than observed in sediments on other Antarctic shelves indicates that the impingement of mantle material results in crustal uplift after continental break-up. Our results show a 10-12 km thick Pratt-type compensated crust on the continental rise and an up to 27 km thick ocean-to-continent transitional crust beneath the continental rise and the shelf. The modelled crust is thicker compared to data from inland of Marie Byrd Land and coincides with the presence of a high density layer beneath the lower crust. We interpret this layer to be related to widespread magmatism.

6.2 Introduction

The continental margin of West Antarctica is of particular interest in reconstructing the tectonic development of West Antarctica. In a broader sense, it is also a key region in understanding the current rapid changes in climate, marine circulation and in particular the dynamic behavior of the West Antarctic

Ice Sheet (WAIS). The region is tectonically active despite its intraplate location which has been related to the presence of anomalously warm upper mantle, interpreted from unusually slow seismic velocities (Sieminski et al., 2003). Marie Byrd Land (MBL) is part of the West Antarctic continental margin, bounded by the West Antarctic Rift System (WARS) in the south and by an elevated, dome-like structure in the north (Fig. 47). This dome has been attributed to plume-related tectonic uplift (LeMasurier and Landis, 1996; LeMasurier, 2008). The plume seems to be similar in petrologic character, geologic history and size to the Kenyan and Ethiopian domes (LeMasurier, 2008).

Contrary to the plume model, recent studies propose that the elevated area is supported by a warm Pacific mantle rising beneath it following the end of subduction at the MBL continental margin, and that its volcanoes are part of a much larger SW Pacific Diffuse Alkaline Magmatic Province (DAMP) (Finn et al., 2005). Other studies propose two hot mantle anomalies of which the larger one is centred in the Ross Sea sector, resulting in up to 1 km of dynamic topography (Spasojevic et al., 2010). Sutherland et al. (2010) illustrated this topography in the seafloor off West Antarctica, which is elevated by 0.5 to 1.2 km above the level of its conjugate area south of New Zealand and predictions using the lithospheric age-subsidence relationship (e.g. Stein and Stein, 1992).

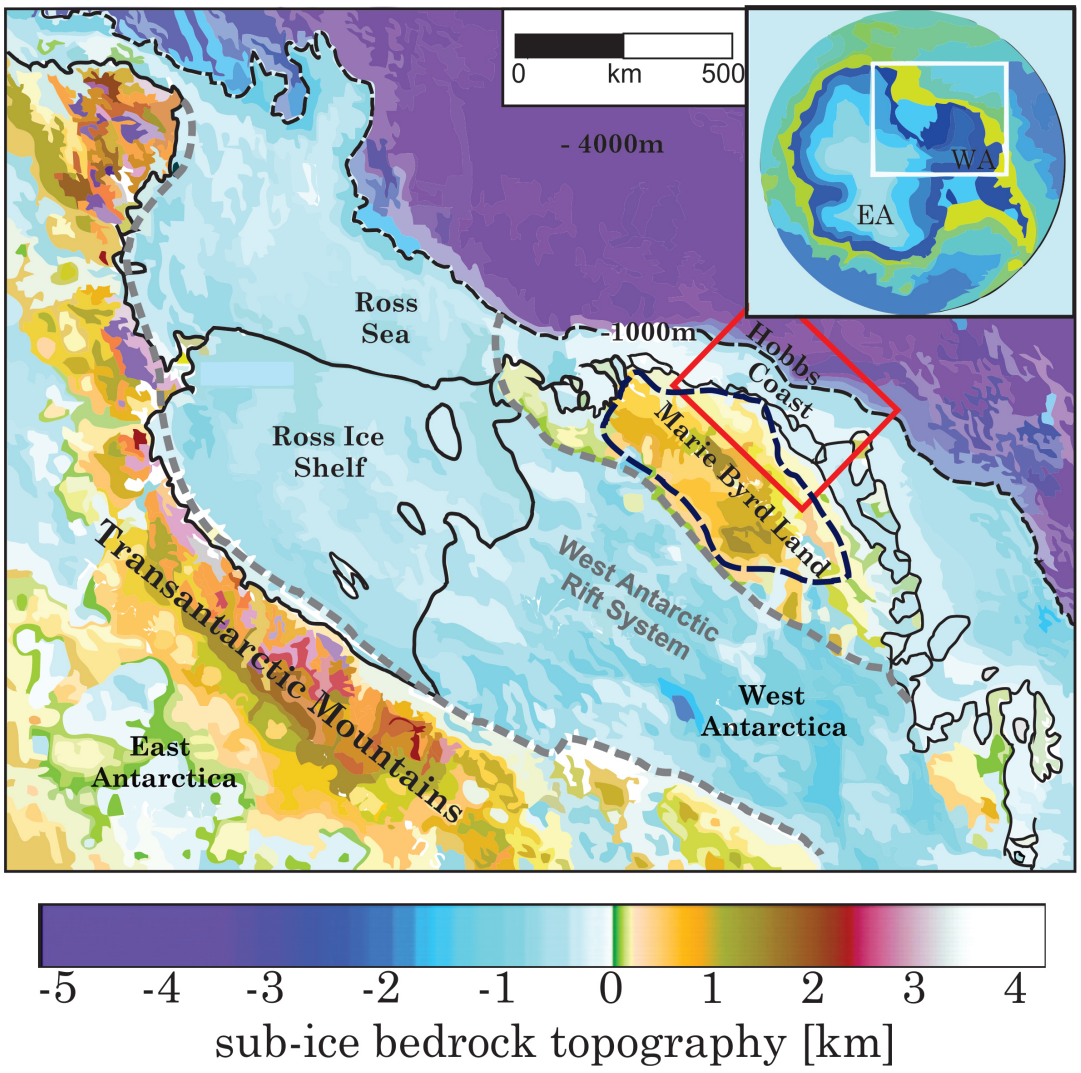

Figure 47: Subglacial elevation and bathymetry of West Antarctica, the Transantarctic Mountains, Ross Embayment and the Amundsen Sea Embayment. Inset shows reference location map. Both based on BEDMAP 2 (Fretwell et al., 2013). The Ross Sea is characterized by a series of basins and basement highs. Marie Byrd Land is highlighted by the dashed dark blue area. Ross Embayment: Ross Sea plus Ross Ice Shelf. West Antarctic Rift System: Ross Embayment plus extended parts of West Antarctica marked by thick grey dashed lines. Study area is highlighted in the red box. WA: West Antarctica, EA: East Antarctica.

Within the continents, mantle upwelling lead to tectonic uplift and widespread magmatism (Cox, 1989) such as in the Afar region of the East African Rift System (e.g. Marty et al., 1996) or the western cordillera in the United States (Parsons et al., 1994). LeMasurier and Landis (1996) and Sieminski et al. (2003) suggested that a mantle plume caused this uplift of central MBL beginning as early as 30 to 28 Ma and coincides with the inception of alkaline volcanism (Hole and LeMasurier, 1994).

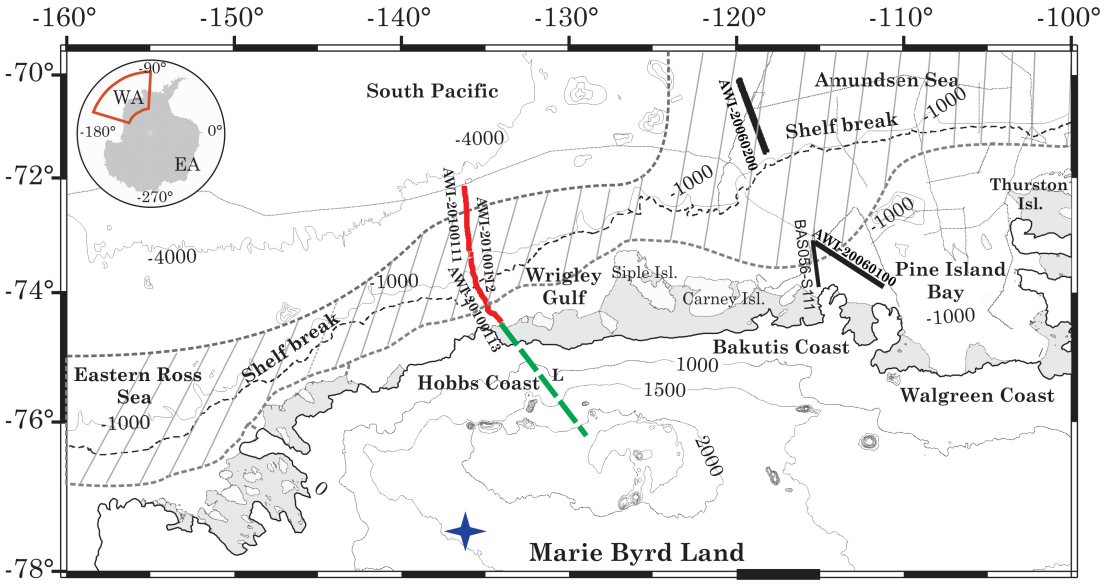

Figure 48: Overview map of the West Antarctic continental margin. Transect A includes seismic reflection profiles AWI-20100111, AWI-20100112 and AWI-20100113 (red). Thin black dashed lines are other seismic reflection profiles. AWI-20060100 (shelf) and AWI-20060200 (continental rise) annotate deep crustal seismic refraction profiles in the Amundsen Sea to the east. BAS056-S111 is a seismic reflection profile in the western Amundsen Sea Embayment (Gohl et al., 2013). The grey hatched area marks the continent-ocean transition after Wobbe et al. (2012). The green dashed line marks the distance L [km] of the dipping shelf sediments to the apex of the MBL dome. The blue star marks the seismic receiver function data point of Winberry and Anandakrishnan (2004).

However, two different hypotheses exist regarding the geomorphology of MBL and greater New Zealand during their Cretaceous continental break-up. One hypothesis suggests that the conjugate margins were at or near sea-level during break-up, and than MBL uplifted thereafter (LeMasurier and Landis, 1996; Rocchi et al., 2006). A contrary hypothesis postulates that the region was already elevated during continental break-up because of the presence of a mantle anomaly which causes uplift (Luyendyk et al., 2001; Sutherland et al., 2010).

This study uses the first geophysical data from Wrigley Gulf off Hobbs Coast, West Antarctica (Fig. 47), that were collected for their relevance to studies of the tectonic evolution and sedimentary architecture of this part of the continental margin. A seismic reflection transect from the continental rise onto the shelf (Fig.48) images the sedimentary architecture and the basement structure for the first time. In combination with seismic data from the neighbouring western Amundsen Sea Embayment (Gohl et al., 2007, Weigelt et al., 2009, Gohl et al., 2013, Kalberg and Gohl, 2014), the eastern Ross Sea (Luyendyk et al., 2003) and onshore receiver function results south of central MBL (Winberry and Anandakrishnan, 2004), a suite of simple 2D gravity models provide new constraints on crustal thickness estimations and mantle density beneath the MBL margin. Built from these constraints, our preferred model involves the presence of regional magmatic underplating, which can be associated with an anomalous mantle (Finn et al., 2005) or mantle plume (LeMasurier, 2008).

Uplift of central MBL has left its signature in the tectono-sedimentary architecture of the adjacent post-break up sediments on the inner shelf. The sedimentary architecture of the inner shelf off Hobbs Coast further provides indications for a near sea-level break-up between New Zealand and West Antarctica and uplift of MBL thereafter. Additionally, seismic reflection data from the continental rise and the inner shelf image changes in the reflection character which in turn represent changing environmental conditions during deposition and episodes of alternating major ice sheet advance and retreat that can be correlated to environmental changes.

6.3 Geological setting

Wrigley Gulf, off Hobbs Coast, is part of the West Antarctic continental margin which is conjugate to Campbell Plateau, south of New Zealand. Following their

separation 90-83 m.y. ago (Eagles et al..; 2004, Wobbe et al., 2012), Campbell Plateau underwent long-term subsidence. MBL, on the other hand, was affected by pure shear extension orthogonal to the Transantarctic Mountains until 28 Ma (Cande et al, 2000), and alkaline magmatism starting around 34 Ma (Rocchi et al, 2006) as part of activity of the West Antarctic Rift System (Fig. 47). Unlike the subsided Campbell Plateau, central MBL is characterized by a large (800 x 500 km) structural dome with an average elevation of 2700 m above sea-level and 3200 m above the glacial-isostatically corrected bedrock-surface elevation (Fig.1).

Late Cenozoic mafic igneous rocks are widespread in the Ross Sea and MBL with a geochemistry of HIMU-type magmatic rocks (high time-integrated 238U/204Pb) (Behrendt et al., 1991; Rocchi et al.,2002, Finn et al., 2005). Panter (2006) considered metasomatized lithosphere as source for alkaline magmatism in the area of greater New Zealand and adjacent continental fragments of Gondwana such as Marie Byrd Land. The timing of onset of metasomatic magmatism is constrained to between 500 and 100 Ma which coincides with subduction and the distribution of HIMU volcanism in the area (Panter, 2006). Rocchi et al. (2002) discussed a model alternatively to the plume hypothesis (e.g. LeMasurier and Landis, 1996; LeMasurier, 2008) to explain and correlate the regional tectonics, magmatism and plate dynamics in the WARS. They propose that origin and emplacement of magmatic material in West Antarctica are related to the reactivation of pre-existing trans-lithospheric faults, which triggered local decompression melting of an enriched mantle that was previously veined during a decompression episode associated with an amagmatic late Cretaceous extensional rift phase of the WARS.

A seismic shear-wave tomographic model of the upper mantle beneath the Antarctic plate shows a low-velocity structure extending from the asthenosphere down to the transition zone beneath the volcanic region of MBL (Sieminski et al., 2003). Teleseismic receiver function studies (Fig. 48) showed a 24 km thin crust just

south of the crest of the elevated part of MBL. The thinned crust is interpreted to be the result of crustal extension from the Cretaceous to middle Cenozoic (Winberry and Anandakrishnan, 2004). The MBL dome is 1 km higher than the top surface of this thickness of crust ought to lie if in simple isostatic equilibrium with normal-density mantle (Winberry and Anandakrishnan, 2004).

The timing of the onset of glaciation in Wrigley Gulf off Hobbs Coast is not tightly constrained, but drilling data and seismic profiles along the Pacific margin of Antarctica reveal extensive aggradation and progradation of the continental shelf during the late Cenozoic, which can be associated with glacial processes (Cooper et al., 2008). Weigelt et al., (2009) infer the onset of major glacial advances onto the continental shelf around West Antarctica in Miocene times and emphasize that the ice sheet in the Amundsen Sea Embayment responded sensitively in its expansion to environmental changes throughout the late Cenozoic. The first seismo-stratigraphic model of the ASE (Gohl et al. 2013) infer similar reflection characteristics compared to those on the Ross Sea shelf for which age models exist from drill records. A chrono-stratigraphic model for seismic units on the ASE shelf assign an Early Cretaceous age to the oldest sedimentary unit and a Pliocene to Pleistocene age to the top unit (Gohl et al., 2013).

6.4 Data acquisition and processing

A 290 km long transect of multichannel seismic reflection data (profiles AWI-20100111, -0112 and -0113) was acquired from the continental rise onto the shelf of Wrigley Gulf off Hobbs Coast during RV Polarstern cruise ANT-XXVI/3 in 2010 (Fig. 49). Three GI-Guns with a total generator volume of 2.2 liters (450 in^3) were used as seismic source. Shot interval of 10 s corresponds to a shot distance of 25 m. Profile AWI-20100111 was recorded with a 3000 m long digital streamer with 240 channels. Sea-ice required the deployment of an 600 m long

analogue streamer of 96 channels for profiles AWI-20100112 and AWI-20100113, both with a sampling rate of 1 ms. Standard data processing include common-depth-point sorting with a binning interval of 25 m, bandpass filtering, velocity analysis, stacking and poststack migration.

Various attempts were made to suppress sea-floor multiples on the shelf using FK-filtering, radon transformation and predictive deconvolution, but due to the small source energy and short offsets all attempts produced minimal results. Ship-borne gravity data were collected continuously with a KSS-31 sea gravimeter at a sampling rate of 1 s. The data were drift corrected by onshore reference measurements in Wellington, New Zealand and Punta Arenas, Chile. We reduced the data to free-air anomaly (FAA) with respect to the GRS80 gravity model using a standard processing procedure (Torge, 1989), including an Eötvös correction calculated with the ships navigation.

6.5 Results

6.5.1 seismic reflection data

Data from the continental rise reveal a relative smooth top of basement (Fig. 49). Four sedimentary units can be identified with a total two-way-time (TWT) thickness up to 1.5 s, corresponding to 1.5-2 km sediment thickness at CDP 66 - 7000, interrupted by two small seamounts. We distinguish several high-amplitude reflectors separating at least 4 distinct units apart from each other in the basin. These units are mostly continuous and with a nearly horizontal strata (Fig. 49). Unit 1 is of homogeneous, transparent and undisturbed strata and characterised by low reflectivity and little internal structure. Some internal, nearly horizontal reflectors can be identified within Unit 2. Unit 3 also shows some horizontal reflectors and internal structure which is of higher reflectivity than Unit 2. Unit 4 is characterised by high reflectivity. The top of basement reflector on the continental rise becomes slightly shallower towards the foot of the shelf slope. Chaotically deposited sediments, identified from undulating and rough reflectors, lie at the foot of the shelf. Other high-reflectivity strata near the bottom of the slope indicate turbidity currents and gravity slides.

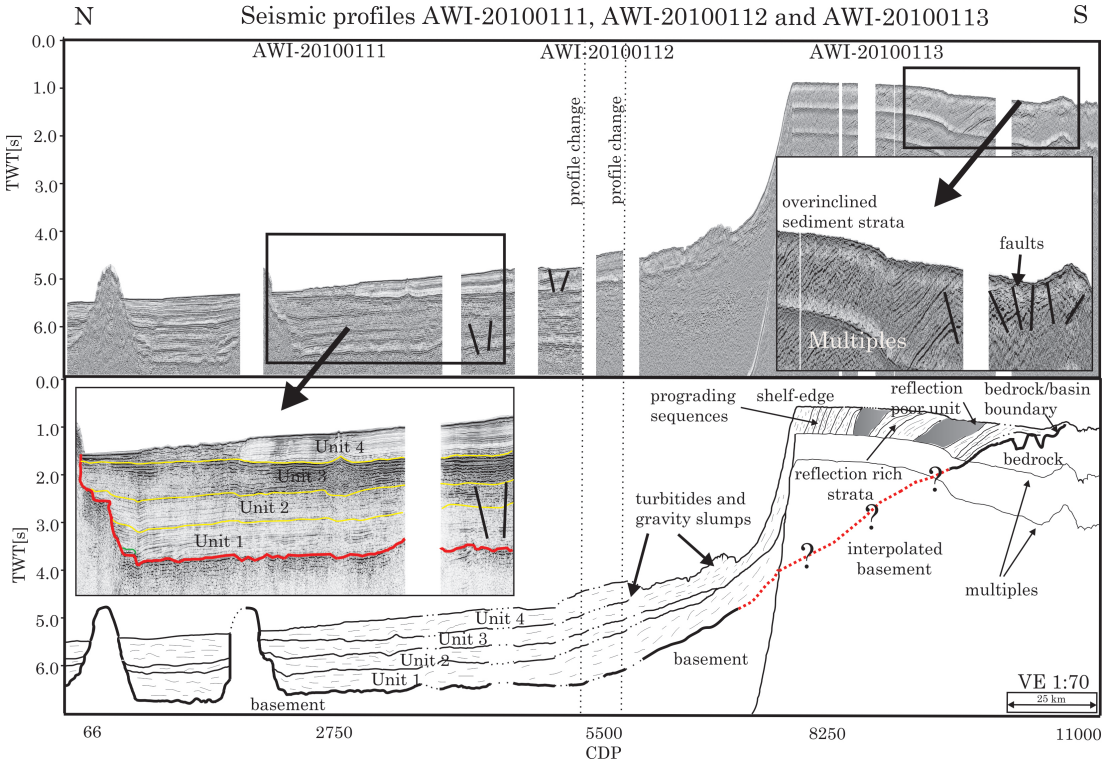

Figure 49: Compilation (top) and horizon interpretation (bottom) of seismic transect A from the continental rise to the inner shelf. Gaps in the data are airgun shutdowns. Continental rise Units 1, 2, 3 and 4 can be distinguished based on their reflection characteristics. Grey filled zones on the shelf mark sediment sequences alternating with sequences of closely-spaced, continuous reflectors within the over-inclined oceanward dipping strata. CDP distance: 25 m.

Seafloor multiples mask the signal from the top of basement and it disappears beneath the shelf edge. Seafloor relief on the 400-700 m deep shelf is relatively smooth. The seafloor deepens towards the inner shelf, which is typical for polar shelves (Anderson, 1999). A series of oceanward dipping units characterize the inner and middle shelf strata (Fig. 49). These units occur in packages that alternate between reflection-rich and reflection-poor.

Between CDP 7000 and 9500, the top of basement is interpolated to the inner shelf where it crops out. The dip of strata on the shelf increases from towards the shelf edge. Middle and inner shelf strata dip at around 4°, calculated based on a CDP interval of 25 m, a distance of 22.5 km (900 CDPs) and the thickness of the middle shelf sediments of about 1.5 km (Fig 51). Accuracy of the dip calculation is limited by the resolution of seismic reflection observations and can estimated to 0.2°. Sedimentary strata on the inner shelf are disrupted by basement-cutting normal faults (Fig. 49).

6.5.2 Gravity modelling

In order to test the model response of a suspected low-density upper mantle (LeMasurier and Landis, 1996, Sieminski et al., 2003, Finn et al., 2005) underneath central MBL, we calculated a suite of simple 2D gravity forward models (Fig. 50) of the measured FAA. We derived the constraints for our starting model from our bathymetric and seismic data as well as from supplementary geophysical data in adjacent regions (e.g. Wobbe et al., 2012; Gohl et al., 2013; Kalberg and Gohl, 2014).

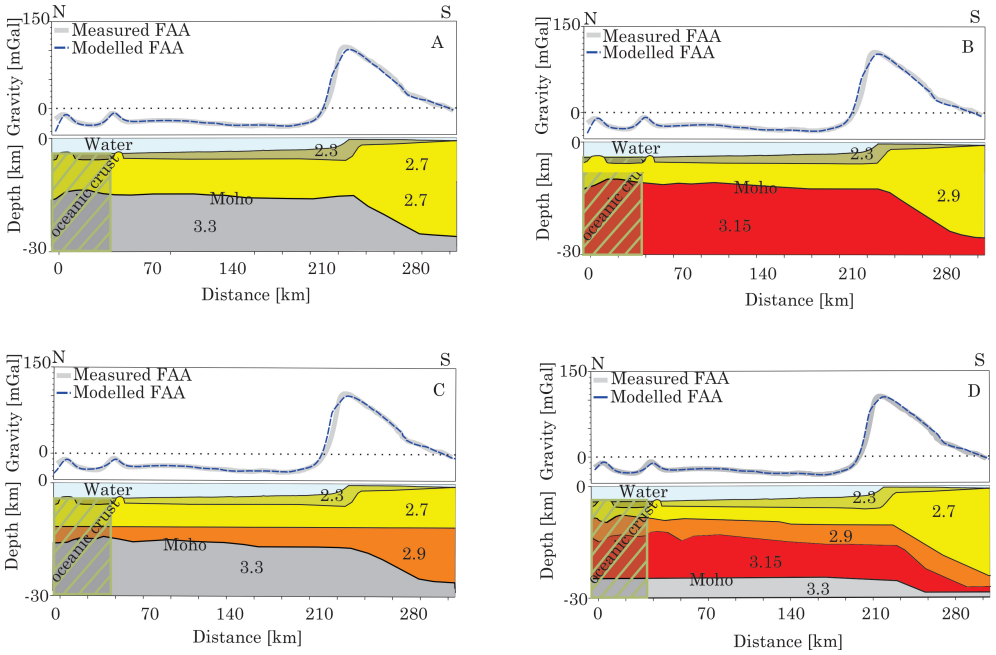

Figure 50: Suite of IGMAS forward gravity models along the seismic transect (Götze and Lahmeyer, 1988). Thick grey lines represent the measured shipborne free-air gravity anomaly. Blue lines: calculated free-air gravity anomaly. Layer densities are given in $10^3 kg/m^3$. Standard deviation between the measured and the calculated free-air gravity is less than 1 $mGal$ in all models. Model D is our preferred model. The semi-transparent and striated layers in the northern part of the models show areas of suspected oceanic crust according to Wobbe et al. (2012).

Sediment thickness was adopted from seismic reflection data and the sediments were modelled as single layer with a constant density of 2050 kg/m^3 adopted from P-wave velocities of the nearest seismic refraction data from the western Amundsen Sea Embayment (Fig. 48, AWI-20060200) (Kalberg and Gohl, 2014). Crustal thickness beneath the western Amundsen Sea Embayment varies between 12 and 27 km (Kalberg and Gohl, 2014). To the south, near the crest of the MBL dome, onshore receiver function analysis suggests crustal thickness of 24 km (Winberry and Anandakrishnan, 2004). The crust of the eastern Ross Sea shelf region is around 23 km thick (Luyendyk et al., 2003). Hence, we use a crust of 25 km in

our starting model assuming that no significant changes in the crustal structure occurs along the margin.

For simplificity, we exclude a distinct oceanic part in the northern part of the model (Fig. 50) as interpreted by Wobbe et al. (2012). We argue that this has no significant influence to our interpretation, which concerns the continental part of MBL. We used a background density of 2760 kg/m^3, seawater density of 1030 kg/m^3, a normal mantle density of 3300 kg/m^3, and warm mantle density of 3150 kg/m^3. Layer boundaries in all models are smooth, and no intrusions or dykes are required to fit the measured FAA. Differences between the measured and modelled FAA can be explained by out-of-plane effects for the shelf-edge and the two seamounts on the continental rise. We estimate that an uncertainty of 100 kg/m^3 for the upper-mantle density leads to an uncertainty of 1 km in crustal thickness. The standard deviation between the measured and the calculated FAA is less than 1 $mGal$ in all models.

Model A (Fig. 50) shows the combination of a normal-density mantle and a single-layer crust with a density of 2700 kg/m^3. The Moho depth is 12 to 15 km on the continental rise and 24 km beneath the shelf. Model B (Fig. 50) demonstrates the effect of low-density mantle (3150 kg/m^3) in combination with a single-layer 2700 kg/m^3 crust. Beneath the continental rise, the Moho depth ranges between 10 and 12 km and reaches 24 km beneath the shelf. In Model C (Fig. 50), a normal mantle density is modelled with a lower crust of 2900 kg/m^3 and upper crust of 2700 kg/m^3 are used. The crustal thickness ranges from 10 to 15 km at the continental rise and 24 km beneath the shelf. Finally, model D (Fig. 50) has a two-layered crust with an upper crustal density of 2700 kg/m^3 and a lower crust of 2900 kg/m^3, and mantle with a 'warm' low-density upper part and normal lower part. The crust is 10 to 12 km thick on the continental rise and 27 km thick beneath the shelf.

6.6 Discussion

Continental rise sediments off Hobbs Coast:

The thickness of sediments on the continental rise is 1.5 to 2 km (Fig. 49). Lack of drill control means that only a visual inspection and interpretation of the chronostratigraphy is possible. However, it is widely accepted that changes in seismic facies of sediments indicate changing environmental conditions during deposition. We interpret the low reflectivity and paucity of internal structure in Unit 1 as indications of deposition under conditions with weak or no bottom water currents, and hence at a time before glaciation on Antarctica. Increasing internal structure in Unit 2 infers increasing water current activity, which we interpret in terms of the presence of ephemeral ice sheets during a transitional period. Unit 3 seems to have been deposited in accompaniment to perennial ice-sheet glaciation of Antarctica. Its high reflectivity indicates strong current fluctuations, and the presence of debris flows can be attributed to sediment transport by advances of ice sheets to the shelf edge. Unit 4 is transparent and its origin remains speculative.

At least we suggest, that this framework for understanding the dynamic of sediments in Wrigley Gulf must be considered as a working model because of the lack of borehole control. Lindeque et al. (2013) present a more detailed seismostratigraphic interpretation of the sedimentary setting and its correlation with environmental conditions during deposition along the Pacific margin of West Antarctica but their interpretation also suffers from the lack of drill data.

Shelf sediments off Hobbs Coast:

The inner shelf of Wrigley Gulf is characterized by oceanward dipping strata whose inclination increases from the inner shelf to the shelf break (Fig. 49). Sediments in this part lying directly on top of the basement (Fig. 49) and may

represent the earliest sedimentary rocks in the region. We interpret the increasing northward dip of these sedimentary reflectors as a probable consequence of different extensional phases during deposition. Normal faults indicate that crustal extension affected the shelf (Fig. 49). This extension may correlate with tectonic rifting and the relative movement of East and West Antarctica after break-up and/or during the formation of the West Antarctic Rift System (WARS) (Müller et al., 2007).

Alternating reflection-rich and reflection-poor regions on the middle shelf of Wrigley Gulf (Fig. 49) can be interpreted as indications of major glacial retreats and advances, as in the western Amundsen Sea Embayment (Weigelt et al., 2009, Gohl et al., 2013). Reflection-poor units indicate poorly-stratified, homogenous deposited sediments and/or a strong scattering of acoustic energy by point sources (e.g. large clasts). Several studies, for example at the continental shelf of the Ross Sea (De Santis et al.,1995, De Santis et al.,1997) or the Antarctic Peninsula (Vanneste and Larter, 1995), have shown that glacially-deposited sediments consist of diamictites (tills etc.) which are poorly or non-sorted with a wide range of clast sizes and of acoustically transparent facies.

On the other hand, studies of the sedimentary architecture on Antarctic continental shelves have also interpreted high-amplitude, closely-spaced reflectors to result from marked contrasts in sedimentary physical properties (De Santis, 1995, De Santis, 1997, Bartek et al., 1997). These contrasts are interpreted to be an indication for strong variations in the composition and diagenesis of the deposited material related to changes in depositional character. Open water and/or glaciomarine conditions allow a stronger diversification and stratification of deposits (e.g. Eyles et al., 1985) that produce continuous high-amplitude reflections in the seismic record.

Following the *glacial sequence stratigraphic model* of Powell and Cooper (2002), we propose that reflection-poor units indicate an expanded ice sheet during cold, polar climate intervals. During glacial retreats, stratified deposition of fine grained mud produce sequences of continuous reflectors on the inner and middle shelf of Wrigley Gulf. Sequence boundaries between reflection-poor and reflection-rich seismic units are clear, but unfortunately the absence of chrono-stratigraphic constraints frustrates the task of estimating the temporal distribution of cold and warm periods and the transitional phases between them. In this context it seems likely that dynamic variations and the evolution of the WAIS can be observed in seismic records from the Ross Sea Embayment through Wrigley Gulf to the Amundsen Sea Embayment and beyond, enabling an inference of spatial and temporal similarities in glaciation all along the Pacific margin of West Antarctica.

Crustal architecture:

We modelled four possible crust-mantle configurations along our transect in order to test the hypothesis of a thermal mantle anomaly beneath MBL. Gravity modelling, regardless if forward or inverse, results in inherently non-unique solutions. Hence, additional geological information is necessary to reduce the number of independent model parameters. The sedimentary architecture is constrained by our seismic reflection data. Seismological observations indicate a low-velocity mantle anomaly beneath MBL and its continental margin (Sieminski et al, 2003, Jordan et al., 2010), which is consistent with our gravity models B and D. Models C and A can be rejected. The transect crosses the suspected continent-ocean transition of Wobbe et al (2012) (Fig. 48), which consists of thinned continental crust or oceanic crust interleaved with segments of transitional crust or continental fragments (Wobbe et al., 2012). Therefore, models A and B, which use single layered oceanic crust can also be disregarded. Consequently, we prefer model D as the closest of the four representations of our profile to the real crustal structure.

North of the shelf, this preferred final model presents a 10 to 12 km thick two-layered crust, which is thicker and of lower average density than expected for normal oceanic crust (White et al., 1990). Beneath the shelf, the crustal thickness increases up to 27 km, thicker than the 24 km that results from Winberry and Anandakrishnan's (2004) seismic receiver function analysis onshore to the south. The crustal architecture and densities are similar to seismic refraction observations and gravity modelling results in the western Amundsen Sea Embayment (Kalberg and Gohl, 2014).

The FAA along the transect averages zero, implying isostatically-compensated crust. We interpret the crust on the continental rise as of stretched continental type and to be isostatically compensated by a Pratt-type mechanism. The model's high density crustal layer (3150 kg/m^3) is denser than the 3000 kg/m^3 used by Wobbe et al. (2012) in his 2D gravity model, but similar to that modelled in the ASE (Kalberg and Gohl, 2014). The high density crustal layer can be attributed to magmatic underplating and so correlated with the action of a mantle plume in either its plume-head arrival or plume-tail phase (White and McKenzie, 1989) or related to an anomalously warm Pacific mantle beneath Antarctica (Finn et al., 2005; Panter et al., 2006). However, it is not possible with these 2D forward models to distinguish between high-density lower crust (a result of underplating) and low-density upper mantle.

Tectonic Implications:

As discussed above, we interpret the increasing northward dip of the inner shelf sedimentary reflectors as a probable consequence of different extensional phases during deposition. The around 4° northwards average dip of inner shelf strata (Fig. 51a) is greater than normal for most Antarctic shelf sediments. To confirm this thesis, we calculated the stratal inclinations of other West and East Antarctic shelf regions in the same way as demonstrated in Fig. 51 and compared them with present-day surface elevations of the corresponding hinterland regions using the bedrock topography of Antarctica derived from the BEDMAP2 grid (Fretwell et al., 2013).

Seismic surveys from the middle to inner shelf of the western ASE reveal sediments dipping at between 0.9° and 1.7° (Weigelt et al., 2009). Off Bakutis Coast, Gohl et al. (2013) observed inclinations of 1.0-0.5 ° on the middle shelf and 4.2 °- 2.0° over the inner to mid-shelf transition in profile BAS056-S111 (Fig. 48). The distance between this profile and the apex of the MBL dome is similar to that for profile AWI-20100113 (Fig. 48). Oceanward dipping sedimentary strata in the Eastern Ross Sea (Luyendyk et al., 2001) dip at around 2° away from the around 500 m sub-ice topographic high south of the Ross Ice Shelf - Shirase Coast. Shelf-strata of the western Weddell Sea dip at less than 0.5° (Rogenhagen et al., 2000, 2005); the mean elevation of their hinterland is 1000 m.

The hinterland elevation of the Ingrid Christensen Coast of Prydz Bay is also about 1000 m high, beyond which we calculate an average shelf strata dip oceanward of less than 1° (Cooper et al., 1991). At the Wilkes Land margin, the Adelie Coast is about 500 m high and strata on the middle shelf dip also oceanward at less than 0.5° (Escutia et al., 2003). Hence, an average oceanward dip of 1° - 2° and average margin hinterland elevations of 0.5 - 1 km seem to be usual for shelf sediments around most of Antarctica. Departing strongly from this pattern, the

4° dip of strata on Wrigley Gulf shelf off Hobbs Coast and western ASE shelf off Bakutis Coast (Gohl et al., 2013) correlate with the uplifted (3 km) subglacial topography of central MBL.

A simple calculation demonstrates the possibility of a causal relationship between uplift, tectonic processes and tilting of strata on the shelf (Fig. 51c). A regional tilt of around 1° results directly from a 3 km uplift of the MBL dome crest (Fig. 51b). If we add this result to the 1-2° inclination of 'usual' Antarctic shelf sediments, a total inclination of around 2-3° is likely (Fig. 51c) but the Hobbs Coast sediments dip with around 4°. For completion, further influences can be invoked to account for the difference between the calculated 2-3° and the observed 4° dip that typifies Wrigley Gulf shelf sediments.

Tectonic processes have a marked effect on sediment transport mechanisms, depositional processes, sediment strata and facies distributions on continental shelves. Normal faults on the inner shelf off Hobbs Coast (Fig. 49) imply distinct rifting events, which may have further influenced the sedimentary architecture. Due to the distance of the inner shelf sediments to the apex of central MBL (Fig. 48), flexural effects of the lithosphere to the inclination of inner shelf sediments must be taken into account.

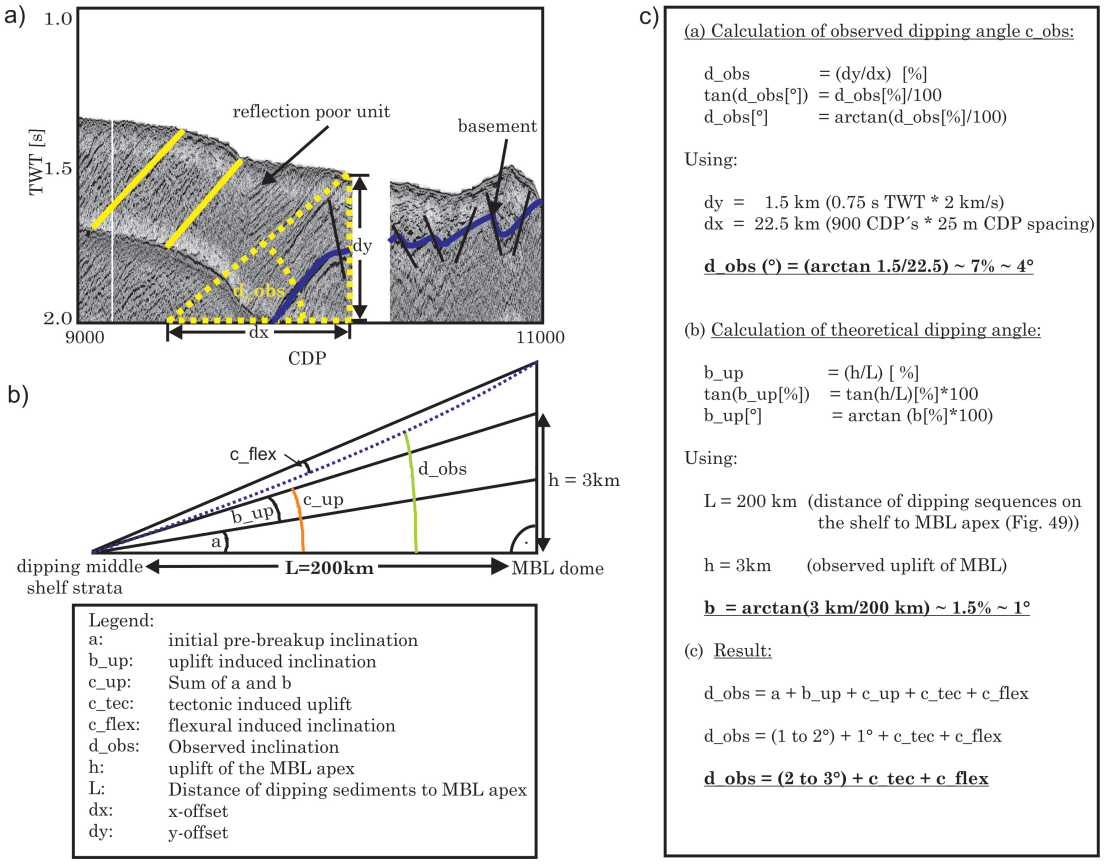

Figure 51: a.) Middle shelf sediments of Wrigley Gulf from CDP 8000 to CDP 11000. Calculation of observed middle shelf sediment dip c_obs. dy is the thickness based on two-way traveltime in (s) of the observed layer, dx is the profile distance in (km) used for dip calculation where 1 CDP = 25 m. b) Schematic image of factors which influence the inclination of the sediments on the continental margin. c) Model calculation of the middle shelf strata inclination. Abbreviations are explained in the legend lower left.

The response of the lithosphere to sedimentary load and rifting can be approximated by an elastic plate with an equivalent thickness Te (e.g. Watts, 2001). Watts et al. (1989) suggested that the stratal geometry of coastal sediments depend on the sediment supply, the amount of subsidence which directly correspond to the elastic thickness Te of the lithosphere. The lithospheres flexural rigidity is primarily controlled by the elastic thickness of the plate (Watts et al., 1982; Watts, 2001). Based on crustal thickness estimations in Wrigley Gulf (Fig. 50)

and topographic load defined by the rock equivalent topography (RET) based on the ships bathymetry (Braitenberg et al., 2007), we estimated the elastic thickness (Te) by using the software LITHOFLEX (Braitenberg et al., 2007) of 5 -10 km. This result is similar to findings in the Amundsen Sea Embayment (Kalberg and Gohl., 2014), under the Pine Island Glacier (Jordan et al., 2010) and also comparable to values from other rift systems such as the Basin and Range Province (Te = 5km) (Lowry and Smith, 1994) or the Afar region, followed by the Main Ethiopian Rift (Te = 7km) (Pérez-Gussinyé et al., 2005).

A first order estimation of the flexural effect of the lithosphere to the sedimentary dip off Hobbs Coast reveals an additional tilt of less than 0.2° which is in the order of the accuracy of the calculation of the inner shelf sediment dips. At this point we mention, that a *sagging* lithosphere due to flexural behavior of the lithosphere and sedimentary load has an increasing effect to the tilt of the inner shelf sediments (Watts et al., 1989). The magnitude of influence depends on the changing rate of the elastic thickness. The model of Watts et al. (1989) predicts an increasing tendency for oceanward coastal sediment tilt as the flexural rigidity changes more rapidly with time. Conversely, the sedimentary load has an weakening effect to the lithosphere because of the lower density of sediments relative to crystalline crust (Lavier et al., 1997).

In summary, we interpret the excess inclination of Wrigley Gulf inner shelf sediments as a consequence of the combined effects of post-break-up thermal subsidence of the continental margin, flexure of the lithosphere, glacial-isostatic compensation due to changes in ice sheet coverage, rifting during the formation of the region and uplift of central Marie Byrd Land.

Situation during break-up:

Luyendyk et al. (2001) suggested that the West Antarctic Erosion Surface was formed at or above sea-level due to absence of thick early Cenozoic sediments on the shelf of the eastern Ross Sea. Rocchi et al. (2006) counter that the lack of early Cenozoic sediments is not inconsistent with a near-sea-level origin. If a thermal anomaly existed since the Cretaceous, the area would have been elevated at break-up times (Campbell and Griffiths, 1990). The reflection-poor units of Wrigley Gulf inner shelf strata (Fig. 49) imply deposition during glacial times, the earliest in Cretaceous pre-glacial times. These sediments were deposited before uplift, because they are concordant with reflectors in the upper basement. Hence, uplift must have been occurred after sedimentation (Fig. 5). We associate the over-inclined reflection-poor sediments of the inner shelf and the significant elevation of Wrigley Gulf with low thermal subsidence and uplift after break-up. The absence of seaward dipping reflectors, however why, in our seismic data is an indication that extensive volcanism associated with a thermal mantle anomaly did not occur at break-up times.

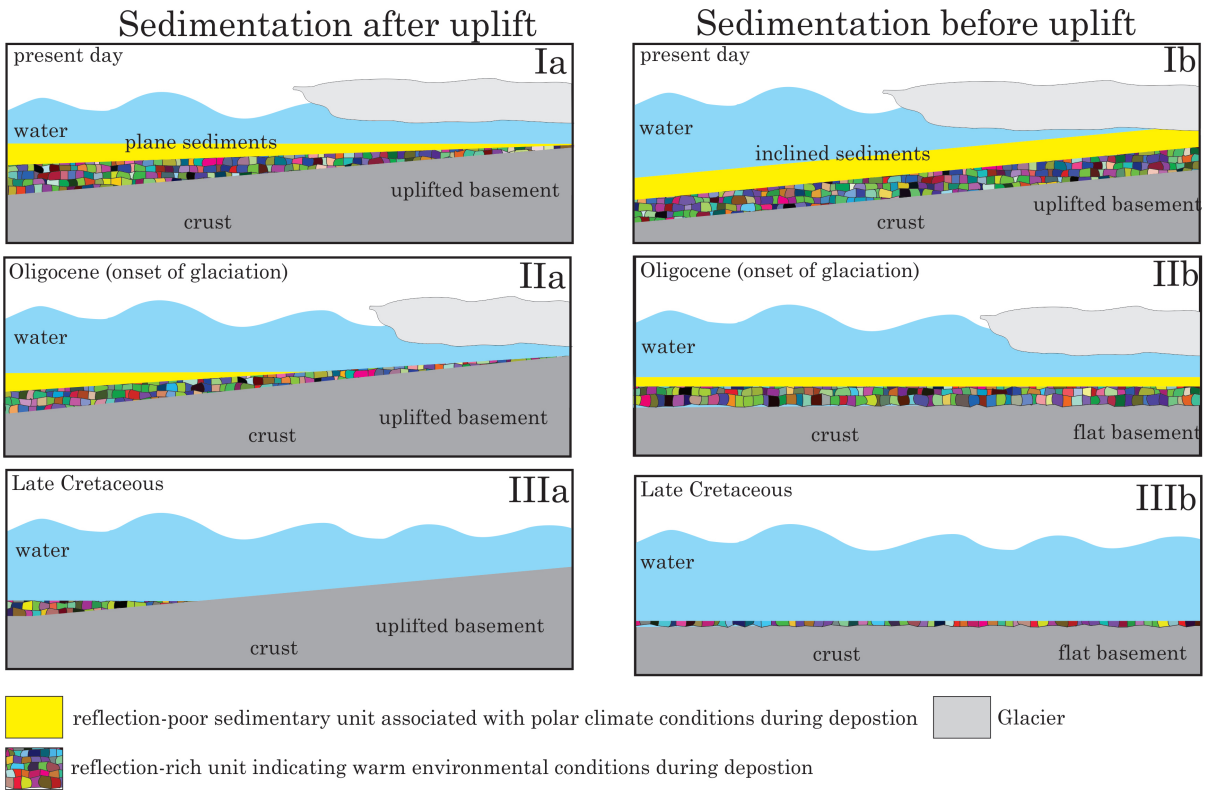

Figure 52: Schematic and exaggerated depiction of the influence of uplift on sedimentary architecture. Figs Ia, IIa and IIIa show the expected onlap that would accompany sedimentation after uplift. Fig. Ib, IIb, and IIIb show the more conformable sedimentary architecture that would form by deposition before uplift.

Comparsion with other regions:

The geomorphology of the MBL uplift area best compares to the uplifted region of the east coast of Brazil. This area was formed in Lower Cretaceous times by continental break-up between South America and Africa. The east coast of Brazil is the conjugate to the Cape Angola topographic high. A mantle plume has been suggested to be responsible for the Paraná continental flood basalts and the Serra do Mar coastal escarpment, which rises up to 2000 m above sea-level over a distance of around 1500 km from Porto Alegre in the south to the inland plateau edge (Peate et al., 1990). The conjugate topographic highs of the east coast of Brazil and Cape Angola are interpreted to be the opposing halves of a single original structure (Cox et al., 1989) which is interpreted as result of pre-break-up uplift.

In contrast, the elevated setting of central MBL and its narrow shelf off Hobbs Coast is not reflected on the conjugate continental submarine plateaus of New Zealand. We interpret this asymmetry as a further, purely geomorphological, indication for a post-break-up uplift of the MBL margin and post-break-up subsidence on New Zealand side (Sutherland et al., 2010).

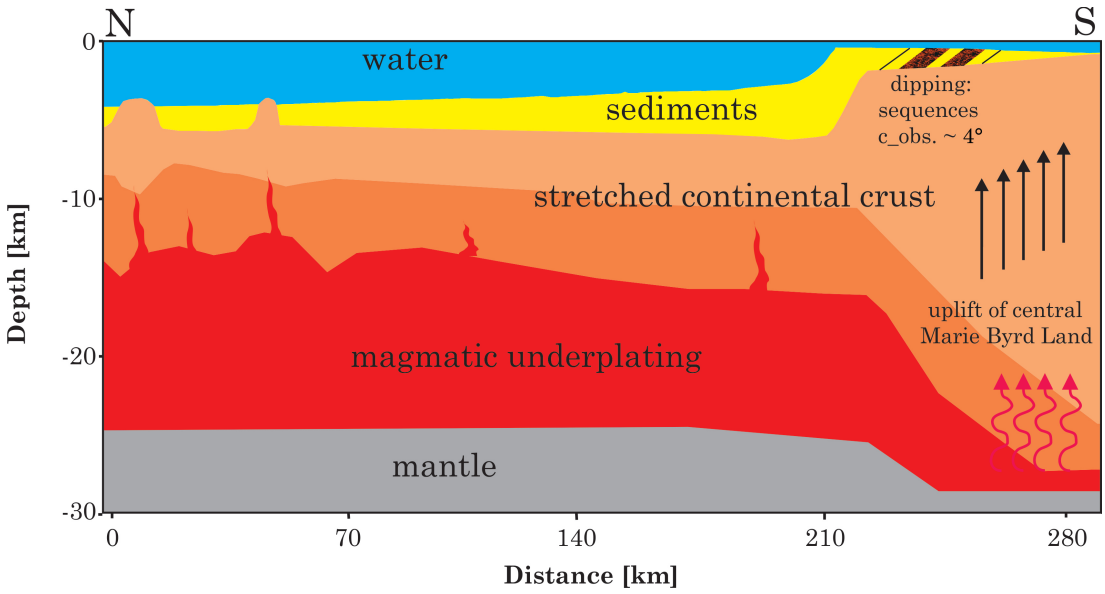

Figure 53: Schematic geological interpretation of 2D forward gravity model D. Black arrows should illustrate the uplift of central Marie Byrd Land due to a thermal mantle anomaly. Red arrows illustrate the influence of this thermal mantle anomaly. On the shelf over-inclined dipping sequences alternating between reflection rich and reflection poor units.

We infer underplating beneath the Marie Byrd Land margin (Fig. 53) is the result of early stage and initial magmatism after break-up may supported by anomalously warm Pacific mantle beneath Antarctica (Finn et al., 2005; Panter et al., 2006). This coincides with the multi-staged tectonic-geodynamic-magmatic model of Rocchi et al. (2002a, b) which explained evolution of the region without the occurrence of a mantle plume. The presence of this warm material may be ascribed to the arrival of a small mantle plume (LeMasurier, 2008) or the escape of low-density mantle material from beneath subducted slabs (Sutherland et al., 2010). Finally, the existence of a mantle plume cannot be verified or neglected from our modelling results.

Conclusion:

The aim of our study is to use simple 2D gravity models to present evidence for the timing and cause of MBL uplift in the crustal configuration and the sedimentary architecture of the region's continental shelf. The models are constrained using seismic observations of the top of basement and the sedimentary architecture as well as supplementary data from nearest geophysical measurements.

1. Gravity modelling shows that Pratt-type compensated stretched continental or transitional crust is underlain by a low-density upper mantle, consistent with a known negative velocity perturbation (Sieminski et al., 2003) and geochemical evidence for warm Pacific mantle beneath West Antarctica (Finn et al., 2005).

2. Changing reflectivity of continental rise sediments represent changes in environmental conditions from pre-glacial through trans-glacial to full glaciated conditions during deposition. We further infer that reflection-poor units on the inner shelf indicate a cold climate period during deposition, whereas reflection-rich units were developed during warmer times.

3. Dynamic variations and evolution of the WAIS can be observed in seismic records from the Ross Sea Embayment through Wrigley Gulf to the Amundsen Sea Embayment and beyond, enabling an inference of spatial and temporal similarities in glaciation all along the Pacific margin of West Antarctica.

4. Inner shelf sediments dip oceanward by up to 4°, about 2° steeper than non-progradational sediment sequences on other Antarctic shelves. This excess inclination can in some parts be correlated to a total surface uplift of 3 km in central Marie Byrd Land, and to multiple tectonic processes affecting the Pacific margin of West Antarctica including rift-related faulting at the continental margin and the West Antarctic Rift System.

5. A low-density upper mantle, over-inclined inner shelf sediments and the absence of flood basalts infer that the central MBL crust is supported by an anomalous mantle which controlled lithospheric uplift after a non-elevated break-up between New Zealand and Marie Byrd Land.

Acknowledgement We are grateful to the master and crews of the RV Polarstern expeditions ANT-XXIII/4 (2006) und ANT-XXVI/3 (2010) for their support in collecting geophysical data. This project was funded by the Deutsche Forschungsgemeinschaft (DFG) under project number GO 724/13-1.

7 Conclusions and Outlook

Most of the questions asked in chapter 1.1 could be answered by analysis and interpretation of the geophysical data which were collected during the expeditions ANT-XXIII/4 in 2006 to the Bellingshausen and Amundsen Sea and ANT-XXVI/3 in 2010 into Wrigley Gulf and the Amundsen Sea Embayment including Pine Island Bay.

The Amundsen Sea Embayment:
The crustal models of the Amundsen Sea Embayment presented in chapters 4 and 5 confirms earlier study conclusions whether the region is composed by stretched and thinned crust. Curstal thickness variies between 10-14 km beneath the continental rise and up to 29 km beneath the shelf of the Embayment. The velocity structure of the crust shows the character of continental crust. The entire crust is underlaid by a high-velocity layer of variable thickness which can be correlated with a postulated continental insulation flow from beneath eastern continental Marie Byrd Land to the Marie Byrd Seamounts (Kipf et al., 2014). Magmatic intrusions are of felsic nature in the western embayment and of more mafic composition in the eastern embayment which I correlate with the prominent Dorrel Rock intrusive complex (Rocchi et al., 2006) onshore eastern Marie Byrd Land.

Potential field data show tectonic lineaments in WSW-ENE orientation. The analysis of lithospheric rigidity reveals an elastic thickness between 10-15 km in the western embayment and 0-5 km in Pine Island Bay indicating a major tectonic event superposed by several minor tectonic events in Oligocene. Further, the occurence of tectonic activity in the embayment indicates an elongation of the West Antarctic Rift System into this part of West Antarctica.

The Marie Byrd Land:

The analysis of the crust of Wrigley Gulf off Hobbs Coast reveals Pratt-type compensated and stretched crust of continental nature which is underlaid by a low-density upper mantle layer of variable thickness. This low-density layer coincides with a known negative velocity pertubation in the area (Simiensky et al., 2013). The crust is between 10 to 12 km thick at the continental rise and thickens up to 27 km beneath the shelf. These values are similar to observations in the western Amundsen Sea Embayment (Kalberg and Gohl, 2014) indicating a relatively homogenous crustal architecture along this part of the West Antarctic continental margin.

Continental rise sediments image environmental changes from pre-glacial through trans-glacial to full glaciated conditions during deposition. These variations can be also observed in the Ross Sea Embayment through Wrigley Gulf to the Amundsen Sea Embayment which implies a common pattern of temporal as well as spatial behavior of the West Antarctic Ice Sheed along the Pacific margin of West Antarctica.

Sediments of the inner shelf dip seaward with around 4° which is about 2° steeper than non-progradational sediment sequences on other Antarctic shelves. I correlate this excess inclination with a surface uplift of up to 3 km in central Marie Byrd Land. Considering the low-density upper mantle and absence of flood basalts I infer that central Marie Byrd Land is supported by an anomalous mantle which controlled lithospheric uplift after a non-elevated break-up between Marie Byrd Land and greater New Zealand.

Finally, my results suggest that the entire West Antarctic continental margin between the Ross Sea Embayment and the Antarctic Peninsula (Fig. 1) was affected by multi-staged rifting processes starting in Cretaceous and culminating in Oligocene times. These rifting stages where superposed by a single major and several minor magmatic episodes whose products I correlate with the SW Pacific Diffuse Alkaline Magmatic Province (Finn et al., 2005) and a suspected magmatic continental insulation flow from beneath eastern Marie Byrd Land towards the Marie Byrd Seamounts (Kipf et al., 2014). My models upgrade knowledge of the West Antarctic continental margin and can be used to constraint new reconstructions of the tectonic develpoment of the South Pacific. Furthermore, my basement and crustal models are indispensable for future models of the dynamic behavior of the West Antarctic Ice Sheet.

It must be kept in mind that my interpretations are based on models, which are always ambiguous. To confirm or extend my models, first and foremost new detailed seismic refraction measurements in Wrigley Gulf off Hobbs Coast and Bakitus Coast would fill the lack of knowledge of the lithospheric architecture. Maybe these models will show also a homogenous crust of stretched continental nature which is underlaid by a high-density layer along the entire West Antarctic continental margin implying a continental wide tectono-magmatic event affecting West Antarctica.

If this hypothesis will be confirmed, it should be discussed why central Marie Byrd Land is elevated whereas the eastern part is near sea-level. My models show a similar crustal architecture both off Hobbs Coast and in the Amundsen Sea Embayment and hence, the cause of uplift is not a miscellaneous response of the crust due to magmatic activity. Potentially, this is an effect of an asymmetric expansion of the West Antarctic Rift system to the Amundsen Sea Embayment and onshore eastern Marie Byrd Land.

Bibliography

Anderson, Don L.,1989. Theory of the Earth. Boston: Blackwell Scientific Publications, http://resolver.caltech.edu/CaltechBOOK:1989.001

Anderson, J. B., 1999. Antarctic Marine Geology. Cambridge: Cambridge University Press

Barker, P. F., B. Diekmann and C. Escutia, 2007a. Onset of Cenozoic Antarctic glaciation. *Deep-Sea Res. II*, 54(21‐22), 2293‐2307. doi:10. 1016/j.dsr2.2007.07.027.

Barker, P. F., G. M. Filippelli, F. Florindo, E. E. Martin and H. D. Scher, 2007b. Onset and role of the Antarctic Circumpolar Current. *Deep-Sea Res. II*, 54(21‐22), 2388‐2398. doi:10.1016/j.dsr2.2007.07.028

Bartek, L.R., Anderson, J., Oneacre, T., 1997. Ice stream troughs and variety of seismic stratigraphic architecture from a high southern latitude section: Ross Sea, Antarctica. In: Davies, T.A., et al. (Ed.), Glaciated continental margins — an atlas Of acoustic images. Chapman & Hall, London, pp. 250–254.

Barton, P., 1986. The relationship between seismic velocity and density of continental crust – a useful constraint? *Geophys. J. R.* astr. Soc., 87, 195-208

Bechtel, T. D., Forsyth, Sharpton, V. L., Grieve, R.A.F. 1990. Variations in effective elastic thickness of the North American Lithosphere. *Nature*. v. 343, 636-638. doi:10.1038/343636a0

Behrendt, J. C., W. E. LeMasurier, A. K. Cooper, F. Tessensohn, A. Trefu and D. Damaske 1991. Geophysical studies of the west Antarctic rift arm, Tectonics, 10, 1257‐1273, doi:10.1029/91TC00868.

Bell, R. E.; Blankenship, D. D.; Finn, C. A.; Morse, D. L.; Scambos, T. A.; Brozena, J. M.; Hodge, S. M., 1998. Influence of subglacial geology on the onset of a West Antarctic ice stream from aerogeophysical observations, Nature, Jul 2, Volume 394, Issue 6688, p.58-62,

Biollot, G., Winterer, E. L. 1988. Drilling on the Galicia Margin: retrospect and prospect. In: Boillot, G., Winterer E. L. et al (eds) Proceedings of the Ocean Drilling Program, Scientific Results, 102. Ocean Drilling Program, College Station. TX. 809-828.

Boillot, G., Beslier, M-O. & Comas, M., 1992. Seismic image of undercrusted serpentinite beneath a rifted margin. *Terra Nova*. 4, 25-33.

Bingham, R.G., Ferraccioli, F., King, E.C., Larter, R.D., Pritchard, H.D., Smith, A.M. and Vaughan, D.G., 2012. Inland thinning of West Antarctic Ice Sheet steered along subglacial rifts. *Nature*, 487, 468-471, doi: 10.1038/nature11292.

Birch, F., 1964. Density and composition of the mantle and core. J. Geophysic. Res., v.69 p. 4377-4388.

Bradshaw, J. D., 1991. Cretaceous dispersion of Gondwana: Continental and oceanic spreading in the south-west Pacific-Antarctic sector, *in* Thomson, M. R. A., et al., eds., Geological evolution of Antarctica:, Cambridge University Press, 581–585. Cambridge, United Kingdom.

Braitenberg, C., Ebbing, J. and Götze, H.-J. 2002. Inverse modeling of elastic thickness by convolution method - The Eastern Alps as a case example, Earth Planet. Sci. Lett., 202, 387-404.

Braitenberg C., Wienecke S., Ebbing J., Born W. & Redfield T., 2007. Joint gravity and isostatic analysis for basement studies, in Proceedings of EGM 2007 International Workshop, Innovation in EM, Grav and Mag *Methods: a new Perspective for Exploration, Extendend Abstracts*. Villa Orlandi, Capri, Italy, 2007 April 15–18.

Brunov, E., Guillou-Frottier, L. 2005. The plume head-continental lithosphere interaction using a tectonically realistic formulation for the lithosphere. *Geophys. J. Int.* 161, 469-490.

Buck, W.R., 1991. Modes of continental lithospheric extension. *Journal of Geophysical Research* 96, 20,161–20, 178.

Buttkus, B. 2000. Spectral Analysis and filter theory in applied geophysics. Springer. Berlin

Campbell, I. H. and Griffiths, R. W., 1990. Implications of mantle plume structure for the evolution of flood basalts. *Earth and Planetary Science Letters*, v.99. p. 79-93.

Cande, S.C., Stock, J. M., Müller, R. D. and Ishihara, T., 2000. Cenozoic motion between East and West Antarctica. *Nature,* 404, 145–150.

Carlson, R. L. and Raskin, G. S., 1984. Density of the ocean crust. *Nature.* v. 311. p. 555-558.

Carlson, R. L., Miller, D. J., 2003. Mantle wedge water contents estimated from seismic velocities in partially serpentinized peridotites. *Geophysical Research Letters*.

Chaput, J., R. C. Aster, A. Huerta, X. Sun, A. Lloyd, D. Wiens, A. Nyblade, S. Anandakrishnan, J. P. Winberry and T. Wilson, 2014. The crustal thickness of West Antarctica, J. Geophys. Res. Solid Earth, 119, 378-395, doi:10.1002/2013JB010642.

Chian, D., Louden, K. E., Minshull, T. A. and Whitmarsh, R. B., 1999. Deep structure of the ocean-continent transition in the southern Iberia Abyssal Plain from seismic refraction profiles: Ocean Drilling Program (Legs 149 and 173) transect, *J. Geophys. Res.,* 104, 7443–7462.

Christensen, N. I., Mooney, W. D., 1995. Seismic velocity structure and composition of the continental crust. A global view. *J. Geophys. Res.*, 100, 9761-9788.

Christensen, N.I., 1996. Poisson's ratio and crustal seismology: *J. Geophys. Res.*, 101, 3139–3156.

Cianciara, B. and Marcak, H, 1976. Interpretation of gravity anomalies by means of local power spectra, Geophys. Prosp. 24, 273–286.

Clark, D.A., 1997. Magnetic properties of rocks and minerals. AGSO Journal of Australien Geology & and Geophysics, 17.

Cochran, J. R., Tinto, K. J., Bell, R. E., 2015. Abbot Ice Shelf, structure of the Amundsen Sea continental margin and the southern boundary of the Bellingshausen Plate se award of West Antarctica. *Geochemistry Geophysics Geosystems.* doi 10.1002/2014GC005570.

Cooper, A., H., Stagg, H., Geist, E., 1991. Seismic Stratigraphy and structure of Prydz Bay, Antarctica: Implications from LEG 119 Drilling. Proceedings of the Ocean Drilling Program, Scientific Results, Vol. 119.

Coxall, H. K., Wilson, P. A., Palike, H., Lear, C. H. and Backman, J. 2005. Rapid stepwise onset of Antarctic glaciation and deeper calcite compensation in the Pacific Ocean. *Nature* 433: p53–-57.

Cunningham, A. P., R. D. Larter, P. F. Barker, K. Gohl and F. O. Nitsche, 2002. Tectonic evolution of the Pacific margin of Antarctica: 2. Structure of Late Cretaceous–early Tertiary plate boundaries in the Bellingshausen Sea from seismic reflection and gravity data, J. Geophys. Res., 107(B12), 2346, doi:10.1029/2002JB001897.

Cox, K.G., 1989. The role of mantle plumes in the development of continental drainage patterns*:* Nature*, v.* 342 pp. 873-877.

Czaja, A. and J. Marshall, 2006. The Partitioning of Poleward Heat Transport between the Atmosphere and Ocean. *J. Atmos. Sci.*, **63**(5), 1498‑1511. doi:10.1175/JAS3695.1.

Dalziel, I.W.D. and Elliot, D.H., 1982. West Antarctica: problem child of Gondwanaland, Tectonics, 1, 3–19.

Davey, F. J., De Santis, L., 2006. A Multi-Phase Rifting Model for the Victoria Land Basin, Western Ross Sea. *Antarctica*. 303-308. doi: 10.1007/3-540-32934-X_38.

Davy, B. and Wood, R.A., 1994. Gravity and magnetic modelling of the Hikurangi Plateau. Marine Geology, 118, 139-151

Denk, A., 2011. Diploma Thesis, Analysis of ship-borne and helicopter-borne magnetic data in the Amundsen Sea, West Antarctica, Universität Köln. hdl:10013/epic.389

De Conto, R., Pollard, D., 2003. Rapid Cenozoic glaciation of Antarctica induced by declining atmospheric CO2. *Nature*, 421: 245-249.

De Santis, L., Anderson, J.B., Brancolini, G., Zayatz, I., 1995. Seismic record of late Oligocene through Miocene glaciation on the central and eastern continental shelf on the Ross Sea. In: Cooper, A.K., Barker, P.F., Brancolini, G. (Eds.), Geology and Seismic Stratigraphy of the Antarctic Margin. Antarctic Research Series. American Geophysical Union, Washington, DC, pp. 235–260.

De Santis, L., Anderson, J.B., Brancolini, G., Zayatz, I., 1997. Glaciomarine deposits on the continental shelf of Ross Sea, Antarctica. In: Davies, T.A., et al. (Ed.), Glaciated continental margins - an atlas of acoustic images. Chapman & Hall, London, pp. 110–113.

Dormack, E. W, Ishman, S., 1992. Magnetic susceptibility of Antarctic glacial marine sediments. Antarctic Journal of the United States, Vol. 27 Issue 5, p64

Dorman, L.M. and Lewis, B.T.R., 1970. Experimental isostasy, 1, theory of the determination of the earth's isostatic response to a concentrated load. *Journal of* Geophysical Research, 75, 3357-3365.

Eagles, G., Gohl, K. & Larter, R.D., 2004a. High-resolution animated tectonic reconstruction of the South Pacific and West Antarctic margin; *Geochemistry, Geophysics, Geosystems (G^3),* 5, doi:10.1029/2003GC000657.

Eagles, G., Gohl, K. & Larter, R. D., 2004b. Life of the Bellingshausen plate. *Geophysical Research Letters 31,* doi: 10.1029/2003GL019127.

Ebinger, C, Deino, J. A., Drake, R. E., Tesha, A. L., Kronenberg, A. and Tullis, F., 1989. low strength of quartz Chronology of volcanism and rift basin propagation: Rungwe volcanic province, East Africa, J. Geophys. Res., 94.

England, P. and Molnar, P., 1990. Surface uplift, uplift of rocks, and exhumation of rocks: *Geology*, v. 18, p. 1173-1177.

Escutia, C., D., Warnke, G. D., Acton, A., Barcena, L., Burckle, M., Canals, M. and Frazee, C.S., 2003. Sediment distribution and sedimentary processes across the Antarctic Wilkes Land margin during Quaternary. Deep-Sea Research Part II 50, p. 1481-1508.

Eyles, C.H., Eyles, N., Miall, A.D., 1985. Models of glaciomarine sedimentation and their application to the interpretation of ancient glacial sequences. Palaeogeography, Palaeoclimatology, Palaeoe-cology 51 (1–4), 15–84.

Fasullo, J. T. and K. E. Trenberth, 2008. The Annual Cycle of the Energy Budget. Part II: Meridional Structures and Poleward Transports. *J. Climate*, 21(10), 2313–2325. doi:10.1175/2007JCLI1936.1.

Finn, C. A., R. D. Müller, K. S. Panter, 2005. A Cenozoic diffuse alkaline magmatic province (DAMP) in the southwest Pacific without rift or plume origin, *Geochem. Geophys. Geosyst.*, 6, Q02005, doi:10.1029/2004GC000723.

Fretwell, P., Pritchard, H. D., Vaughan, D. G., Bamber, J. L., Barrand, N. E., Bell, R., Bianchi, C., Bingham, R. G., Blankenship, D. D., Casassa, G., Catania, G., Callens, D., Conway, H., Cook, A. J., Corr, H. F. J., Damaske, D., Damm, V., Ferraccioli, F., Forsberg, R., Fujita, S., Gogineni, P., Griggs, J. A., Hindmarsh, R. C. A., Holmlund, P., Holt, J. W., Jacobel, R. W., Jenkins, A., Jokat, W., Jordan, T., King, E. C., Kohler, J., Krabill, W., Riger-Kusk, M., Langley, K. A., Leitchenkov, G., Leuschen, C., Luyendyk, B. P., Matsuoka, K., Nogi, Y., Nost, O. A., Popov, S. V., Rignot, E., Rippin, D. M., Riviera, A., Roberts, J., Ross, N., Siegert, M. J., Smith, A. M., Steinhage, D., Studinger, M., Sun, B., Tinto, B. K., Welch, B. C., Young, D. A., Xiangbin, C., and Zirizzotti, A.: Bedmap2: improved ice bed, surface and thickness datasets for Antarctica, The Cryosphere Discuss., 6, 4305-4361.

Gardner, G.H.F., Gardner, L. W. and Gregory, A. R., 1974. Formation velocity and density, the diagnostic basics for stratigraphic traps". *Geophysics* 39: 770–780.

Götze, H. J., Lahmeyer, B., 1988. Application of three-dimensional interactive modelling In gravity and magnetics, *Geophysics* Vol. 53, No. 8, p. 1096-1108.

Gohl, K., Teterin, D., Eagles, G., Netzeband, G., Grobys, J., Parsiegla, N., Schlüter, P., Leinweber, V., Larter, R.D., Uenzelmann-Neben, G. & Udintsev, G.B. 2007. Geophysical survey reveals tectonic structures in the Amundsen Sea embayment, West Antarctica; Proceedings of the 10th Int. Symposium of Antarctic Earth Sciences, edited by A.K. Cooper and C.R. Raymond et al., *USGS Open-File Report 2007-1047*, doi:10.3133/of2007-1047.srp047.

Gohl, K., editor, 2010. The expedition of the Research Vessel Polarstern to the Amundsen Sea, Antarctica, in 2010 (ANT-XXVI/3), volume 617 of Berichte zur Polar- und Meeresforschung = Reports on polar and marine research. Alfred Wegener Institute

for Polar and Marine Research. doi:10013/epic.35668.d001.

Gohl, K., editor, 2007. The Expedition ANTARKTIS-XXIII/4 of the Research Vessel Polarstern in 2006, volume 557 of Berichte zur Polar- und Meeresforschung = Reports on polar and marine research. Alfred Wegener Institute for Polar and Marine Research. doi:10013/epic.27102.d001.

Gohl, K., 2012. Basement control on past ice sheet dynamics in the Amundsen Sea Embayment, West Antarctica; *Palaeogeography, Palaeoclimatology, Palaeoecology*, v. 335-336, p. 35-41, doi:10.1016/j.palaeo.2011.02.022.

Gohl, K., Denk, A., Eagles, G. & Wobbe, F., 2013a. Deciphering tectonic phases of the Amundsen Sea Embayment shelf, West Antarctica from a magnetic anomaly grid. *Tectonophysics*, 585, 113-123, doi:10.1016/j.tecto.2012.06.036.

Gohl, K., Uenzelmann-Neben, G., Larter, R.D., Hillenbrand, C.-D., Hochmuth, K., Kalberg, T., Weigelt, E., Davy, B., Kuhn, G. & Nitsche, F. O. 2013b. Seismic stratigraphic record of the Amundsen Sea Embayment shelf from pre-glacial to recent times: Evidence for a dynamic West Antarctic ice sheet. *Marine Geology*. 344, 115-131. doi:10.1016/j.margeo.2013.06.011.

Granot, R., Cande, S.C., Stock, J.M., Damaske, D., 2013. Revised Eocene-Oligocene kinematics for the West Antarctic rift system. *Geophysical Research Letters,* v. 40, p. 279-284, doi:10.1029/2012GL054181.

Grobys, J. W. G., Gohl, K. & Eagles, G. 2008. Quantitative tectonic reconstructions of Zealandia based on crustal thickness estimates; *Geochemistry, Geophysics, Geosystems (G^3)*, 9, 1, Q01005, doi:10.1029/2007GC001691.

Grobys, J. W. G., Gohl, K., Uenzelmann-Neben, G. & Barker, 2009. Extensional and Magmatic nature of the Campbell Plateau and Great South Basin from deep crustal studies. *Tectonophysics*, v. 472, p.213-225.

Grunow, A.M., Kent, D. V. and Daiziel, I. W. D., 1991. New paleomagnetic data from Thurston Island: Implications for the tectonics of West Antarctica and Weddell Sea opening. *Journal of Geophysical Research 96: doi: 10.1029/91JB01507.*

Hamilton, W., 1987. Crustal extension in the Basin and Range Province, south-western United States. In: Coward, M.P., Dewey, J.F., Hancock, P.L. (Eds.), Continental Extensional Tectonics. *Geological Society Special Publications*, 28, 155–176.

Hay, W.W. 1996. Tectonics and Climate. Geol. Rundschau. 85. p.409-437.

Hole, M. J., and LeMasurier, W.E., 1994. Tectonic controls on the geochemical composition Of Cenozoic, mafic alkaline volcanic rocks from West Antarctica: *Contributions to Mineralogy and Petrology*, v. 117, p. 187-202.

Hopper, J., Dahl-Jensen, T., Holbrook, W., Larsen, H., Lizarralde, D., Korenaga, J., Kent, G. & Kelemen, P., 2003. Structure of the SE Greenland margin from seismic reflection and refraction data: Implications for nascent spreading center subsidence and asymmetric crustal accretion during North Atlantic opening, *Journal of Geophysical Research*, 108, B5, doi:10.1029/2002JB001996.

Jordan, T.A., Ferraccioli, F., Vaughan, D.G., Holt, J.W., Corr, H., Blankenship, D.D., Diehl, T.M., 2010. Aerogravity evidence for major crustal thinning under the Pine Island Glacier region (West Antarctica). Geological Society of America Bulletin 122, 714–726. doi.org/10.1130/B26417.1.

Kalberg, T. and Gohl, K., 2013. Crustal structure of the Amundsen Sea Embayment, West Antarctica: Implications for its tectonic evolution from a geophysical dataset , EGU General Assembly, Vienna, 7 April 2013 - 12 April 2013 .

Kalberg, T. and Gohl, K., 2014. The crustal structure and tectonic development of the continental margin of the Amundsen Sea Embayment, West Antarctica: implications from geophysical data, Geophysical Journal International, 198 (1), pp. 327-341 .

Karner, G.D. and Watts, A. B., 1983. Gravity Anomalies and Flexure of the Lithosphere at Mountain Ranges, *J. Geophys. Res.,* 88, 10449-10477.

Karner, G.D., Studinger, M., Bell, R., 2005. Gravity anomalies of sedimentary basins and their mechanical implications: application to the Ross Sea basins, West Antarctica. Earth and Planetary Science Letters 235, 577–596.

Kipf, A., Mortimer, N., Werner, R., Gohl, K., van den Bogaard, P., Hauff, F. and Hoernle, K. 2012. Granitoids and dykes of the Pine Island Bay region, West Antarctica. *Antarctic Science*, 24(5), 473-484, doi:10.1017/S0954102012000259.

Kipf, A., Hauff, F., Werner, R., Gohl, K., van den Bogaard, P., Hoernle, K., Maicher, D. and Klügel, A., 2014. Seamounts off the West Antarctic margin: A case of non-hotspot intraplate volcanism. *Gondwana Research*. doi:10.1016/j.gr.2013.06.013.

Larter, R.D., Cunningham, A. P., Barker, P. F., Gohl, K. and Nitsche, F. O., 2002. Tectonic evolution of the Pacific margin of Antarctica — 1. Late Cretaceous tectonic reconstructions. *J. Geophys. Res.,* 107 (B12), 2345.

Lavier, L. L. and Steckler, M. S., 1997. The effect of sedimentary cover on the flexural strength of continental lithosphere. *Nature,* v. 389, p. 476-479.

Lawver, L. .A., Gahagan, L.M. and Dalziel, I.W.D., 2011. A different look at gateways: Drake Passage and Australia/Antarctica, *in* Anderson, J.B. and Wellner, J.S., Tectonic, Climatic, and Cryospheric Evolution of the Antarctic Peninsula, Special Publication No. 063, American Geophysical Union, p. 5-33. DOI: 10.1029/2010SP001017.

LeMasurier, W. E. and Rex, D. C., 1989. Evolution of linear volcanic ranges in Marie Byrd Land, Antarctica: *Journal of Geophysical Research*, v. 94, no. B6, p. 7223-7236.

LeMasurier, W.E. and J. W. Thomson, 1990. Volcanoes of the Antarctic Plate and Southern Oceans, Antarctic Research Series: Washington, D.C., American Geophysical Union, p. 512.

LeMasurier, W. E. and Rex, D. C., 1991. The MBL volcanic province and its relation to the Cenozoic West Antarctic rift system, in Tingey, R. J. ed., the geology of Antarctica; Oxford, Clarendon press, p. 249-284.

LeMasurier, W. E., Harwood, D. M., and Rex, D. C., 1994. Geology of Mount Murphey Volcano: An 8 m.y. history of interaction between a rift volcano and the West Antarctic Ice Sheet. *Geological Society of America Bulletin.*

LeMasurier, W. E. and C. A. Landis, 1996. Mantle-Plume, activity recorded by low relief erosion surfaces in West Antarctica and New Zealand: Geological Society of America Bulletin, v.108, p. 1450-1466.

LeMasurier WE, 2008. Neogene extension and basin deepening in the West Antarctic rift inferred from comparisons with the East African rift and other analogs. Geology 36:247–250. doi:10.1130/G24363A.1.

LeMasurier, W., Sung, H. C., Kawachi, Y., Mukasa, S. B., and Rogers N. W., 2011. Evolution pf pantellerite-trachyte-phonolite volcanoes by fractional crystallization of basanite magma in a continental rift setting, Marie Byrd Land, *Antarctica. Contrib. Mineral Petrol.* 162, p. 1175-1199. doi:10.1007/s00410-011-0646-z.

Lindeque, A. , Martos, Y. M. , Gohl, K. and Maldonado, A., 2013. Deep-sea pre-glacial to glacial sedimentation in the Weddell Sea and southern Scotia Sea from a cross-basin seismic transect , Marine Geology, 336 , pp. 61-83. doi:10.1016/j.margeo.2012.11.004

Lindow, J., Spiegel, C., Johnson, J., Lisker, F., Gohl, K., 2011. Constraining the latest stage exhumation of Marie Byrd and Ellsworth Land, West Antarctica, 11th International Symposium on Antarctic Earth Science; Edinburgh, Scotland.

Livermore, R., C.-D. Hillenbrand, M. Meredith, and G. Eagles, 2007. Drake Passage and Cenozoic climate: An open and shut case? *Geochem. Geophys. Geosyst.*, 8, Q01005. doi:10.1029/2005GC001224.

Llubes, M., Florsch, N., Legresy, B., Lemoine, J., Loyer, S., Crossly, D. and Remy, F. 2003. Crustal thickness in Antarctica from CHAMP gravimetry. *Earth and Planetary Science Letters*. 212. 103-117.

Luyendyk, B. P., Sorlien, C. C., Wilson, D.S., Bartek, L.R. and Siddoway, C. H., 2001. Structural and tectonic evolution of the Ross Sea rift in the Cape Colbeck region, Eastern Ross Sea, Antarctica, *Tectonics*, 20, 933-959.

Luyendyk, B., Wilson, D. S., Siddoway, C. S., 2003. Eastern margin of the Ross Sea Rift in western Marie Byrd Land, Antarctic: Crustal structure and tectonic development. *Geochemistry, Geophysics, Geosystems (G^3).* v. 4. doi:10.1029/2002GC000462.

Mackenzie, G. D., Thybo, H., & Maguire, P. K. H., 2005. Crustal velocity structure across the Main Ethiopian Rift: results from two-dimensional wide-angle seismic modelling, Geophysical Journal, Volume 162, Issue 3, pp. 994-1006.

Malahoff, A., Kolotyrkina, I. Y., Midson, B. P. & Massoth, G. I., 2006. A decade of exploring a submarine intraplate volcano: Hydrothermal manganese and iron at Lo¯ʼihi volcano. *Geochemistry, Geophysics, Geosystems (G^3).* 7. 1525-2027.

Marty, B., Appora, I., Barrat, J.-A., Deniel, C., Vellutini, P., Vidal, P., 1993. He, Ar, Sr, Nd and Pb isotopes in volcanic rocks from Afar: evidence for a primitive component and constraints on magmatic sources. Geochem. J. 27, 219–228.

Marty, B., Pik, R., Gezahegn, Y., 1996. Helium isotopic variations in Ethiopian plume lavas: nature of magmatic sources and limit on lower mantle contribution. Earth Planet. Sci. Lett. 144,223–237.

Maus, S., S. Macmillan, S. McLean, B. Hamilton, A. Thomson, M. Nair and C. Rollins, 2010. The US/UK World Magnetic Model for 2010-2015, NOAA Technical Report NESDIS/NGDC.

Mayes, C. L., Lawver, L. A. & Sandwell, D. T., 1990. Tectonic history and new isochron chart of the South Pacific: *J. Geophys. Res.,* 95. 8543–8567.

McAdoo, D.C. & Laxon, D., 1997. Antarctic tectonics: Constraints from an ERS-1 satellite marine gravity field, *Science*, 276, 556-560.

Mjelde, R., J. Kasahara, H. Shimamura, A. Kamimura, T. Kanazawa, S. Kodaira & Shiobara, T., 2002. Lower crustal seismic velocity-anomalies; magmatic underplating

or serpentinized peridotite? Evidence from the Voring Margin, NE Atlantic. *Marine Geophysical Research.* 23. 169-183.

Minshull, T., 2009. Geophysical characterisation of ocean-continent transition at magma-poor rifted margins, *C. R. Geosci.,* 341, 382–393.

Mortimer N., Hoernle K., Hauff F., Palin, J. M., Dunlap, W. J., Werner R. and Faure, K., 2006. New constraints on the age and evolution of the Wishbone Ridge, southwest Pacific Cretaceous microplates, and Zealandia–West Antarctica breakup. Geology 34, 185–188.

Mutter, J. C., M. Talwani and P. L. Stoffa 1984. Evidence for a thick oceanic crust off Norway. Journal of Geophysical Research 89, 483-502.

Müller, R.D., Gohl, K., Cande, S.C., Goncharov, A., Golynsky, A.V., 2007. Eocene to Miocene geometry of the West Antarctic rift system. Australian Journal of Earth Sciences 54, 1033–1045. http://dx.doi.org/10.1080/08120090701615691.

Nafe, J. E. & Drake, C. L., 1963. Physical properties of marine sediments, in *The Sea, Vol. 3*, edited by M. N. Hill, pp. 794–815, Interscience, New York.

Nettleton, L. L. 1942. Gravity and magnetic calculations. Geophysics, 7. p. 293-310

Nitsche, F.O., Jacobs, S., Larter, R. D. & Gohl, K., 2007. Bathymetry of the Amundsen Sea Continental Shelf: Implications for Geology, Oceanography, and Glaciology. *Geochemistry, Geophysics, Geosystems (G^3)*,8: Q10009, doi:10.1029/2007GC001694.

Nitsche, F.O., Nitsche, K. Gohl, R.D. Larter, C.-D. Hillenbrand, G. Kuhn, J.A. Smith, S. Jacobs, J.B. Anderson, M. Jakobsson, 2013. Paleo ice flow and subglacial meltwater dynamics in Pine Island Bay, West Antarctica Cryosphere, 7, pp. 249–262 http://dx.doi.org/10.5194/tc-7-249-2013.

Panter, K.S., Blusztanjn, J., Hart, S.R., Kyle, P.R., Esser, R., McIntash, W.C., 2006. The origin of HIMU in the SW Pacific: evidence from intraplate volcanism in southern New Zealand and Subantarctic islands. Journal of Petrology 47, 1673–1704.

Parker, R.L., 1972. The Rapid Calculations of Potential Anomalies, *Geophysical Journal of the Royal Astromical Society* 31, 447-455.

Parsons, T., Thompson, G. A. and Sleep, N. H., 1994. Mantle plume influence on the Neogene uplift and extension of the U S. western Cordillera?, Geology, 22, p. 83 – 86.

Peate, D. W., Hawkesworth, C. J., Mantovani, M. S. M., and Shukowsky, W., 1990. Mantle Plumes and flood basalt stratigraphy in the Paraná, South America., 1990. Geology, 18, p. 1223-1226.

Pérez-Gussinyé, M., M. Metois, M. Fernández, J. Vergés, J. Fullea, and A. Lowry, 2009. Effective elastic thickness of Africa and its relationship to other proxies for lithospheric structure and surface tectonics, Earth Planet. Sci. Lett. , 287(1-2), 152-167.

Pollard, D., DeConto, R. M., 2009. Modelling West Antarctic ice sheet growth and collapse through the past five million years. *Nature* 458, 329-332.

Powell, R.D., and J.M. Cooper, 2002. A glacial sequence stratigraphic model for temperate, glaciated continental shelves. In: Dowdeswell, J.A., Cofaigh, Ó (Eds.), Glacier influenced sedimentation on high-latitude continental margins, 203. Geological Society, London, pp. 215–244. Special Publications.

Pritchard, H.D., Arthern, R.J., Vaughan, D.G., Edwards, L.A., 2009. Extensive dynamic thinning on the margins of the Greenland and Antarctic ice sheets. Nature 461. doi:10.1038/nature08471.

Reid, I., 1994. Crustal structure of a non-volcanic rifted margin east of Newfoundland. *J. Geophys. Res*, 99. 161-180.

Rignot, E.J., Bamber, J.L., van den Broeke, M.R., Davis, C., Li, Y., van de Berg, W., van Meijgaard, 2008. Recent Antarctic ice mass loss from radar interferometry and regional climate modelling. Nature Geoscience 1. doi:10.1038/ngeo102.

Rignot, E. J., J. Mouginot, and B. Scheuchl, 2011. Ice Flow of the Antarctic Ice Sheet, Science, 333 (6048), 1427{1430, doi:10.1126/science.1208336.

Rocchi, S., Armienti, P., D'Orazio, M., Tonarini, S., Wijbrans, J., Di Vincenzo, G., 2002a. Cenozoic magmatism in the western Ross Embayment: role of mantle plume versus plate dynamics in the development of the West Antarctic Rift System. Journal of Geophysical Research 107 (B9), 2195.

Rocchi,S.,LeMasurier,W.E.,DiVincenzo,G.,2002b. Uplift and erosion history in Marie Byrd Land as a key to possible mid-Cenozoic plate motion between East and West Antarctica. Geological Society of America Abstracts with Programs 34.

Rocchi, S., LeMasurier, W. E. & Di Vincenzo, G., 2006. Oligocene to Holocene erosion and glacial history in MBL, West Antarctica, inferred from exhumation of the Dorrel Rock intrusive complex and from volcano morphologies. 118, 991–1005.

Rogenhagen, J. and Jokat, W., 2000. Marine Geology. The sedimentary structure in the western Weddel Sea, v.168, p. 45-60.

Rogenhagen, J., Jokat, W., Hinz, K. and Kristoffersen, Y., 2005. Marine Geophysical Researches. Improved seismic stratigraphy of the Mesozoic Weddel Sea, v. 25, p. 265-283.

Rosenbaum, G., Lister, G.S. & Duboz, C., 2002. Relative motions of Africa, Iberia and Europe during Alpine orogeny. Tectonophysics 359, 117-129.

Rosenbaum, G., Weinberg, R. F., Regenauer-Lieb, K. 2008. The geodynamics of lithospheric extension. Tectonophysics, v. 488. p. 1-8.

Sanger, E.A. and Glen, J.M.G., 2003. Density and magnetic susceptibility values for rocks in the Talkeetna Mountains and adjacent region, South-Central Alaska. U.S. Geological Survey Open-File Report 03–268.

Schaeffer, A. J. and S. Lebedev, 2013. Global shear-speed structure of the upper mantle and transition zone. Geophys. J. Int. doi:10.1093/gji/ ggt095.

Schubert, G., Trucotte, D. L. & Olsen, P., 2001. *Mantle Convection in the Earth and Planets*. 1st ed. Cambridge: Cambridge University Press.

Siddoway, C., 2008. Tectonics of the West Antarctic rift system: New light on the history and dynamics of distributed intra-continental extension. Antarctica: A Keystone in a Changing World, Proceedings of the 10th International Symposium on Antarctic Earth Sciences. Washington, DC: The National Academies Press, p. 91-114.

Siedner, G. and Mitchell, J.G., 1976. Episodic mesozoic volcanism in Namibia and Brazil: A K–Ar isochron study bearing on the opening of the South Atlantic. Earth and Planetary Science Letters 30, 292–302.

Sieminski, A., Debayle, E. and Leveque, J-J. 2003. Seismic evidence for deep low-velocity anomalies in the transition zone beneath West Antarctica. *Earth and Planetary Science Letters* v. 216, p. 645-661.

Smith, W. H. F. and Sandwell, D.T., 1997. Global seafloor topography from satellite altimetry and ship depth soundings, *Science*, v. 277, p. 1957-1962, 26 Sept.

Smith, A. M., T. A. Jordan, F. Ferraccioli and R. G. Bingham, 2013. Influence of subglacial conditions on ice stream dynamics: Seismic and potential field data from Pine Island Glacier, West Antarctica. *J. Geophys. Res,* doi:10.1029/2012JB009582.

Spasojevic, S., Gurnis, M. and Sutherland, R., 2010. Inferring mantle properties with an evolving dynamic model of the Antarctic-New Zealand region from late Cretaceous. *Journal of Geophysical Research*, Vol. 115.

Spector, A. and Grant F.S., 1970. Statistical models for interpreting aeromagnetic data, *Geophysics*, 35, 293-302.

Stein, C. A. and Stein, S., 1992. A model for the global variations in oceanic depth and heat flow with lithospheric age. Nature. v. 359. p. 123-129.

Sterritt, V. A., 2006. Understanding physical property: mineralogy relationships in the context of geologic processes in the ultramafic rock-hosted mineral deposit environment : aiding interpretation of geophysical data. Retrospective Theses and Dissertations, 1919-2007, Earth and Ocean Sciences Theses and Dissertations.

Stewart, J., and Watts, A.B., 1997. Gravity anomalies and spatial variations of flexural rigidity at mountain ranges: Journal of Geophysical Research, v. 102, p. 5327–5352, doi: 10.1029/96JB03664

Stickley, C. E., H. Brinkhuis, S. A. Schellenberg, A. Sluijs, U. Röhl, M. Fuller, M. Grauert, M. Huber, J. Warnaar, and G. L. Williams, 2004. Timing and nature of the deepening of the Tasmanian Gateway. *Paleoceanography*, 19(4), PA4027. doi:10.1029/2004PA001022.

Storey, B. C., 1991. The crustal blocks of West Antarctica within Gondwana: Reconstruction and breakup model. In Geological Evolution of Antarctica, eds. M. R. A. Thompson, J. A. Crame, and J.W. Thompson, 587-592. Cambridge University Press.

Storey, B. C., 1995. The role of mantle plumes in continental breakup:case histories from Gondwanaland. Nature377, 301– 308.

Sutherland, R., Spasojevic, S. and Gurnis, M., 2010. Mantle upwelling after Gondwana subduction death explains anomalous topography and subsidence histories of eastern New Zealand and West Antarctica. *Geology*, v. 38, no. 2, p.155-158.

Syberg, F.J.R., 1972. A Fourier method for the regional-residual problem of potential fields, Geophysica l Prospecting, 20, 47-75.

Tessensohn, F., Wörner, G., 1991. The Ross Sea rift system (Antarctica). Structure, evolution and analogues. In: Thompson M. R. A., Crame J.A., Thomson, J.W.. Geological evolution of Antarctica. Cambridge University Press, Cambridge, 273-277.

Trenberth, K. E. and J. M. Caron, 2001. Estimates of Meridional Atmosphere and Ocean Heat Transports. *J. Climate*, 14(16), 3433–3443. doi:10.1175/1520-0442(2001)014 <3433:EOMAAO>2.0.CO;2.

Trey, H., A. K. Cooper, G. Pellis, B. Della Vedova, G. Cochrane, G. Brancolini, *and* J. Makris, 1999. Transect across the West Antarctic rift system in the Ross Sea, Antarctica, Tectonophysics, 301, 61–74.

Trua, T., Deniel, C., Mazzuoli, R., 1999. Crustal control in the genesis of Plio-Quaternary bimodal magmatism of the Main Ethiopian Rift (MER), geochemical and isotopoic (SR, ND, Pb) evidence, Chem. Geol, 155, 201-131

Torge W., 1989. Gravimetry. Walter de Gruyter, 465.

Uenzelmann-Neben, G., Gohl, K., Larter, R.D., Schlüter, P., 2007. Differences in ice retreat across Pine Island Bay, West Antarctica, since the Last Glacial Maximum: Indications from multichannel seismic reflection data; Proceedings of the 10th ISAES, edited by A.K. Cooper and C.R. Raymond et al., *USGS Open-File Report 2007-1047*, doi:10.3133/of2007-1047.srp084.

Uenzelmann-Neben, G., Gohl, K., 2012. Amundsen Sea sediment drifts: Archives of modifications in oceanographic and climatic conditions, *Marine Geology*, v. 299-302, p. 51-62, doi:10.1016/j.margeo.2011.12.007.

Uenzelmann-Neben, G., Gohl, K., 2014. Early glaciation already during the Early Miocene in the Amundsen Sea, Southern Pacific: Indications from the distribution of sedimentary sequences. *Global and Planetary Change,* 120, 92-104.

Vanneste, L. E., Larter, R.D., 1995. Deep-tow boomer survey on the Antarctic Peninsula Pacific Margin: an investigation of the morphology and acoustic characteristcs of late Quaternary sedimentary deposits on the outer continental shelf and upper slope. In: Cooper, A.K., Barker, P.F., Brancolini, G. (Eds.), Geology and Seismic Stratigraphy of the Antarctic Margin, Antarctic Research Series, 68. AGU, Washington, D.C., pp. 97–121.

Voss, M., Jokat, W., 2007. Continent-ocean transition and voluminous magmatic underplating derived from P-wave velocity modelling of the Greenland continental margin. *Geophys. J. Int.,*170. 580-604.

Watts, A.B., Karner, G. D., Steckler, M.S., 1982. Lithospheric Flexure and the Evolution of Sedimentary Basins, *Phil. Trans. R. Soc. Lond,* v. 305, p. 249-281.

Watts, A. B., 1989, Lithospheric flexure due to prograding sediment loads: implications for the origin of offlap/onlap patterns in sedimentary basins, Basin Research, v. 2, p. 133-144.

Watts, A. B. & Fairhead, J. D., 1999. A process-oriented approach to modelling the gravity signature of continental margins, *The Leading Edge*, 18(2), 258–263.

Watts, A.B., 2001. Isostasy and flexure of the lithosphere: Cambridge, Cambridge University Press, 458 p..

Weigelt, E., Gohl, K., Uenzelmann-Neben, G., Larter, R. D., 2009. Late Cenozoic ice sheet cyclicity in the western Amundsen Sea Embayment – Evidence from seismic records. Global and Planetary Change, 69, 162-169.

Whitmarsh, R.B., White, R.S., Horsefield, S. J., Sibuet, J., Recq, M. & Louvel, V., 1996. The ocean-continent boundary off the western continental margin of Iberia: Crustal s structure west of Galician Bank. *J. Geophys. Res.* 101. 291-314.

White, R. S. and McKenzie, D. P., 1989. Magmatism at rift zones: The generation of Volcanic continental margins and flood basalts: *Journal of Geophysical Research*, v. 94, p. 7685-7729.

Wilson, D. S., D. Pollard, R. M. DeConto, S. S. Jamieson, and B. P. Luyendyk, 2013. Initiation of the West Antarctic Ice Sheet and estimates of total Antarctic ice volume in the earliest Oligocene. *Geophys. Res. Lett.*, 40(16), 4305‐4309. doi:10.1002/grl.50797.

Winberry, J. P., and S. Anandakrishnan 2004. Crustal structure of the West Antarctic rift system and Marie Byrd Land hotspot, Geology, 32(11), 977‐980, doi:10.1130/G20768.1.

Wienecke, S., Braitenberg, C. and Götze, H.J. 2007. A new analytical solution for the differential equation of the 4th order estimating the flexural rigidity in the Central Andes (15°- 33° S). in editorial process, Geophys. J. Int.

Wobbe, F., Gohl, K., Chambord, A. & Sutherland, R., 2012. Structure and break-up history of the rifted margin of West Antarctica in relation to Cretaceous separation from Zealandia and Bellingshausen plate motion. *Geochemistry, Geophysics, Geosystems.* Q04W12, doi:10.1029/2011GC003742.

Zelt, C. A. & Smith, R.B., 1992. Seismic traveltime inversion for 2-D crustal velocity structure, *Geophys. J. Int.,* 108(1), 16‐34.